THE UNIVERSITY OF ALBERTA

PILE FOUNDATIONS IN PERMAFROST

by

Jeffrey Stephen Weaver

A THESIS

SUBMITTED TO THE FACULTY OF GRADUATE STUDIES AND RESEARCH

IN PARTIAL FULFILMENT OF THE REQUIREMENTS FOR THE DEGREE

OF DOCTOR OF PHILOSOPHY

IN

GEOTECHNICAL ENGINEERING

DEPARTMENT OF CIVIL ENGINEERING

EDMONTON, ALBERTA

FALL 1979

THE UNIVERSITY OF ALBERTA

FACULTY OF GRADUATE STUDIES AND RESEARCH

The undersigned certify that they have read, and recommend to the Faculty of Graduate Studies and Research, for acceptance, a thesis entitled PILE FOUNDATIONS IN PERMAFROST submitted by Jeffrey Stephen Weaver in partial fulfilment of the requirements for the degree of DOCTOR OF PHILOSOPHY in GEOTECHNICAL ENGINEERING.

N.R.Morgenstern .....
Supervisor

R.R.Gilpin .....

T.M.Hrudey .....

S.Thomson .....

B.Ladanyi .....
External Examiner

Date...July 31, 1979

THE UNIVERSITY OF ALBERTA

RELEASE FORM

NAME OF AUTHOR Jeffrey Stephen Weaver

TITLE OF THESIS PILE FOUNDATIONS IN PERMAFROST

DEGREE FOR WHICH THESIS WAS PRESENTED DOCTOR OF PHILOSOPHY

YEAR THIS DEGREE GRANTED FALL 1979

Permission is hereby granted to THE UNIVERSITY OF ALBERTA LIBRARY to reproduce single copies of this thesis and to lend or sell such copies for private, scholarly or scientific research purposes only.

The author reserves other publication rights, and neither the thesis nor extensive extracts from it may be printed or otherwise reproduced without the author's written permission.

(SIGNED) .....

PERMANENT ADDRESS:

.....

.....

.....

DATED.....19

Best wishes,

Jeff

To Mom and Dad

ABSTRACT

This thesis deals with the construction and design of pile foundations on permafrost. Laboratory creep tests were carried out and support the use of a simple shear analysis to predict pile creep in permafrost. On the basis of this model, design charts were prepared for piles in a wide variety of frozen soils. A detailed review of the literature on pile creep has confirmed the validity of these charts. Numerical methods have been developed to assist data interpretation of pile creep tests and recommendations are given for conducting field pile tests in permafrost.

The wave equation analysis has been adapted for frozen soils and the dynamics of pile driving in permafrost has been studied. A review of the literature on driving records in frozen soils has confirmed the applicability of this model. Recommendations are given for the use of bored cast-in-place piles in permafrost. These recommmendations are based on the results of a detailed literature review and laboratory tests.

RESUME

L'objet de cette thèse est d'étudier la construction et le calcul des fondations sur pieux dans le pergélisol. Des essais de fluage en laboratoire ont confirmé l'intérêt d'une analyse en cisaillement simple des sols, pour prédire les déformations différées des pieux dans le pergélisol. On a préparé des abaques, basées sur ce modèle, pour le calcul des pieux mis en place dans de nombreux types de sols gelés. Une étude approfondie de la littérature sur le fluage des pieux a confirmé la validité de ces abaques. On a développé des méthodes de calcul numérique pour faciliter l'analyse des résultats d'essais de fluage de pieux. On donne également des directives pour effectuer des essais de chargement de pieux dans le pergélisol.

Une adaptation aux sols gelés de l'analyse dynamique de battage des pieux permet d'étudier cette technique dans le pergélisol.Une revue de compte-rendus de battage de pieux dans les sols gelés confirme que cette analyse s'applique. On donne des recommandations pour l'utilisation des pieux forés coulés en place dans le pergélisol; elles sont basées sur une étude détaillée de la littérature et sur des essais de laboratoire.

ACKNOWLEDGEMENTS

The author would like to thank Dr.N.R.Morgenstern for suggesting this thesis topic and for his continual guidance and support during all stages of this thesis.

The author also wishes to thank Dr.S.Thomson for his invaluable comments and discussion of the project.

The author is also grateful to the University of Alberta, Franki of Canada, the Transportation Development Agency and the Boreal Institute for Northern Studies for providing financial support.

Special thanks are extended to my fellow graduate students and the staff within the Department of Civil Engineering who have given me encouragement and friendship during my stay in Edmonton.

In closing, the author especially wishes to thank his future wife, Donna, for her love and understanding during the past five years.

Table of Contents

Chapter Page

List of Tables

List of Figures

CHAPTER 1

INTRODUCTION

1.1 General

Exploration and development of energy resources within the arctic circle in the last two decades has given unprecedented impetus for the geotechnical engineering profession to improve piling practice in permafrost regions. Considerable progress has been made with regard to the use of analytical models to study the interaction between piles and permafrost. In spite of this, the constitutive relationships of frozen soils are still poorly defined and hence the effectiveness of these analyses is somewhat reduced.

Studies of pile construction on permafrost in North America have been modest. Much of the research has been directed at improving existing construction technology (Woodward-Lundgren (1971) and Rooney et al. (1976)). The advent of thermal piles is a notable exception to this trend.

The major objectives of this thesis are to present a less conservative design procedure for piles in frozen soils

and to qualify the use of bored and driven piles in permafrost.

1.2 Scope of the Thesis

The geotechnical properties of frozen soils are reviewed in Chapter 2. Existing creep data are examined and constitutive relationships are proposed for a wide range of frozen soils. Fracture strength/time-to-failure relationships with regard to pile driving are also presented.

The state-of-the-art of piling in permafrost is reviewed in Chapter 3.

Chapter 4 summarises the results of long-term simple shear creep tests on various frozen soils conducted as part of this thesis. The experiments modeled stress transfer at the pile/soil interface. In the light of these results an analytical model to determine pile creep in frozen soils was proposed and design curves for piles in a wide range of frozen soils were presented in Chapter 5. These predictions are based on the constitutive relationships outlined in Chapter 2. In addition a new method of evaluating adfreeze strengths is proposed.

Chapter 6 presents a theoretical basis for analysing pile driving in frozen soils. Blowcounts and end-bearing driving stresses are predicted using a modified version of the wave equation analysis (Smith (1962)). In addition guidelines are given for analysing vibratory driving in

permafrost.

Chapter 7 evaluates the feasibility of using bored cast-in-place concrete piles in permafrost. Recent advances in cementing technology in permafrost are reviewed and their application to sub-surface concreting is assessed.

Guidelines for conducting pile load tests in permafrost are given in Chapter 8. These recommendations are based on the results of theoretical studies of incremental test data interpretation, short-term creep of compressible piles and short-term freezeback pressures generated around frozen-in piles.

Chapter 9 summarises briefly the results of this research and presents recommendations for pile selection and design in frozen soils.

CHAPTER 2

GEOTECHNICAL PROPERTIES OF PERMAFROST RELATIVE TO FOUNDATION DESIGN

2.1 Introduction

This review includes only the geotechnical properties of frozen soils that are pertinent to design and construction of pile foundations in permafrost. This includes creep behaviour at low stresses with regard to pile design, and fracture behaviour at very high stresses with regard to pile driving.

2.2 Composition of Frozen Ground

Frozen soil is a complex 4-phase system comprised of mineral soil particles, ice, water and gases. The interfacial behaviour of these components is governed by thermodynamic considerations and influenced by external variables such as stress and temperature.

The size and shape of the mineral grain and the physico-chemical nature of its surface strongly influence the geotechnical properties of frozen ground. Notwithstanding this, ice is the most important component of

frozen soils. The mechanical properties of frozen soil are dominated by the visco-plastic nature of ice. The most important ice type in frozen soils is ice 1 which has a hexagonal structure.

Unfrozen water exists in two states in frozen soil; namely, strongly bound water and loosely bound water. The strongly bound water is a layer of water surrounding the mineral particle. The very high intermolecular forces within this layer suppress freezing, even at very low temperatures. The loosely bound water is a water layer surrounding the strongly bound water. The intermolecular forces in this layer are weaker and the water can be frozen. The amount of unfrozen water present in the frozen soil at a certain temperature has been empirically related to the specific surface area of the mineral particles (Anderson and Tice (1971)) and approximately related to the liquid limit of the soil (Tice et al. (1973)).

The gaseous phase consists predominantly of water vapour and is the least important component with respect to mechanical behaviour.

For a more detailed review the reader is referred to Anderson and Morgenstern (1973) and to Tsytovich (1975) .

2.3 The Geotechnical Properties of Ice

2.3.1 Rheological Deformation Processes in Polycrystalline Ice

Ice is a visco-plastic crystalline material. In general, a sample of ice will exhibit an instantaneous elastic response upon application of stress. Thereafter, time-dependent plastic deformations occur, for which three modes of creep have been defined; namely, primary, secondary and tertiary creep. The major factors that control the development of a particular creep mode are the magnitude and duration of the applied load and the ice temperature. During primary creep the creep rate continuously decreases; during the secondary stage the creep rate is constant and during tertiary creep the creep rate continuously increases. At high stress levels ice exhibits all three stages of the classical creep curve. At low stress levels ice deforms in the primary and secondary modes only. Further, the mode of deformation may change and the ensuing creep rate will increase with an increase in temperature.

For a detailed review of the mechanics of ice creep the reader is referred to Langdon (1973) , Weertman (1973) , Hobbs (1974) , Glen (1975) , Roggensack (1977) and Baker (1978) . Briefly, creep is a thermally activated process and, as such, can be described by an Arrhenius-type relationship of the form,

$$\dot{\varepsilon} = B'\sigma^n e^{-\frac{Q}{kT}} \qquad \text{.....2.1}$$

where Q denotes the activation energy, k denotes the absolute temperature and B' and n are constants.

In the stress and temperature ranges of interest to geotechnical engineers (i.e. less than 100 kPa and warmer than -10 ^{0}C) there are several deformation processes which may contribute to the creep of polycrystalline ice (Langdon (1973)). From this it emerges that creep activated energies, obtained from creep tests on polycrystalline ice at warm temperatures, are meaningless since they cannot be attributed to a single creep process. This prompted Roggensack (1977) to state

> "...at present, there exists no physical evidence suggesting an equation more complex than a simple power law to relate strain rate to stress."

At temperatures colder than -1 ^{0}C the dominant creep process is thought to be either "Nabarro-Herring" creep or dislocational creep (Weertman (1973)). At warmer temperatures the creep process is accelerated as a result of pressure-melting at intergranular contacts, and intergranular sliding (Barnes _et al_. (1971)).

More recently, Baker (1978) has shown that the creep rate of polycrystalline ice is strongly influenced by the average ice crystal grain size

> "...For coarse-grained ice (average diameter greater than about 1.0 mm), it appears that creep is dominated by internal dislocation movement with creep rate controlled by the mobility of

dislocations in their glide planes. Crystal boundaries are obstacles to dislocation motion; reducing the crystal size thus results in a reduction in secondary creep rate in proportion to about the square of the average grain diameter... For fine-grained ice, creep appears to be dominated by diffusional processes. Reduction of ice-crystal size results in an increase in secondary creep rate in proportion to about the inverse-square of the average grain diameter."

2.3.2 A Review of Creep Relationships for Randomly Oriented Polycrystalline Ice

The flow law for random polycrystalline ice, under multiaxial conditions, may be described in terms of the second invariants of deviatoric stress and strain rate. In this way the creep behaviour is assumed to be independent of hydrostatic pressure and the third invariant of stress. Glen (1975) has discussed the limitations of these assumptions and concludes

"For the present it seems reasonable to continue to use the second invariant theory, while awaiting further experimental verification of its validity."

Emery and Nguyen (1974) and Ladanyi (1972b) recommend adoption of the effective shear stress and effective shear strain rate as defined by Odqvist (1966) for general engineering problems,

$$\sigma_e = \sqrt{3}\sqrt{I_2} \qquad \text{.....2.2a}$$

$$\dot{\varepsilon}_e = \frac{2}{\sqrt{3}}\sqrt{J_2} \qquad \text{.....2.2b}$$

where I_2 and J_2 denote the second invariants of deviatoric stress and strain rate, respectively. The flow law now becomes

$$\dot{\varepsilon}_e = B\,\sigma_e^{\,n} \qquad \text{.....2.3}$$

The advantage of this definition is that Norton's Law can be recovered in the uniaxial case.

A detailed review of secondary creep rates in random polycrystalline ice was recently conducted by Morgenstern et al. (1979), and is presented in this thesis as Figure 2.1. The authors determined the following values for the creep parameters, B and n

	B ($kPa^{-n}.yr^{-1}$)	n
-1°C	4.5×10^{-8}	3.0
-2°C	2.0×10^{-8}	3.0
-5°C	1.0×10^{-8}	3.0
-10°C	5.6×10^{-9}	3.0

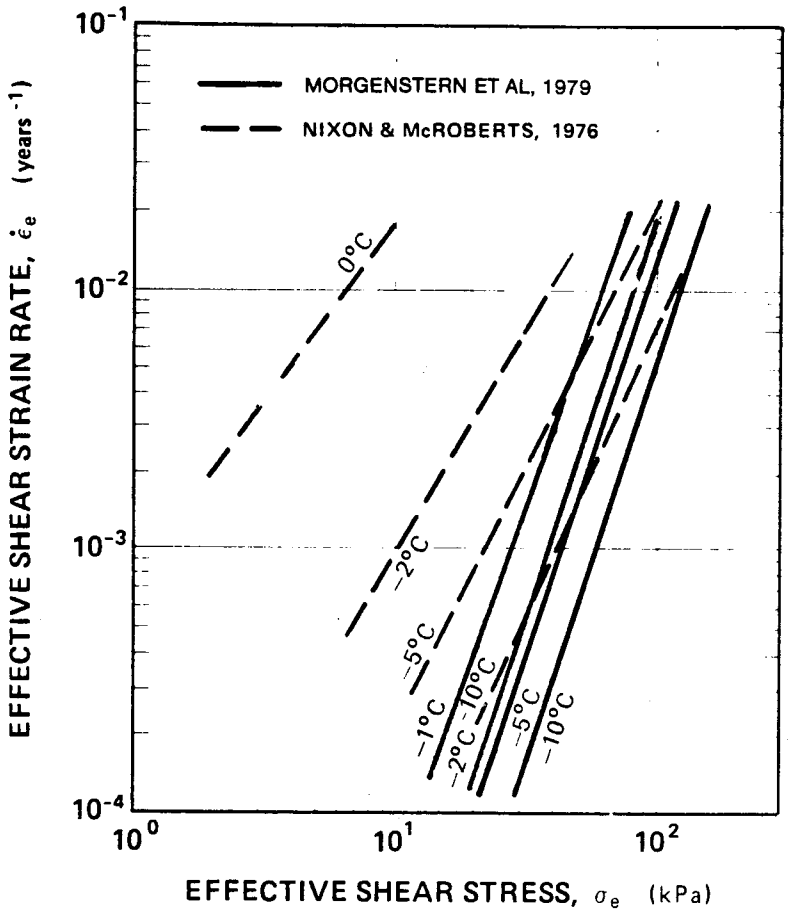

Figure 2.1

Flow Law for Ice

2.3.3 A Review of the Strength Properties of Polycrystalline Ice

When ice fractures rapidly it does so in a brittle manner. The process is commenced by cracks which are initiated following plastic deformation of the crystals (Gold (1972)). However, at lower stresses ice yields in an apparently plastic manner as a result of recrystallisation (Steinemann (1958)).

The strength of ice depends upon temperature, rate of load application, type of loading, type of ice and the direction of the stress relative to the grain structure. Studies of the strength of ice, however, have not usually been carried out with sufficient completeness or control to outline the influences of the preceding factors. Much of the information on the strength of ice, therefore, is qualitative and of little general value. Reviews on this subject have been prepared by Voitkovskii (1960) , Gold (1972) and Glen (1975) .

Voitkovskii (1960) suggests that the fracture stress increases linearly with decreasing temperature. Hawkes and Mellor (1972) have shown that fracture stresses determined from compression tests are much higher than those determined from tensile tests. Voitkovskii (1960) also suggests that the fracture stress determined from shear tests is approximately equal to half the fracture stress determined from tension tests. Finally, the anisotropic nature of the

ice mono-crystals renders the fracture stress dependent upon the direction of stressing in relation to the optical axis of the crystal (Gold (1972)). It appears that in the ductile yield range the yield stress decreases with decreasing stress application rate and in the brittle fracture range the fracture stress is rate-independent.

2.4 The Geotechnical Properties of Frozen Soils

2.4.1 Rheological Deformation Processes in Frozen Soils Subjected to Low Stresses

The structure of frozen soil is complex. The presence of soil particles in a body of ice can modify or entirely alter the indigenous creep mechanisms. The degree of modification is particularly sensitive to the bulk density of the frozen soil and the grain size of the soil particles.

In general, the presence of soil particles impedes the movement of dislocations within the ice crystals, thereby suppressing ice creep. However, the soil particles may also cause a reduction in the average grain-size of the ice crystals and at very low concentrations (i.e. bulk densities less than 0.95 Mg/m^3) the creep rate may be enhanced (Hooke et al. (1972) ; Baker (1978)). At higher concentrations of solids, the suppressive mechanism dominates and the creep rate is reduced. This phenomenon is analogous to the problem of dispersion hardening of polycrystalline metals (Reed-Hill (1973)), and has been shown to exist in frozen soils whose

bulk densities are less than 1.5 Mg/m^3 (Hooke et al.(1972)).

The long-term creep characteristics of frozen soils whose bulk densities are higher than 1.5 Mg/m^3 are ill-defined. The creep mechanism in dense, fine-grained frozen soils is further complicated by the presence of an interconnecting network of unfrozen water. Vialov (1959) points out that for such soils, time-dependent consolidation will occur, resulting in increased effective stresses and, therefore, a strengthening of the soil matrix. Further, the presence of unfrozen water reduces the average ice crystal size and also assists grain-boundary sliding, thus facilitating plastic flow of the ice matrix. Sayles and Haines (1974) reported unconfined compression creep tests (greater than 1500 hours) on frozen silts and clays of bulk densities approximately equal to 1.8 Mg/m^3. They indicated that secondary creep does not exist for such soils, throughout the time range 0 to 2000 hours and in the stress range 35 to 250 kPa. Therefore, it is probable that for frozen fine-grained soils, secondary creep either does not exist or is insignificant and can be ignored in geotechnical considerations.

Similarly, the experimental works of Sayles (1968) and Sayles (1973) have shown that secondary creep does not exist at low stresses for dense coarse-grained frozen soils.

2.4.2 A Proposed Classification of Frozen Soils

On the basis of the experimental evidence summarised in

the previous section, the low stress creep behaviour of permafrost may be classified according to frozen bulk density. In this regard, the following terms are introduced.

1. Dirty ice - this term applies to ice that has very low solid concentrations. Typical bulk densities are between 0.9 and 0.95-1.0 Mg/m^3. Introduction of soil particles into the ice matrix reduces the average grain size of the ice crystals, thereby giving rise to higher creep rates than pure ice.
2. Very dirty ice - this term applies to ice that has medium to high solids concentrations. These materials display secondary creep rates much lower than that of polycrystalline ice. It is speculated that these soils do not have extensive grain to grain contact. Typical bulk densities are between 0.9 - 1.0 and 1.6 - 1.8 Mg/m^3.
3. Ice-poor frozen soil - this term applies to saturated frozen soils whose deformation behaviours are characterised by primary creep. This definition encompasses all grain sizes and typical bulk densities are between 1.7 - 1.8 and 1.9 - 2.0 Mg/m^3.
4. Ice-rich frozen soil - this term applies to frozen soils having a continuous network of segregated ice. It is expected that the mineral layers will creep in a primary mode and that the ice will deform according to a secondary creep law. Thus, the overall creep response of the composite material is complex and is very sensitive

to the reticulate structure of the segregated ice, the bulk density and grain size of the mineral layers and the ground temperature.

It is noted that no distinction has been made between coarse-grained and fine-grained frozen soils. However, it is speculated that the creep of frozen fine-grained soils at temperatures very close to the melting point may be considerably accelerated by high unfrozen water contents. Under these conditions it appears reasonable to suggest that such soils will undergo large creep displacements and may display secondary creep behaviour.

This classification is tentative and is only intended to provide an approximate framework in which to categorise the creep behaviour of frozen soils. The bulk density demarcations have been estimated on the basis of the aforementioned creep data and as more data becomes available, the boundaries may be more clearly defined.

2.4.3 A Review of Constitutive Relationships of Frozen Soils in the Low Stress Range

In situ freezing of coarse-grained soils generally results in ice-poor frozen soil. Similarly, *in situ* freezing of fine-grained soils creates a composite network of segregated ice and ice-poor frozen soil. Very dirty ice is seldom encountered in permafrost soils. Therefore, this review is limited to the creep relationships in the low stress range for ice-rich and ice-poor frozen soils.

Long-term creep tests have been conducted on undisturbed ice-rich frozen soils containing varying amounts of segregated ice (Thompson and Sayles (1972), Roggensack (1977) and McRoberts *et al.* (1978)). The field data of Thompson and Sayles indicate that the ice-rich Fairbanks silt in the vicinity of Fox, Alaska, displays creep rates comparable to that of polycrystalline ice. In contrast to this, the data presented by McRoberts *et al.* (1978) indicate that Norman Wells silt displays lower creep rates than that of polycrystalline ice. Roggensack (1977) observed creep rates in frozen clays, at -0.8 ^{0}C, higher than that of polycrystalline ice.

The data of Roggensack (1977) and McRoberts *et al.* (1978) have been normalised to -1.0 ^{0}C by Nixon (1978) and these data are summarised in Figure 2.2. The discrepancies in these data reflect the sensitivity of the creep behaviour to the variables outlined in the previous section. Since the frozen mineral soil layers are characterised by primary creep, it is logical to assume that the short- to middle-term creep response of an ice-rich soil will also be characterised by primary creep, and that true steady-state creep will only be realised when the transient creep in the mineral layers has become very small. Hence, the long-term creep response of ice-rich soil is characterised by secondary creep occurring in the reticulate ice structure.

The short-term response will depend very largely on the relative magnitudes of the primary creep in the frozen soil

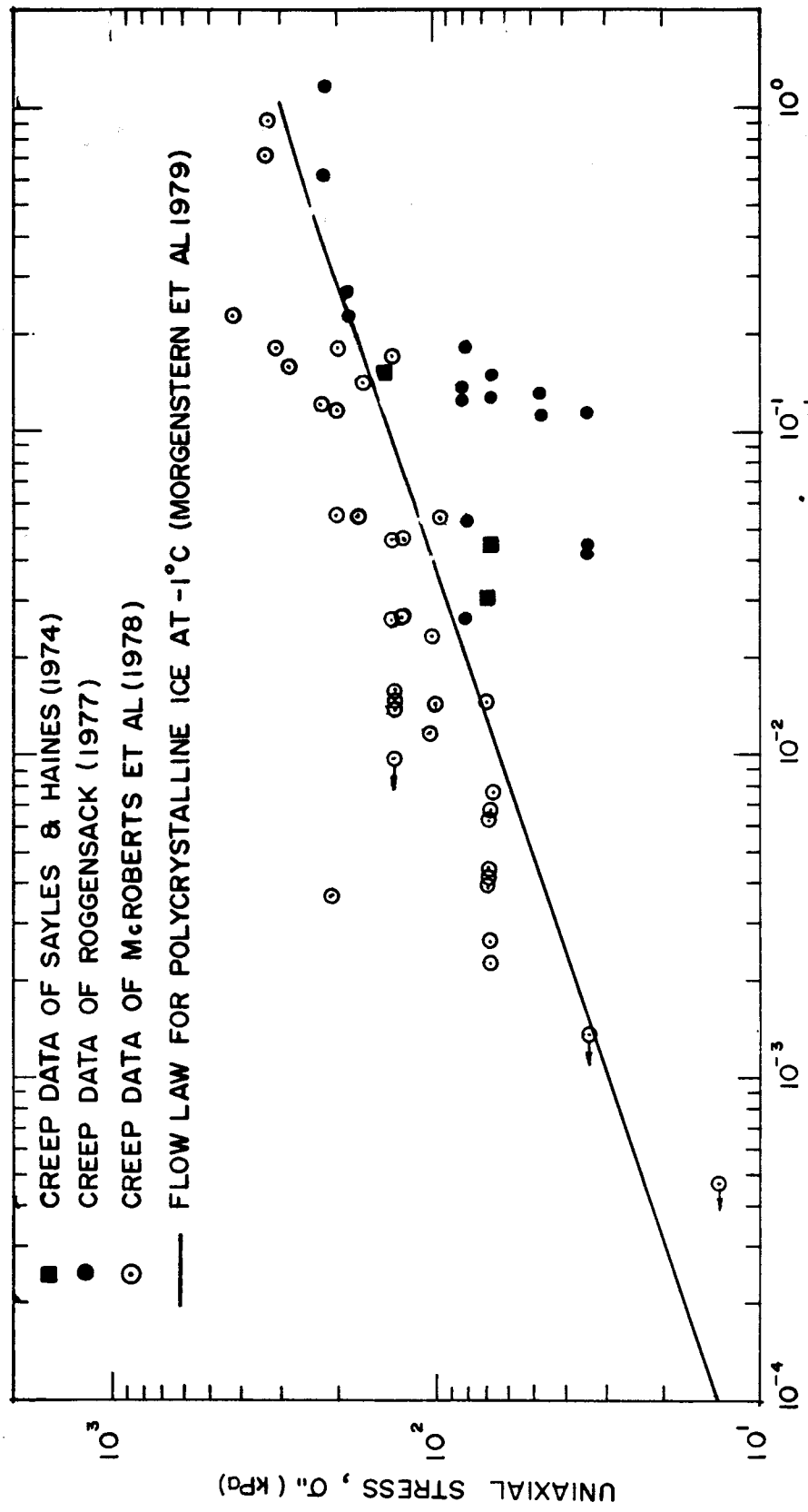

Figure 2.2

Creep Data for Ice-Rich Frozen Soils, Adjusted to −1°C

and the ice lenses. For example, dense warm fine-grained frozen soils possess a high unfrozen water content, and it is probable that primary creep in these soils is more pronounced than in ice. Thus, for such an ice-rich frozen soil the stiffer ice lenses will support most of the applied load, in the short term, and the overall material may appear to creep in the secondary mode at a rate higher than that of ice.

In this context, consider the data of Roggensack (1977). These tests were conducted in the temperature range 0 to -1 ^{0}C and the soil mineral layers were characterised by frozen bulk densities in excess of 1.9 Mg/m^{3}. Thus, it is probable that the soil layers were more deformable in the short-term than ice. Hence, these samples may appear to creep at faster secondary creep rates than those predicted for analogous samples of pure ice. It is anticipated that in the long-term the frozen soil layers would stiffen and therefore, arrest the creep of the overall material.

The above reasoning provides a rational explanation for the anomalies in the observed creep behaviour of ice-rich frozen soils, and supports the view that the flow law for ice provides a conservative estimate of the creep of an ice-rich frozen soil.

Hult (1966) proposed the following multiaxial creep law to describe the primary creep of high temperature metals

$$\varepsilon_e = \left[\dot{\varepsilon}_c(1+\mu)\right]^{\frac{1}{1+\mu}} \left(\frac{\sigma_e}{\sigma_c}\right)^{\frac{m}{1+\mu}} t^{\frac{1}{1+\mu}} \qquad \text{.....2.4}$$

where ε_e and σ_e are defined in Equation 2.2, t is the time elapsed after application of load (hr), $\dot{\varepsilon}_c$ is an arbitrarily selected strain rate, σ_c is the creep proof stress and m and μ are creep exponents. For frozen soils equation 2.4 may be more simply stated as follows

$$\varepsilon_e = K\sigma^c t^b \qquad \text{.....2.5}$$

where K, c and b are temperature-dependent material parameters. Vialov (1962) proposed that the temperature dependence of K may be stated as follows

$$K = \left[\frac{1}{w(\theta+1)^k}\right]^c \qquad \text{.....2.6}$$

where θ is the temperature below freezing in centigrade degrees and w and k are material-dependent parameters.

Equation 2.5 does not take into account the influence of the mean normal pressure $(\sigma_1 + \sigma_2 + \sigma_3)/3$, where σ_1 , σ_2 and σ_3 are the three principal stresses. Recognising this, Ladanyi (1972b) used the Von Mises failure criterion to model the influence of hydrostatic pressure on the steady-state creep rates. This approach may be extended to non-steady creep rates; thus the dependence of strain on the confining pressure in the primary creep range can be stated as follows,

$$\varepsilon_e = K\left[\left(\frac{f+2}{3}\right)\sigma_e + (1-f)\sigma_m\right]^c t^b \qquad \text{.....2.7}$$

where $f=(1+\sin\phi)/(1-\sin\phi)$ and ϕ is a "pseudo" internal angle of friction. The applicability of Equation 2.7 to represent the creep of ice-poor frozen soils can be explored by back-analysis of the confined compression creep data of Sayles (1973). Such a synthesis has been undertaken as part of this thesis and is described in Appendix A. The constants in Equation 2.7 were determined from analysis of the creep data and are presented in Table A.3. The applicability of this type of constitutive relationship was then assessed by comparing the strain/time behaviour, predicted by Equation 2.7, with the actual observed behaviour. This comparison is presented in Figure 2.3. The agreement between observed and predicted behaviour is good. Thus, this set of data supports the use of Equation 2.7 to describe the confined compression creep behaviour of ice-poor frozen soil. Finally, the predictive capacity of Equation 2.7 was also checked against unconfined compression creep data (Sayles (1968). Inspection of Table A.3 shows that the creep exponents as determined from the two data sets are in reasonable agreement. Further, examination of Figure 2.4 which presents a comparison of creep data as observed by Sayles (1968) and as predicted by Equation 2.7, confirms that the predictions are also good.

The accuracy of Equation 2.7 is reduced as the ratio $\frac{\sigma_1}{f\sigma_3}$ approaches unity and for $\frac{\sigma_1}{f\sigma_3}$ less than 1.25, better accuracy can be obtained if 'f' is taken as unity. Unfortunately, at this time lack of multiaxial creep data

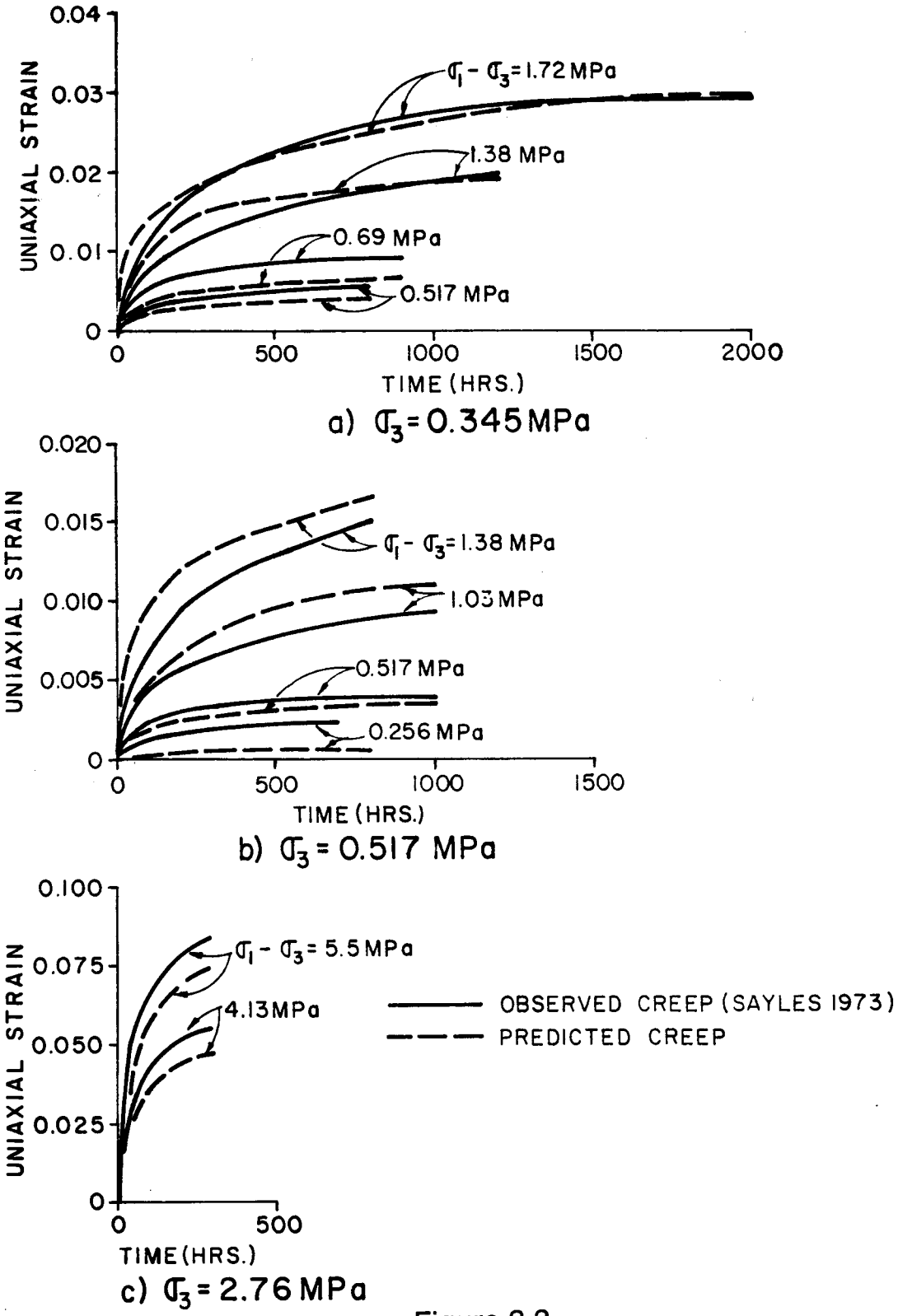

Figure 2.3
Comparison of Predicted and Actual Creep Behaviour for Ottawa Sand (Data from Sayles (1973))

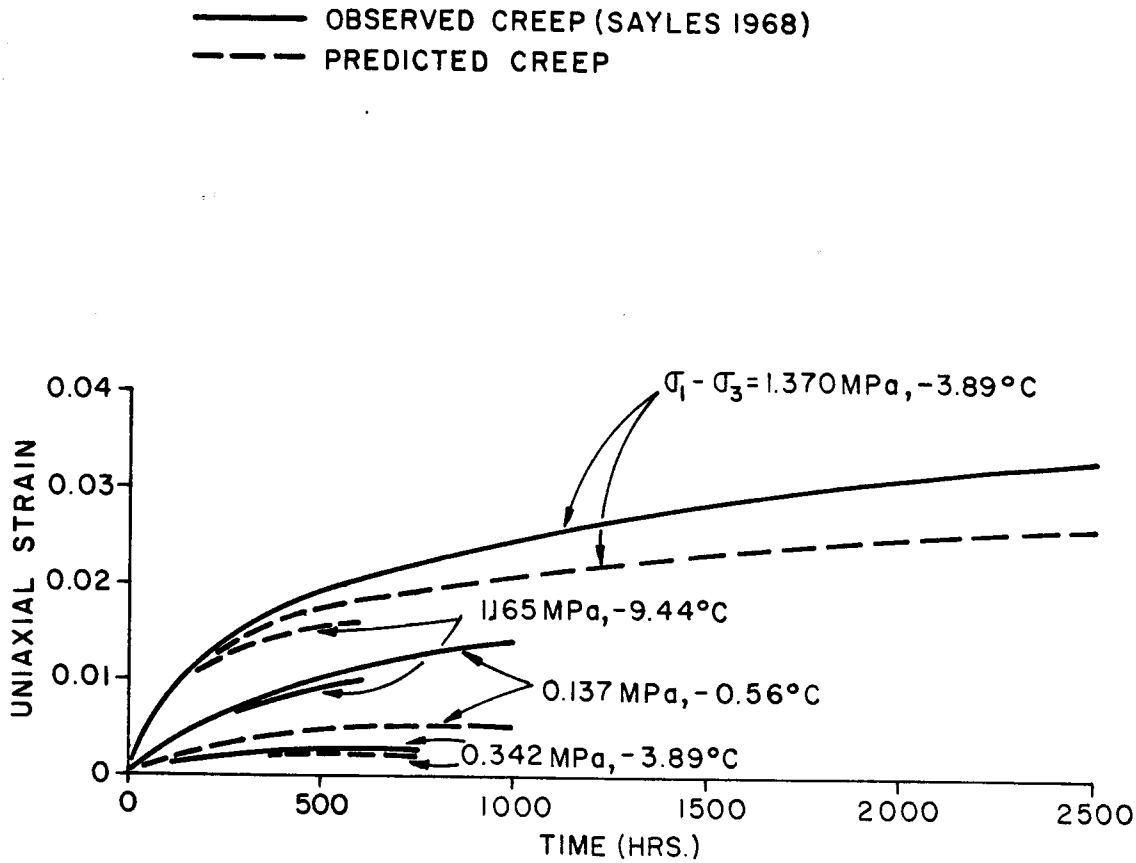

Figure 2.4
Comparison of Predicted and Actual Creep Behaviour for Ottawa Sand (Data from Sayles (1968))

precludes verification of Equation 2.7 and therefore, it should be used with caution.

2.4.4 A Review of the Rheological Strength Properties of Frozen Soils Subject to High Strain Rates

This review includes only the strength properties which are pertinent to pile driving analysis, i.e., strengths associated with high strain rates.

A review of possible failure mechanisms for brittle fracture of frozen soils can be found in Haynes et al. (1975) and Haynes and Karalius (1977) .

The compressive strength of frozen Fairbanks silt has been determined for a wide range of temperatures and strain rates (Haynes et al. (1975) and Haynes and Karalius (1977)). The relationship between the compressive strength of frozen Fairbanks silt, temperature and time-to-failure (analogous to strain rate) are summarised in Figures 2.5 and 2.6, and can be described by the following equation

$$\sigma_{cu} = D t_f^{m} \qquad \text{.....2.8}$$

where σ_{cu} is the unconfined uniaxial compressive strength (MPa), t_f is the time to failure (seconds), D is a temperature dependent parameter and m is a constant. From Figures 2.5 and 2.6 the following relationship was obtained

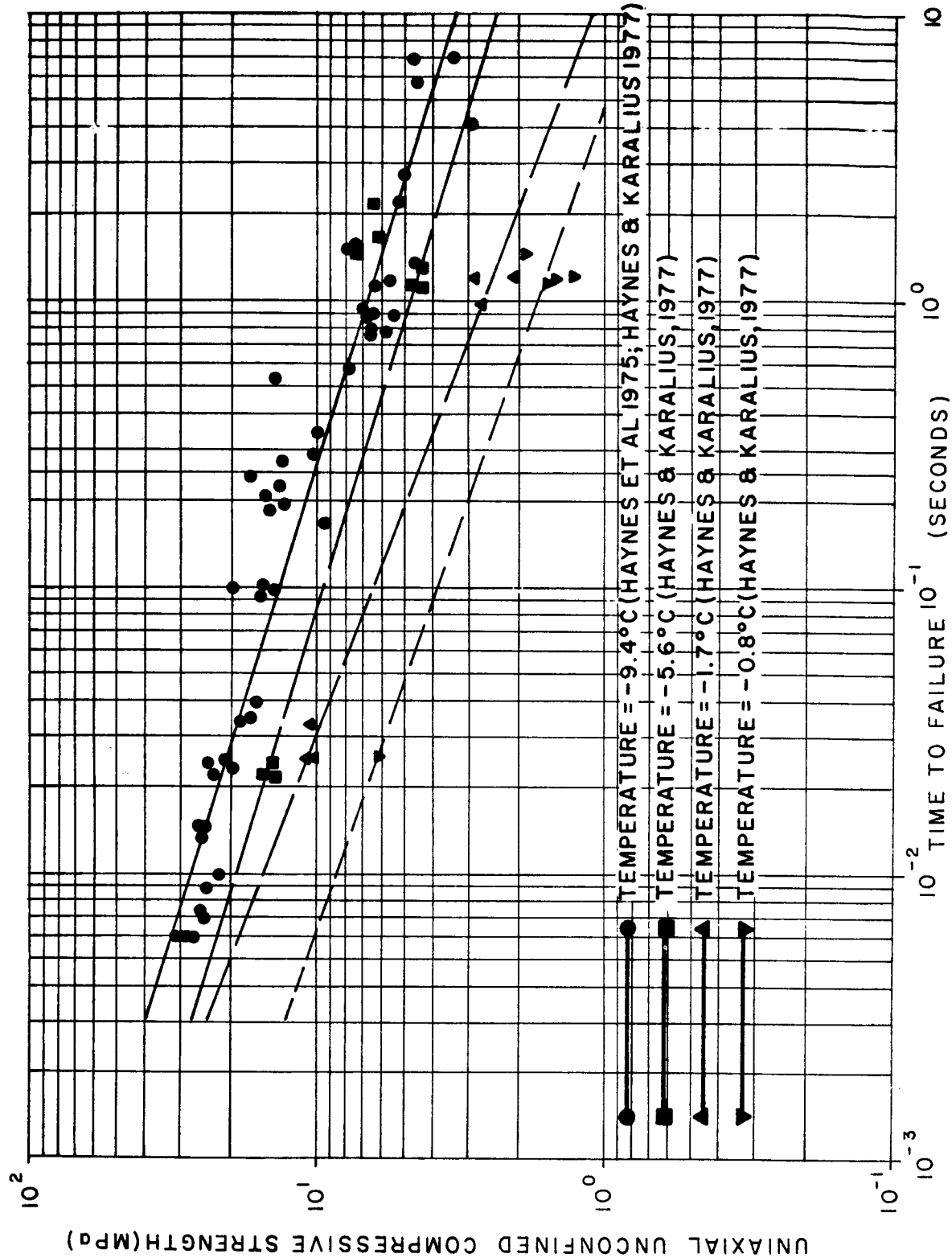

Figure 2.5
Relationship Between Compressive Strength and Time to Failure for Frozen Fairbanks Silt

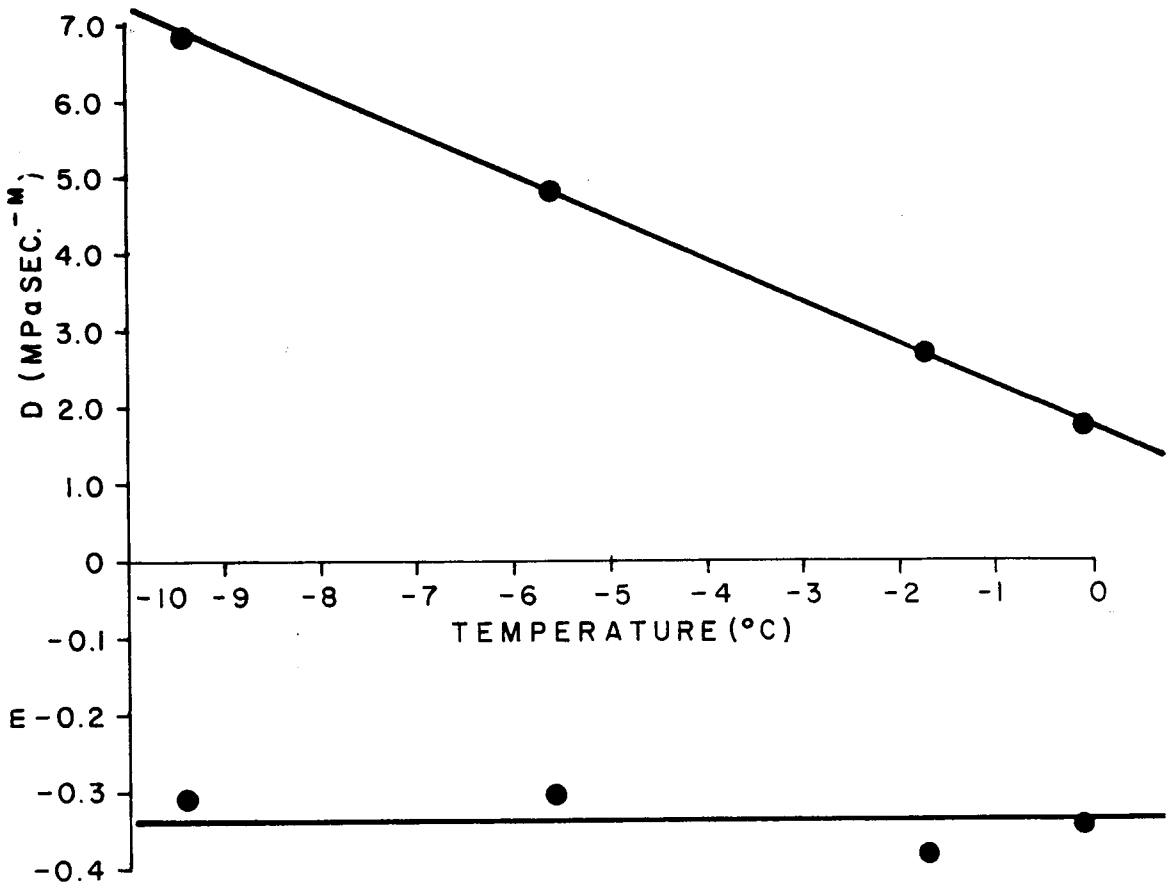

Figure 2.6

Variation of Parameters D and m for Frozen Fairbanks Silt

$$D = 1.7 + 0.545T \qquad \text{.....2.9}$$

where T is the temperature in centigrade degrees below 0 ^{o}C, and m = -0.34. Therefore, for frozen Fairbanks silt (bulk density = 1.83 Mg/m^3), Equation 2.8 becomes

$$\sigma_{cu} = (1.7 + 0.545T)\, t_f^{-0.34} \qquad \text{.....2.10}$$

Haynes and Karalius (1977) found that the compressive strength of polycrystalline ice is approximately 50-67 % greater than that of frozen Fairbanks silt. The results of Sayles (1973) indicate that the compressive strength of frozen Ottawa sand (bulk density = 2.00 Mg/m^3) may be as much as an order of magnitude greater than that of frozen Fairbanks silt. Finally, the results of Perkins and Ruedrich (1973) indicate that the compressive strength of Penn sand (bulk density = 2.07 Mg/m^3) is approximately 500 % greater than that of frozen Fairbanks silt. Thus, the parameters in Equation 2.9 may be approximated for polycrystalline ice, Ottawa sand and Penn sand.

CHAPTER 3

A REVIEW OF CURRENT PILING TECHNIQUES IN PERMAFROST

3.1 Geotechnical Problems Associated with Design and Construction of Pile Foundations in Permafrost

In frozen fine-grained soils, the volume of ice may be greater than that of the soil solids. Thawing of this ice can change a perennially frozen soil from a firm bearing material into a slurry with no supporting capacity.

Permafrost conditions at a site are often in a delicate state of thermal equilibrium, which renders permafrost a very difficult material on which to carry out construction without some thawing of the frozen soil. The situation is further aggravated by the impervious nature of the permafrost; rainfall and water from melting snow cannot drain into the ground, but instead forms pools and lakes. This induces a net increase of heat flux into the permafrost, thereby lowering the permafrost table. This is particularly important during the design life of a structure when a degrading thermal regime can reduce the effective pile embedment area and increase the downdrag loading on the piles.

During autumn the ground refreezes and in fine-grained soils piles may experience considerable uplift forces in the active layer. The heave is seldom uniform and differential movements may disrupt the foundation.

The occurence of ice in frozen soil also renders

permafrost a non-linear visco-elastic material. To this extent, the instantaneous strength is comparable to that of concrete, while the long-term strength is several orders of magnitude lower. This decrease in strength is associated with time dependent deformation behaviour.

Long term observations on polar glaciers and ice shelves suggest that the deformation behaviour of ice is characterised by undamped creep. This characteristic of ice strongly influences the stress-strain behaviour of frozen soils and due consideration must be given to this phenomenon in the design of pile foundations.

It should not be inferred that all permafrost soils present the above problems. Clean, coarse-grained materials rarely contain appreciable ice and this obviates frost heave and thaw consolidation and minimises time-dependent considerations. In fact, frozen granular materials usually provide a very competent foundation base.

3.2 A Review of Pile Types Used in Permafrost

3.2.1 Timber Piles

Timber piles are generally the least expensive pile type and have been used extensively in the permafrost areas of Canada. Local spruce and Douglas fir are the most common source of timber and are readily available in lengths from 6 to 15 m and diameters from 0.15 to 0.35 m. Timber piles must be protected in the active layer against deterioration and

decay. This is achieved using either a "brush-on" preservative or pressure creosoting techniques.

Timber piles offer favourable insulation and seismic properties and develop higher adfreeze bond strengths with permafrost than steel piles. The principle disadvantage of a timber pile is its comparatively low structural strength. To this extent, wooden piles cannot be driven and cannot be used to support large loads.

3.2.2 Steel Piles

Steel pipes and H piles are the most common pile type in Alaska and are now common in northern Canada. Drill stem, rails and hollow box sections are also used occasionally.

Steel piles must be protected against oxidation and corrosion in the active layer. This is easily achieved using a protective paint. Steel piles are usually more expensive than timber piles. Further, the adfreeze bond between steel and frozen soil is less than that between wood and frozen soil. However, this may be overcome by using a corrugated steel section.

The principle advantages of steel piles are that they can be driven into most types of warm permafrost (Davison et al. (1978)) and can support higher structural loads than timber piles.

3.2.3 Concrete Piles

In North America, economic considerations have led to a

preference for steel piles over concrete piles. However, precast, reinforced square and circular concrete piles are used extensively in the USSR where steel is a relatively expensive commodity. Concrete piles may be driven and can also support high loads. Further, the thermal properties of concrete render it a more favourable construction material than steel in permafrost regions.

The major concern with a concrete pile relates to its low tensile strength, which generally precludes its use in areas where substantial frost heave forces are allowed to develop on the pile in the active layer.

Cast-in-place piles have been used only occasionally in permafrost regions because of the strength and thermal problems associated with curing concrete in a cold environment.

3.2.4 Thermal Piles

Thermal piles consist essentially of one or more concentric steel pipes. They are most often used in areas of marginal permafrost where extra assurance of freezeback and/or maintenance of design adfreeze bond is needed.

These self-refrigerated piles remove the heat from the ground surrounding the embedded portion of the pile, and transfer it to the top of the pile, where the heat is dissipated to the atmosphere. Thermal piles of various designs are in use. The most common is the two phase system which operates on an evaporation and condensation cycle, in

which the pile is charged with propane, carbon dioxide or other suitable evaporative materials (Long (1963) and Long (1973)). The ground heat causes the fluid to evaporate, which in turn condenses in the upper, colder above-ground portion of the pile, thus effecting a heat transfer mechanism which functions only in the winter. Fixed radiation surfaces are commonly used above ground to facilitate heat transfer.

3.3 A Review of Pile Emplacement Methods in Permafrost

The following methods have been used to place piles in permafrost

1. Placement in a steam-thawed hole of diameter greater than the pile diameter.
2. Placement in a bored hole of diameter greater than the pile diameter.
3. Direct driving using an impact hammer.
4. Direct driving using a vibratory hammer.
5. Driving into steamed or bored holes of diameters less than the pile diameter.

Various combinations and modifications of the above have also been used.

3.3.1 Placement in a Steam-thawed, Oversized Hole

Prior to 1960, piles were traditionally installed in permafrost by prethawing an oversized hole using steam

points. The method is quick and cheap and has been successful when applied with knowledge and control. However, the consequences of the improper use of this method are very serious. Sanger (1969) has documented several instances when piles have failed as a result of poorly controlled steaming. Further, injection of steam into permafrost introduces large quantities of heat and water, which can increase considerably the time required for pile refreezing. Sanger (1969) recommends that "steamed" piles in warm permafrost should be placed one year in advance of building construction. Artificial refrigeration may be used to hasten freezeback, but this technique is expensive and hence is not particularly attractive.

Steam may be used for all shapes and types of piles, but in the past has most commonly been used in conjunction with timber piles. Steaming oversized holes is no longer recommended in warm permafrost. A more detailed account of this method is given by Sanger (1969).

In an attempt to obtain improved steaming control, and therefore reduce the amount of heat put into the permafrost, Goncharov (1964) proposed drilling a small pilot hole in advance of steaming. This method has proved successful in the USSR in frozen clays, silts and sands (Goncharov (1964)). However, it cannot be used in coarse-grained frozen soils.

A more recent modification to the steaming technique has been developed in the USSR (Porkhaev *et al.* (1977)). In

this method a hole is advanced using a "steam vibroleader", into which the pile is lightly driven. The steam vibroleader consists of a hollow tube with a cutting bit attached to its lower end to which steam is supplied. The steam thaws the frozen soil around the leader perimeter and then escapes to the surface through the interior of the leader. A vibratory pile driver, fixed to the upper section of the tube, forces the leader down into the thawed soil. In this way, thawing of the ground precedes the advance of the leader thereby minimising mechanical interaction between the cutting bit and the permafrost hence increasing the service life of the cutting bit.

Upon removal of the leader, the pile is driven into the thawed column of soil. The pile displaces the slurry thereby filling the annulus around the pile. This is a particularly attractive feature in winter when artificial slurry preparation is often very difficult. This method has been highly acclaimed in the USSR, where it has been applied with much success, even in gravelly and bouldery frozen soils.

3.3.2 Placement in a Bored Oversized Hole

In this method the pile is placed in a pre-bored oversized hole and the annulus around the pile is backfilled with a soil/water slurry. Sanger (1969) recommends a sand slurry of the following grading for an annulus greater than 12 mm

Sieve Size	% Finer by Weight
3/8"	100
#4	93-100
#10	70-100
#40	17-57
#200	0-17

and for an annulus less than 12 mm a water or silt/clay slurry is suggested.

Slurries are normally prepared in portable concrete mixers to the consistency of 0.15 m slump concrete, and placed in approximately one metre lifts around the pile and vibrated with a small diameter concrete spud vibrator. Sanger (1969) recommends that the temperature of the slurry should not be greater than 5 ^{0}C.

This method may be used for all shapes and types of piles and has been used extensively in all permafrost soil types but is particularly useful when site conditions do not permit driving or steaming.

3.3.3 Direct Driving Using Impact Hammers

If ground conditions permit, pile driving is the preferred installation method. The advantages of driving have been summarised by Davison et al. (1978) as

1. Minimal disturbance of soil physical and thermal regime during installation.
2. Construction speed during placement.

3. Immediate load support potential.

4. Placement under severe environmental conditions.

5. Minimization of discrete work operations.

6. Minimization of different trades involvement.

The low compressive strength of wood precludes the use of driven timber piles. Structural steel members of various sections have been driven in North America in a wide range of permafrost soils with the exception of very dense granular deposits. The most successful steel sections have been H and hollow pipe piles. Davison et al. (1978) recommend an H pile modified with angle pockets on either side of the web, for use in coarse-grained soils. Piles have been driven in permafrost using a wide range of impact driving equipment with rated hammer energies varying from 20 kJ to 54 kJ.

3.3.4 Vibratory Pile Driving

In this method, the pile is vibrated longitudinally at frequencies of up to 135 cps with an amplitude of 0.02 to 0.03 m. The vibrations are produced by rotating eccentric weights, whose horizontal components cancel one another, but whose vertical components are additive and are transmitted to the pile through a mechanical or hydraulic clamp. The net downward force on the pile is supplied by the dead weight of the machine and/or a crowd force from the driving mast.

The vibration generates frictional and exothermal heat at the pile/soil interface, thereby thawing the adjacent

soil and hence facilitating driving.

This method is best suited to piles of small cross-sectional area, i.e. H and open ended hollow pipe piles.

3.3.5 Driving into Undersized Holes

In order to expedite driving in difficult ground conditions a small diameter pilot hole may either be steamed or drilled. This also assists in maintaining correct pile alignment during driving. This method is frequently used in North America to drive steel H piles and is used extensively in the USSR to drive reinforced concrete piles. However, recently in the USSR attention has been given to the zone of thawed soil which is produced at the tip of large area piles during driving. This contained zone of thawed soil refreezes in a closed system, thus generating considerable upward pressure beneath the tip. In light of this problem, Sivanbaev and Kolesov (1976) recommend that such piles be allowed to stand for 4 to 5 months prior to loading.

3.3.6 An Overview of Pile Emplacement Methods

Pile installation techniques now utilize modern steaming, drilling or driving techniques and effectively minimise permafrost thermal disturbance. Installation methods are determined by ground temperatures, the type of soil, the required depth of embedment, the type of pile, and the difficulty and cost of mobilising the required equipment

and personnel at the site.

Pile driving is the preferred installation technique in frozen fine-grained warm permafrost soils. The effectiveness of pile driving is still not clearly defined in cold permafrost and coarse-grained frozen soils, particularly in relation to vibratory driving. At present in North America, frozen-in piles are considered the only reliable means of placing piles in these soils. However, the Soviets have recently developed a new pile installation tool that employs both steaming and vibratory driving techniques. Using this method piles have satisfactorily been driven in all types of frozen soils.

3.4 A Review of Design Techniques for Piles in Permafrost

The design of pile foundations in permafrost must satisfy both rheological and thermal considerations. The thermal aspect of pile design addresses the following issues

1. The design must guard against unacceptable changes in the ground thermal regime which may be imposed by the above-ground structure.
2. The design must guard against unacceptable changes in the ground thermal regime which may arise from heat conduction down the pile. Analytical solutions to this problem are given by Nees (1951) and Nixon (1978).
3. The time for freezeback of slurried piles must be determined. Closed-form solutions to this problem are

based on radial heat flow from an infinite composite cylinder (Scott (1956), Lee (1963) and Maksimov (1967)).

4. The design of thermo-piles requires a computer solution to the complex problem of transient, three-dimensional heat flow around a pile in permafrost. This problem has been addressed by Long (1963), Reid *et al.* (1975), Buchko *et al.* (1975), and Nixon (1978).

The rheological aspect of pile design ensures safety against gross failure or excessive settlement. A pile embedment depth is determined which can support the imposed loads on the pile under the worst loading conditions, unless suitable end-bearing in a competent material can be obtained.

The stresses acting on a pile in permafrost during winter and summer are shown in Figure 3.1. Wherever the pile is frozen to the soil the loads are transferred via the adfreeze bond. The adfreeze bond strength is a function of time, temperature, the roughness of the pile and the nature of the frozen soil at its interface. Load transfer in the thawed zone is effected via adhesion and friction.

In winter the pile must resist both frost heave and downdrag forces in the active layer. The magnitude of frost heave will depend upon the frost susceptibility of the soil and the availability of water.

Consideration of vertical equilibrium gives

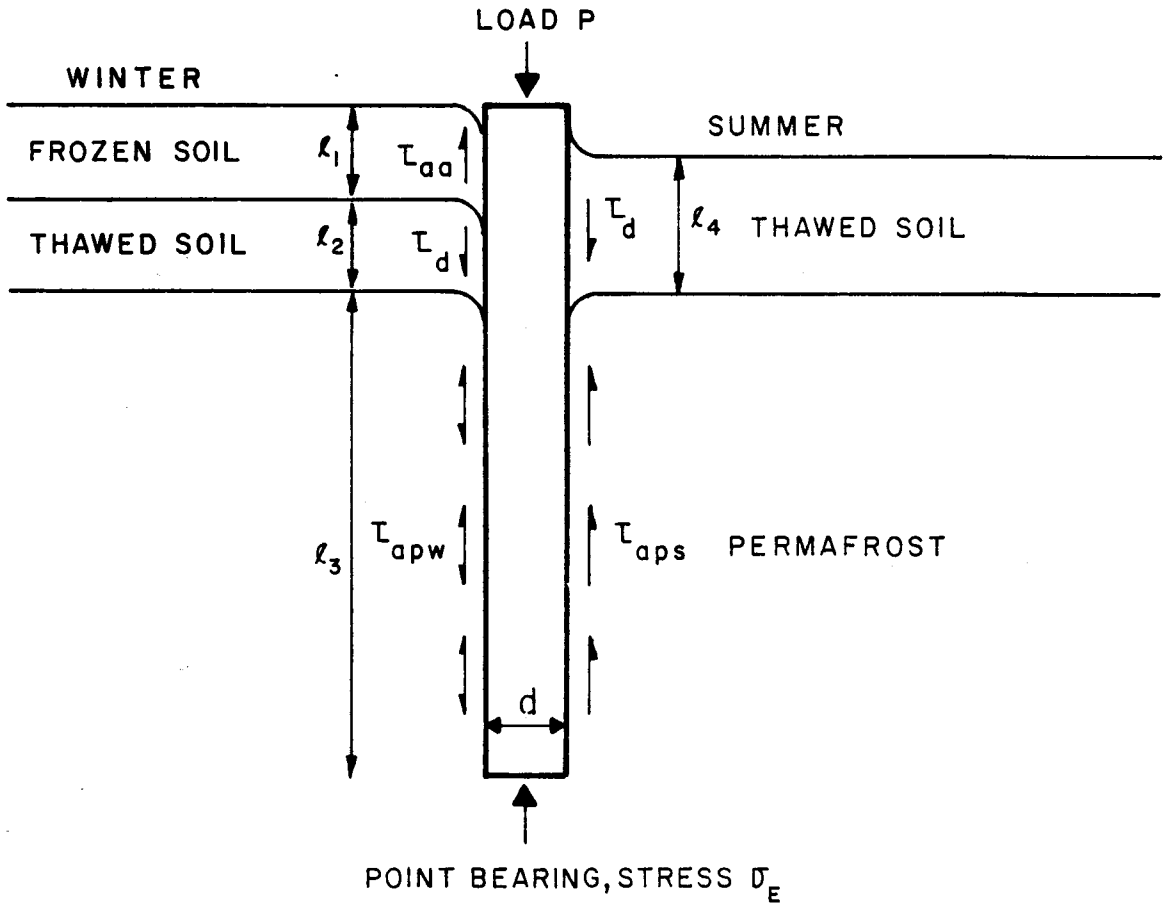

Figure 3.1
Stresses Acting on a Pile During Winter and Summer

$$(\tau_{aa} l_1 - \tau_d l_2 - \tau_{ap\omega} l_3)\pi d + \sigma_\epsilon \frac{\pi d^2}{4} - P = 0 \qquad \text{.....3.1}$$

The temperatures in the refreezing active layer are much colder than in the permafrost, consequently, the adfreeze strength in the active layer, τ_{aa} is much greater than that in the permafrost, τ_{ap} . Therefore, a design against frost-heave based on embedment area alone is usually impractical and designs usually employ passive measures to combat frost heave. One or more of the following techniques have been used

1. The adfreeze bond may be reduced in the active layer by isolating the pile in the active layer using an oil-wax grease.
2. The overall stability of the pile may be increased by either using a corrugated pile or grouting the pile into a firm bearing horizon.
3. The frost-susceptible soil around the pile in the active layer may be replaced with nonfrost-susceptible material.
4. The water table may be lowered.
5. The dead load on the pile may be increased.

If the problem of frost heave is obviated then equation 3.1 reduces to

$$(\tau_{ap\omega} l_3 - \tau_d l_2)\pi d + \sigma_\epsilon \frac{\pi d^2}{4} - P = 0 \qquad \text{.....3.2}$$

In summer the equation becomes

$$(\tau_{aps} l_3 - \tau_d l_4)\pi d + \sigma_c \frac{\pi d^2}{4} - P = 0 \qquad \text{.....3.3}$$

As mentioned at the outset pile failure can occur in the form of either gross disruption of the adfreeze bond or excessive settlement engendered by creep of the frozen soil. A design against adfreeze bond failure is based upon published adfreeze strength values and carried out for the worst loading conditions as defined by Equations 3.2 or 3.3. In ice-poor soils creep settlements are damped and the design focuses on allowable adfreeze strengths. However, ice-rich frozen soils display non-attenuating creep characteristics and Nixon and McRoberts (1976) have shown that for such soils, the design load is determined from consideration of tolerable creep settlements during the service life of the structure and not by allowable adfreeze strengths. They modeled the behaviour of a vertically loaded pile in a non-linear visco-elastic material and presented design curves based on limiting creep settlements for piles in ice and ice-rich permafrost.

The problem of laterally loaded piles in permafrost has been addressed by Ladanyi (1972a) who proposed a design based on the analysis of an expanding cylindrical cavity.

The problem of vibratory loaded piles is still largely undefined and, as yet, no rational analytical basis for design has been presented. The problem is circumvented by

employing vibration dampers to isolate the foundation from the vibration source. Additional precautions are usually taken to ensure that the imposed vibrations do not cause resonance in the pile.

3.4.1 Current Pile Design Philosophies in North America

At present there are no standards for the design and construction of pile foundations in permafrost in North America. In 1971 the U.S. Army/Air Force released a preliminary draft proposing guidelines for foundation design in permafrost (U.S.Army /Airforce (1967)). However, this is still under review and at this time has not yet been publicly released.

The choice of pile type and implementation method for small-scale piling operations is usually dictated by the availability of local materials and equipment. However, economic considerations on large-scale piling projects usually justify the use of a comprehensive field investigation to determine the most suitable construction procedures. Such investigations often include both sub-surface logging and pile load test programs. In this way, Alyeska Pipeline determined that a frozen-in steel pile would be the most suitable pile for the trans-Alaska pipeline.

The thermal aspect of design is normally undertaken using the procedures, outlined in the previous section. The problem of frost-heave is usually obviated by use of

suitable passive techniques also outlined in the previous section. Therefore, the rheological aspect of design reduces to determining an allowable load which satisfies both frozen soil strength and deformation considerations.

In the past the phenomenon of pile creep in frozen soils was not recognized as a major geotechnical concern and hence pile design was based on adfreeze bond strengths. Adfreeze strengths for very rough piles (i.e. wood or corrugated steel piles) approach the shear strengths of the frozen soils. However, the adfreeze strengths of smooth piles are strongly influenced by the presence of ice at the pile interface and therefore, by the method of installation. At present there is no comprehensive set of guidelines which gives recommended adfreeze strength values for various pile configurations. The selection of adfreeze strength is left to the discretion of the engineer.

Current design methodology recognises the importance of pile creep in ice-rich soils and so advocates a "limiting deformation" based design. Such designs are based either on predicted deformation behaviour as obtained from analysis or, on the results of long-term pile load tests. Nixon and McRoberts(1976) have proposed a design approach for ice-rich soils, based on the flow law of ice. The design of piles for the Trans-Alaska pipeline was based on field pile creep tests (Morgenstern (1978)).

In summary, there appears to be general agreement that pile design in ice-rich soils should be based on limiting

creep deformations and in ice-poor soils should be based on allowable adfreeze strengths. However, at this time there have been no attempts to define the range of applicability of either of these designs. Pile design in semi-ice-poor/ice-rich soils is, therefore, left to the discretion of the design engineer.

3.4.2 Current Pile Design Philosophies in the USSR

Pile design in the USSR is based upon two design codes entitled SNiP II-B 6-66 and RSN 41-72. A summary of these codes is presented in a recent National Research Council of Canada Technical Translation (National Research Council of Canada (1976)).

The intent of the codes is not to provide the definitive word on pile design, but rather to recommend a rational systematic framework in which design can be carried out. In this way, the codes encourage the use of supportive field and laboratory test programs, especially in areas of difficult sub-soil conditions. The codes are based both upon a very impressive collection of field and laboratory data and experience accumulated over the last fifty years.

The thermal aspect of pile design is similar to that used in North America.

The rheological aspect of design involves the determination of pile bearing capacity and is based both upon adfreeze and end-bearing support. The allowable adfreeze bond strength is defined to be the maximum adfreeze

stress which does not generate secondary creep at the pile-soil interface. In this way, the pile time-dependent deformations are limited to primary creep. This type of approach generally precludes excessive creep settlements. However, if structure settlement tolerances are critical then the code recommends the use of field pile tests to quantify expected settlements.

The procedure for selecting an allowable adfreeze strength is very thorough and conveys a considerable understanding as to pile load transfer mechanisms. Allowable adfreeze bond strengths are presented in Table 14(5), page 5-14 in NRCC TT-1865(1976) and have been included in Figure 5.1 of this thesis for comparison with North American data. It should be remembered that the values contain an inherent factor of safety.

The procedure for selection of allowable end-bearing support is also impressive. Details of this procedure are described on pages 5-5 to 5-44 (NRCC,1976). Briefly, the end-bearing support is determined from the long-term compressive strength of the material. This approach can be extended to account for the case of ice buried at some depth below the pile tip. The potential for steamed and frozen-in piles to heave during freeze-back exists and so the code recommends that no end-bearing contribution be allowed for these piles. Further, end-bearing is ignored if the pile tip is founded directly on ice.

Design against frost-heave is based on adfreeze

strength considerations and is explained in detail on pages 5-58 to 5-69 (NRCC,1976). Briefly, frost heave is ignored if the composition of the active layer contains less than 30 % by weight of particles less than 0.1 mm. For fine-grained soils with favourable ground water conditions, the adfreeze strength in the active layer is assumed to be 60 to 80 kPa. If ground water conditions are unfavourable then it is recommended that the adfreeze strength in the active layer be determined from field tests.

Much of northern USSR is unglaciated and large amounts of sub-surface ice are uncommon. Consequently, the codes are oriented towards design in ice-poor frozen soils. More recently, however, increased development along the Arctic coast where ground ice is more extensive has stimulated Soviet interest in pile design in ice-rich frozen soils. Vialov (1973) and Eroshenko and Fedoseev (1976) acknowledge this deficiency in the Soviet Design Codes and recommend the use of pile load tests to determine the bearing capacity of piles in these soils. Eroshenko and Fedoseev (1976) proposed modifications to the design recommendations in SNiP II-B 6-66 to account for segregated ice within the permafrost. However, no definitive statement has been issued, concerning the predicted creep behaviour of piles in these soils.

CHAPTER 4

LABORATORY STUDIES OF PILE-LOAD TRANSFER MECHANISMS

4.1 Test Objectives

Pile creep in frozen soils has been predicted using a simple shear analytical model (Johnston and Ladanyi(1972) and Nixon and McRoberts(1976)). This analysis implicitly assumes that there is no slip at the pile/soil interface. However, this assumption has never been verified. The accuracy of these predictions is further restricted by the lack of good reliable constitutive relationships. The objectives of this study were as follows

1. To elucidate the load transfer mechanisms between a pile and various frozen soils and in particular to determine the creep characteristics of the adfreeze bond.
2. To study the influence of frozen bulk density on the creep of frozen soil.
3. To determine the influence of pile roughness on the creep characteristics of the adfreeze bond.
4. To evaluate the effect of stress history on the creep of frozen soils.
5. To determine the influence on load transfer mechanisms, of varying normal loads on the lateral surface of the pile.

The above issues were explored using a simple shear apparatus.

4.2 Test Materials

The issues investigated in this study were not unique to any one particular soil type but were applicable to all forms of frozen soil. In this regard, three classes of frozen soils were selected as representative of the majority of soil types encountered in permafrost areas. These materials were frozen concrete sand, frozen Devon silt and polycrystalline ice.

The grain-size curves for the concrete sand and Devon silt are presented in Figures 4.1 and 4.2. The specific gravity of the Devon silt was 2.75 and the plastic and liquid limits were 21 % and 46 %, respectively.

The maximum and minimum dry densities of the concrete sand were determined to be 1.44 and 1.92 Mg/m^3, respectively.

4.3 Description of the Apparatus

Three identical sets of apparatus were constructed to permit simultaneous testing of the three different frozen materials. Each set consisted of a loading frame, five linear voltage displacement transducers (LVDTs), one thermistor, and two aluminum plates, 20.3 cm by 7.6 cm.

A frozen soil sample (20.3 cm by 7.6 cm by 10 cm high) was sandwiched between each pair of plates. The lower plate was held in an encastre position and the upper plate was subjected to both constant horizontal shear and vertical

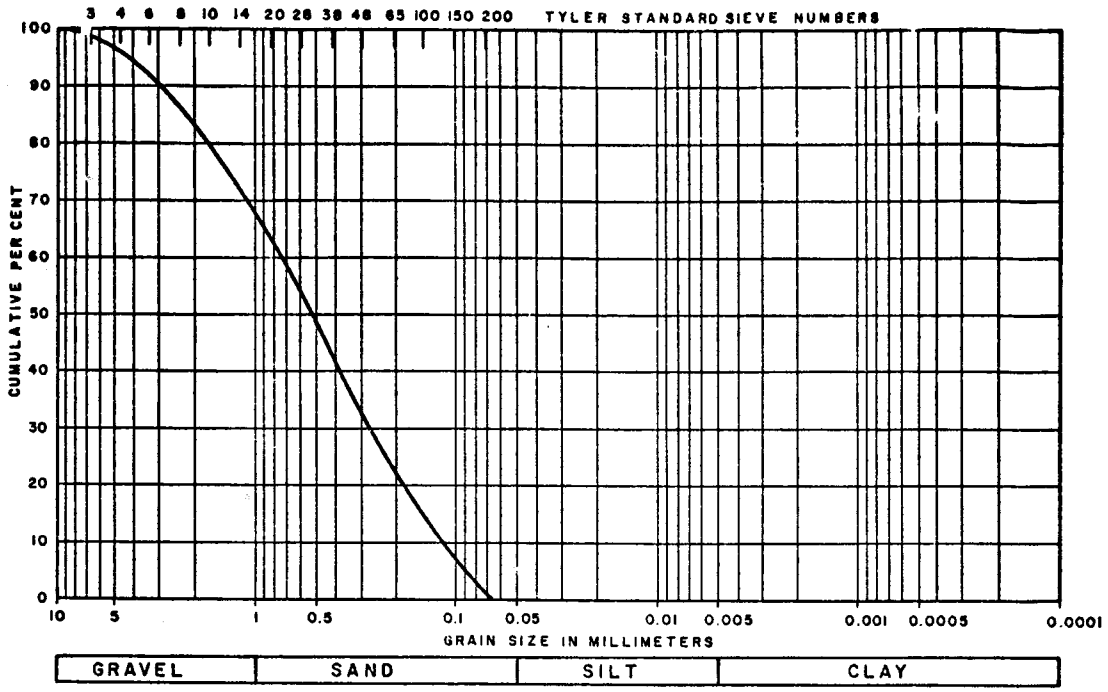

Figure 4.1 Grain Size Distribution Diagram for Concrete Sand

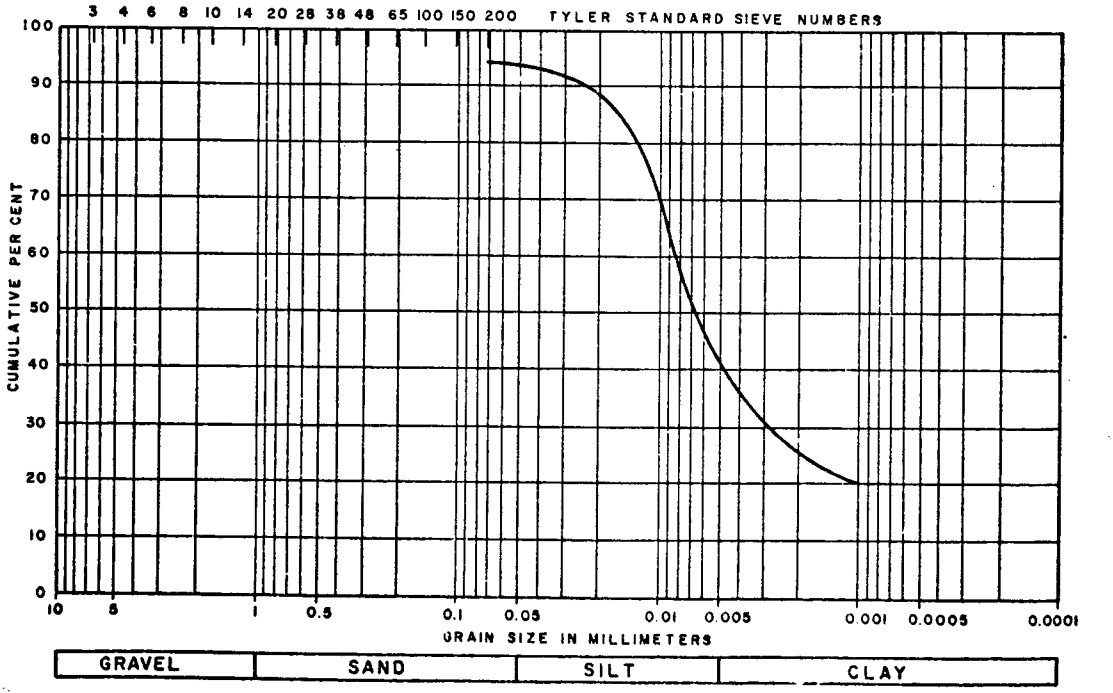

Figure 4.2 Grain Size Distribution Diagram for Devon Silt

normal loadings. Horizontal creep displacements of the upper plate and the frozen soil at intermediate points between the plates were monitored in the direction of applied shear. Vertical creep displacements of the upper plate were monitored in the direction of normal loading. Hewlett Packard 24 DCDT LVDTs monitored deformations to an accuracy exceeding 0.0001 cm.

Normal loads were applied via a direct hanging system to which weights were added. Shear loads were applied via an adjustable pulley system to which weights were added. Photographs of the apparatus are presented in Figures 4.3 and 4.4.

The three creep cells were located inside a controlled environment laboratory where ambient temperatures were maintained between -2 ^{0}C and -3 ^{0}C. Sample temperature fluctuations were further reduced by enclosing the apparatus in a large insulated box and circulating ethylene glycol from a constant-temperature bath through pipes in the plates. This technique reduced short-term temperature fluctuations to ±0.5 ^{0}C. Sample temperatures were monitored directly by freezing a thermistor into a pre-drilled hole at the centre of each sample. The thermistors were calibrated at the outset and on completion of the test program to an accuracy of ±0.01 ^{0}C, using a ±0.001 ^{0}C quartz thermometer.

Output signals from the LVDTs and thermistors were monitored and recorded at 6 hour intervals using a data acquisition system. Information obtained included a record

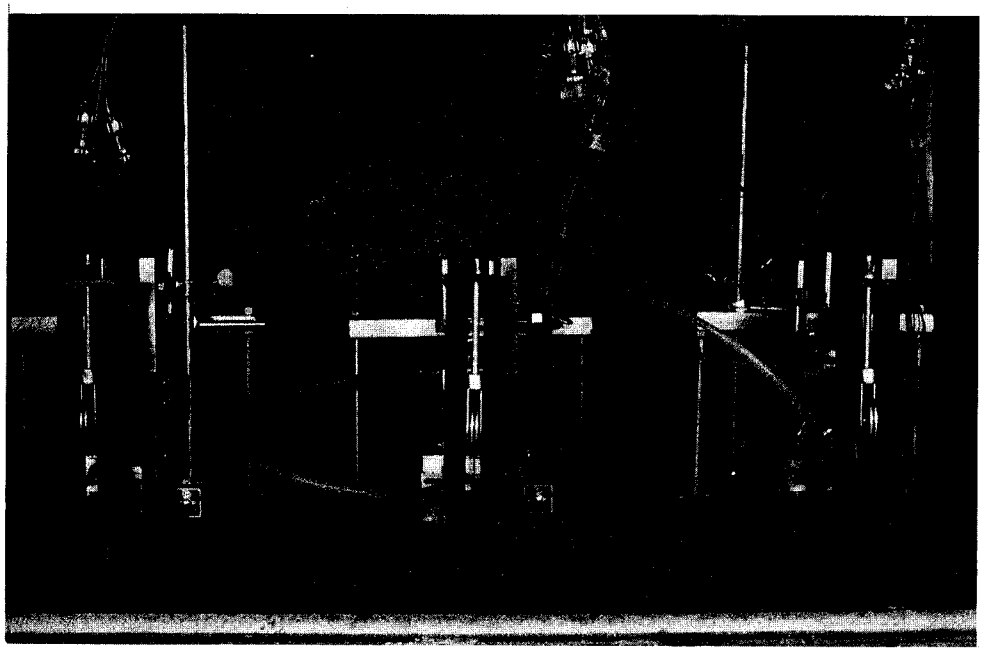

Figure 4.3 Simple Shear Apparatus

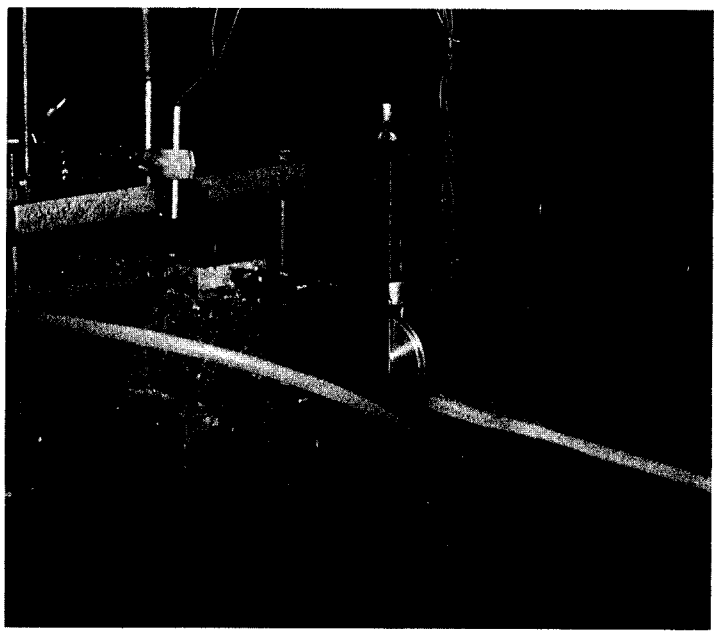

Figure 4.4 Simple Shear Apparatus

of vertical and horizontal deformations and temperature. A schematic layout of the apparatus is presented in Figure 4.5.

Preliminary tests indicated that the horizontal shear strain was approximately constant throughout the sample. Thus, in the test program, horizontal soil displacements were monitored 5 mm below the upper plate and 5 mm above the lower plate. In the ensuing analysis it was assumed that the shear strain rate was constant between these points.

An integral part of this study was the investigation of the influence of plate roughness on the creep characteristics of the adfreeze bond. In this regard, three plates of different roughnesses were tested. Roughness is conveniently quantified using centre-line averages. The centre line average (CLA) is defined as the average distance from peaks to valleys on the material surface. CLA values for the three plates were 2.5μm, 125.0μm and 5.0 mm. The roughness of the lower plate was 5.0 mm for all the tests.

4.4 Material Preparation

4.4.1 Polycrystalline Ice

It was desirable to test fine-grained (grain size, 1 to 2 mm), homogeneous, isotropic, air-free, polycrystalline ice (Glen (1955)).

Hoar-frost was collected from the pipes of a cold chamber and sieved in the ice laboratory. Ice crystals passing a number 8 sieve, but retained by a number 16 sieve

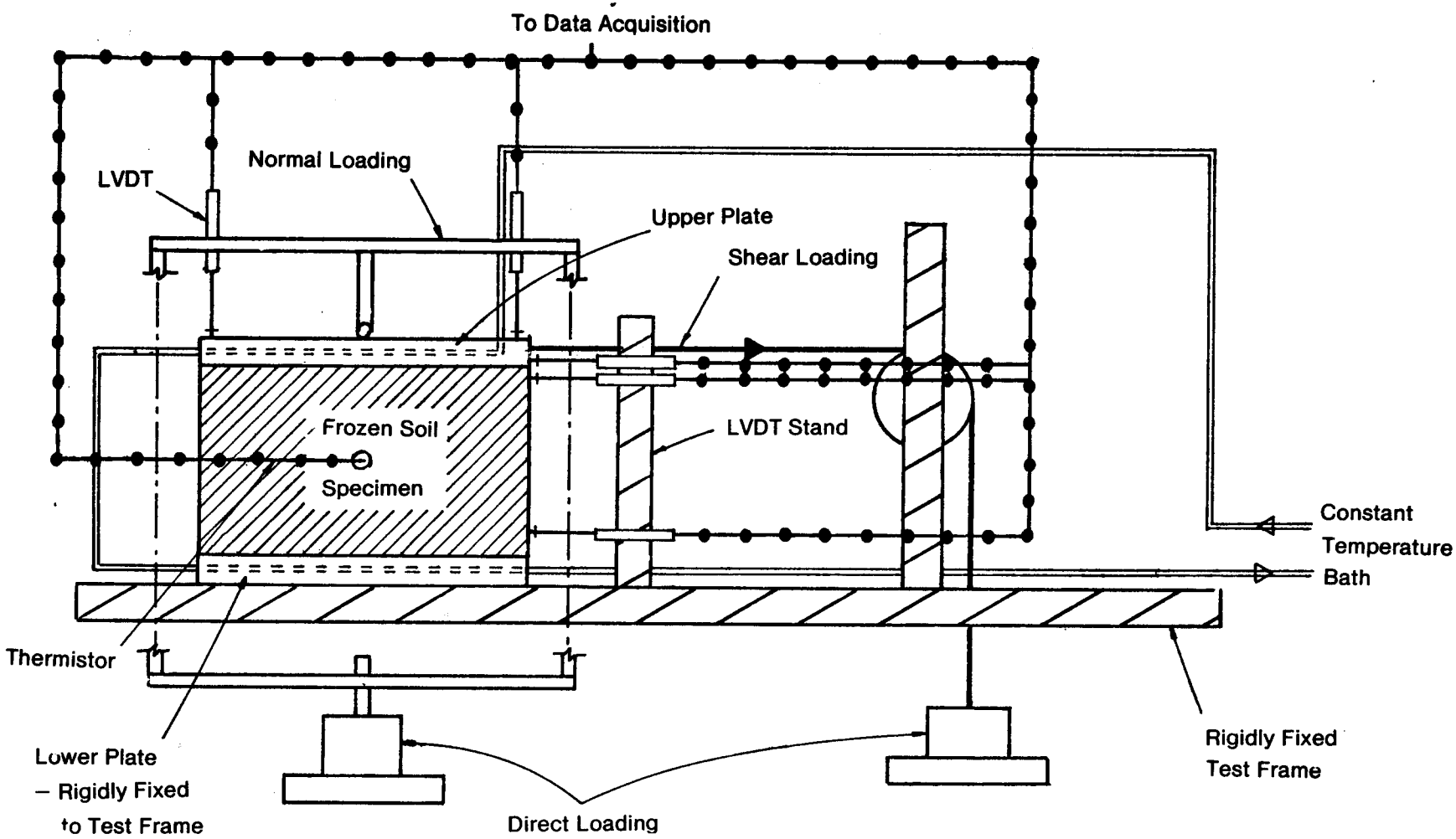

Figure 4.5
Schematic Layout of Simple Shear Experiments.

were loosely placed in a prechilled (-5 ^{0}C) P.V.C. mould having a diameter of 25 cm and a height of 30 cm. Air-free, double distilled water prechilled to 0 ^{0}C, was then introduced into the mould via the bottom aluminum plate under a vacuum of 62 cm of mercury. Upon completion of saturation the vacuum was released and the top plate was removed. The sample was frozen unidirectionally by placing the bottom plate on dry ice and surrounding the P.V.C. walls of the mould with zonolite insulation.

Specimens prepared in this way were slightly cloudy, probably because of air bubbles within the original ice crystals, however their densities were similar to that of clear ice.

Thin sections were prepared from the ice specimen (Glen (1955)) and viewed between crossed polaroids. It was observed that the peripheral 5 cm of the sample consisted of preferentially oriented crystals. However, the crystals in the remainder of the sample were randomly oriented, uniform and typically 2 mm in size.

4.4.2 Frozen Sand

Prechilled (-5 ^{0}C) concrete sand was placed loosely inside a prechilled (-5 ^{0}C) cylindrical P.V.C. mould having a diameter of 15 cm and a height of 22.5 cm. Air-free double distilled water prechilled to 0 ^{0}C was then introduced into the mould via the bottom plate under a vacuum of 60 cm of mercury. Upon completion of saturation, the vacuum was

released and the top plate was removed. To ensure sample uniformity the mould was subjected to a nominal vibration. The sample was then frozen unidirectionally by placing the bottom aluminum plate on dry ice and surrounding the walls of the P.V.C. mould with zonolite insulation.

Specimens prepared in this way possessed uniform moisture contents of approximately 17 %, frozen bulk densities of approximately 2.05 Mg/m^3 and degrees of saturation of approximately 98 %.

4.4.3 Frozen Silt

Frozen Devon silt specimens were prepared at three different moisture contents and are referred to as Silt 1, Silt 2 and Silt 3.

4.4.3.1 Preparation of Silt 1

Devon silt was mixed with distilled water to produce a slurry of moisture content approximately 70 %. The slurry was placed in a vacuum flask and a vacuum of 60 cm of mercury was applied while the flask was simultaneously vibrated on a vibrating table. This procedure was continued until the sample was de-aired.

The slurry was then poured into a cylindrical P.V.C. mould having a diameter of 15.0 cm and a height of 40.0 cm. The bottom aluminum plate of the mould incorporated a drainage outlet, over which was placed a porous stone and two filter papers. Two additional filter papers and one

additional porous stone were carefully placed on top of the slurry. Uniaxial loading was applied to the sample, taking care not to cause extrusion of the slurry around the upper porous stone. Loads were applied incrementally, up to a maximum consolidation pressure of 225 kPa and the sample was consolidated under two-way drainage conditions.

Upon completion of primary consolidation, the sample was unloaded and allowed to attain stress equilibrium under atmospheric conditions. The sample was then transferred to a controlled temperature environment and allowed to equilibrate to a temperature of +1 ^{0}C; thereafter, the sample was frozen unidirectionally by placing the bottom aluminum plate of the mould on dry ice and surrounding the walls of the P.V.C. pipe with zonolite insulation. Samples prepared in this way were completely frozen within 24 hours and produced a uniform silt having a frozen bulk density of 1.9 ±0.05 Mg/m^{3}. Hairline ice lenses were observed throughout the samples.

4.4.3.2 Preparation of Silt 2

A de-aired slurry having a moisture content of 70 % was prepared in the same way as described for Silt 1. The slurry was then prechilled to +1.0 ^{0}C and then poured into a prechilled (+1.0 ^{0}C) P.V.C. mould. The slurry was then frozen unidirectionally by placing the lower aluminum plate of the mould on top of dry ice and surrounding the walls of the P.V.C. pipe with zonolite insulation.

Samples prepared in this way were frozen within 24 hours and produced a uniform frozen silt having a frozen bulk density of 1.5 ±0.1 Mg/m^3. Hairline ice lenses were observed throughout the samples.

4.4.3.3 Preparation of Silt 3

Prechilled (-5 ^0C) Devon silt was mixed with ice crystals and prepared in the same way as described for polycrystalline ice.

Samples prepared in this way consisted of a silty ice having a bulk density of 0.95 Mg/m^3.

4.5 Sample Preparation

The preparation was identical for all frozen soil samples.

The cylindrical specimen was removed from the P.V.C. mould and trimmed in the ice laboratory on a milling machine. The finished sample was 20.3 cm long by 7.6 cm wide by 10.0 cm high. The two aluminum test plates were cleaned and thoroughly rinsed in distilled water, and frozen to the top and bottom of the specimen. A thin coating of water droplets was sprayed onto the four exposed faces of the sample, and a moist sheet of Saran Wrap was wrapped around the entire sample to effect an air-tight seal to reduce desiccation of the sample during testing.

The shafts of two 2.54 cm long flat-head nails were frozen into two predrilled horizontal holes. The nails were located 5 mm above the bottom plate. They provided a stable monitoring datum, against which the two LVDTs were to be placed. The exact position of the two nails and the upper plate with respect to the lower plate were recorded.

A thermistor was frozen into a predrilled 2.5 mm diameter hole which extended to the centre of the sample.

The sample was then assembled within the loading frame and placed within the insulated test housing unit. Hoses from the constant temperature bath were cornected to swagelock fittings on the two plates and ethylene glycol was circulated through the pipes in the plates. Two LVDTs were positioned vertically, at either end of the top plate and three LVDTs were positioned horizontally, against the two nails and the upper plate. The "shear loading" pulley was adjusted to impart horizontal shear loading to the top plate and the normal loading hanger was assembled around the sample.

The three apparatuses were positioned beside one another within the insulated housing unit and allowed to stand for either 48 hours or until thermal equilibrium was attained within the samples.

Normal loading and then shear loading were applied insta taneously.

4.6 Analysis of Results

4.6.1 Stress Distribution Within a Simple Shear Apparatus

The non-uniform stress conditions which develop within simple shear test specimens complicated interpretation of the test results. Both the linear stress analysis performed by Roscoe (1953) and the non-linear finite element analysis, described by Duncan and Dunlop (1969) show that the stress nonformities in simple shear are most severe near the ends of the specimen.

Simple shear differs from pure shear by the absence of complimentary shear stresses at the ends of the sample. The magnitudes of shear stresses on planes parallel to the ends increase toward the centre, however, and stresses in the centre of the specimen correspond closely to pure shear (Duncan and Dunlop (1969)). For the purpose of this study, it suffices to approximate non-uniform simple shear stress conditions by uniform pure shear stress conditions hence simplifying interpretation of the results.

The average values of shear and normal stress on any horizontal plane may be calculated from equilibrium considerations. It is convenient to analyse shear and normal loading separately and then superimpose the results to yield the stress distribution for the combined loading configuration. In this testing program, the boundary condition along the lower plate is one of zero displacement and, as such, the lower face of the specimen is considered

encastré. This is shown in Figure 4.6.

Normal loading produces a constant uniform vertical stress distribution throughout the height of the sample (Figure 4.7). Uniform horizontal shear loading on the upper plate yields a constant shear stress distribution with depth and a bending moment about the horizontal that increases uniformly with increasing distance from the top plate. The bending moment on any horizontal plane is conveniently represented by a triangular normal stress distribution on that plane. The normal stress varies from 0 at the top plate to $-6Th/l^2$ at the left hand corner of the lower plate and $6Th/l^2$ at the right hand corner of the bottom plate (Figure 4.8). The variation of normal stress, σ_y , in the y-direction, is described by the relation

$$\sigma_y = \frac{6T}{l^2 A}(h-y)(2x-l) + \frac{P}{A} \qquad \text{.....4.1}$$

The shear stress, τ_x , in the x-direction is independent of co-ordinates. Thus,

$$\tau_x = \frac{T}{A} \qquad \text{.....4.2}$$

The creep behaviour of ice is markedly different under tensile and compressive loading (Voitkovskii (1960)). Therefore, it is desirable to eliminate tensile forces in the y-direction. This condition is satisfied if

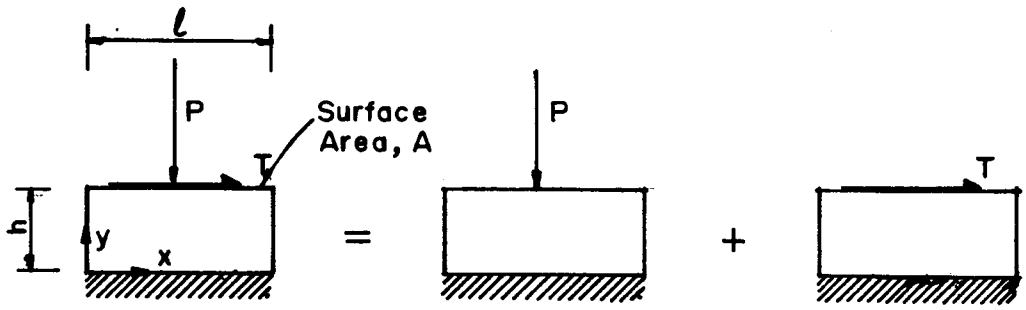

Figure 4.6
Superposition of Normal and Shear Loading in Simple Shear

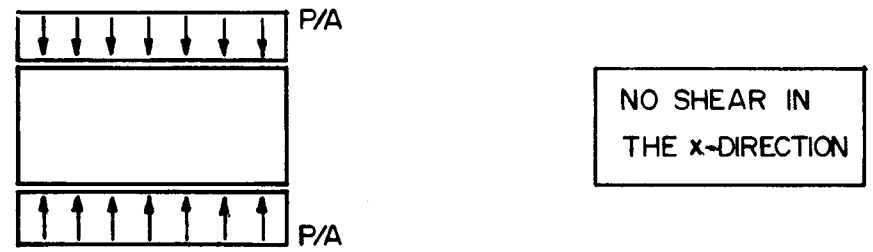

a) Normal stresses in the y - direction

b) Shear stresses in the x - direction

Figure 4.7
Stresses Arising from Normal Loading

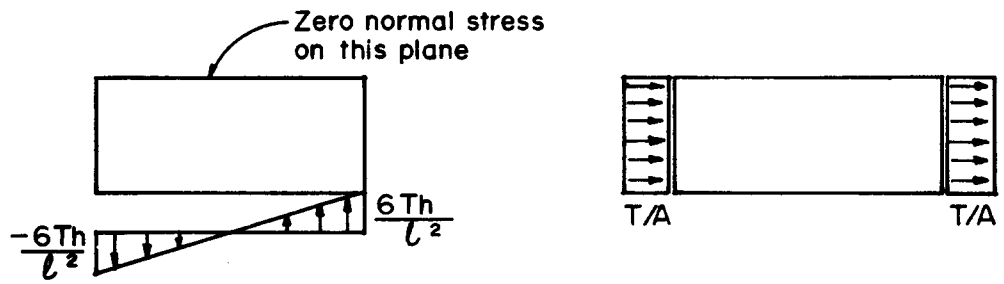

a) Normal stresses in the y - direction

b) Shear stresses in the x - direction

Figure 4.8
Stresses Arising from Shear Loading

$$P \geq \frac{6Th}{\ell} \qquad \text{.....4.3}$$

In this study, h/l = 0.5 and Equation 4.3 reduces to

$$P \geq 3T \qquad \text{.....4.4}$$

4.6.2 Presentation of Results

Displacement and temperature data were entered into the computer at six-hour intervals and data reduction and data plotting were executed with the aid of the computer.

Chronological plots were presented for temperature, applied normal and shear stresses, horizontal shear strain, horizontal shear strain rate, vertical normal strain and vertical normal strain rate.

Horizontal shear strains relative to the lower nail were computed for both the upper nail and the upper plate. The vertical normal strain was defined to be the average vertical displacement of the upper plate, divided by the distance between the upper and lower plates. Shear strain rates of the upper nail and normal strain rates of the upper plate were computed using a five-point moving average procedure. This technique smoothed the experimental data, thus rendering the curves more amenable to analysis.

4.6.3 Discussion of Results

The test program comprised of seven series of tests.

Each series consisted of isothermal, isochronal creep tests on three artificially frozen soils.

The intent of test series 1 was to study the influence of varying shear stresses on the observed shear strain rate for frozen sand, silt 2 and polycrystalline ice.

The intent of test series 2 was to study the influence of normal stress on the observed shear strain rate for frozen sand, silt 2 and polycrystalline ice.

The objectives of test series 3, 4 and 5 were to study the influence of frozen bulk density on the observed creep behaviour of frozen silt.

Finally, the intent of test series 6 and 7 was to evaluate the effect of plate roughness on the observed creep of the adfreeze bond for frozen sand, silt 1 and polycrystalline ice.

The results are shown in graphic form in Figures B.1 to B.27. A summary of the data is presented in Table 4.1.

The data are conveniently examined under the following sub-sections.

4.6.3.1 Influence of Plate Roughness on the Load Transfer Mechanism

Inspection of Figures B.1 to B.5 demonstrates that for shear stresses less than 25.0 kPa there is no slipping between the very rough aluminum plates (CLA = 5 mm) and the frozen soil specimens. Adfreeze bond failure, under suppressed dilatancy conditions, is characterized by

Test Series	Soil Type	Frozen Bulk Density (Mg/m^3)	Average Temperature (°C)	Upper Plate Roughness (mm)	Shear Stress (kPa)	Shear Strain Rate (Yr^{-1})	Normal Stress (kPa)	Normal Strain Rate (Yr^{-1})
1	Ice	0.901	-0.92	5	17.8	0.0162	57.0	<0.0157
					25.0	0.0317		0.0131
					17.8	0.0166		0.0187
	Silt2	1.59	-0.89	5	17.8	0.0030	57.0	<0.0003
					25.0	<0.0033		0
					17.8	0		0
	Sand	2.03	-0.92	5	17.8	0.0053	57.0	0.0073
					25.0	<0.036		<0.0131
					17.8	0		0.0012
2	Ice	0.900	-0.78	5	17.8	0.0126	57.0	0.026
						0.0136	75.0	<0.076
						0.0127	100.0	0.123
	Silt2	1.54	-0.80	5	17.8	<0.0017	57.0	0.0027
						0	75.0	<0.0092
						0	100.0	<0.0020
	Sand	2.05	-0.80	5	17.8	0.0095	57.0	0.011
						0.0084	75.0	<0.058
						0.0061	100.0	<0.095
3	Silt1	1.76	-0.92	5	17.8	<0.0011	57.0	<0.0068
	Silt2	1.42	-0.85	5	17.8	<0.0008	57.0	<0.002
	Silt3	0.96	-0.92	5	17.8	<0.0179	57.0	<0.012
4	Silt2	1.42	-0.83	5	17.8	<0.0023	57.0	0.0018
	Silt3	0.96	-0.92	5	17.8	<0.021	57.0	<0.017
5	Silt1	1.85	-0.94	5	17.8	<0.0081	57.0	<0.014
	Silt2	1.42	-0.86	5	17.8	0.0012	57.0	0.0022
	Silt3	0.96	-0.93	5	17.8	0.019	57.0	0.014
6	Ice	0.89	-0.78	0.0025	6.0	failed	57.0	0.048
	Silt1	1.89	-0.79	0.0025	17.8	0.021	57.0	0.024
	Sand	2.05	-0.85	0.0025	17.8	0.03	57.0	<0.042
7	Ice	0.89	-0.80	0.0125	9.7	0.0066	57.0	0.017
					13.5	<0.066		unsteady
					17.8	<0.046		0.016
					21.3	0.033		0.016
	Silt1	1.89	-0.81	0.0025	17.8	<0.012	57.0	<0.018
					21.3	0.022		<0.014
	Sand	2.05	-0.83	0.0025	17.8	<0.0091	57.0	<0.011

Table 4.1 Summary of Laboratory Test Data

shearing along frozen soil-frozen soil interfaces. Thus, the adfreeze bond strength is expected to be comparable to the shear strength of the frozen soil.

The load transfer mechanisms for smooth (CLA less than 2.5 μm) plates are complex. It has been hypothesised that a continuous liquid-like layer exists on the surface or internal boundaries of ice (Barnes et al. (1971)). The theoretical work of Fletcher (1968) indicates that for temperatures above -5 ^{0}C, clear ice crystals may be covered by a quasi-liquid film whose thickness is of the order of 1 to 4 nm. The thickness of this film increases as the temperature approaches 0 ^{0}C.

The significance of this quasi-liquid film on the adhesive properties of ice has been addressed by Jellinek (1959) . He observed that the adhesive bonds of ice to polished stainless steel plates were much greater in tension than in shear, and this, he argued, could be attributed to a quasi-liquid film at the plate-ice interface. Jellinek assumed the liquid-like layer to be a Newtonian liquid of viscosity, η , and proposed the following relationship between the velocity of the top plate, v_t , the shear stress, τ_t, at any time, t, and the thickness of the viscous film, L

$$v_t = \eta \frac{\tau_t}{L} \qquad \text{.....4.5}$$

The parameters, η and L are not known experimentally. However, Jellinek determined an upper bound for L to be 20 nm at -5 ^{0}C.

In this study, the asperities on the smoothest plates were measured to be 2.5μm. Therefore, a single asperity was at least ten orders of magnitude larger than the thickness of the proposed quasi-liquid film. Therefore, if the interface were completely air-free, the viscous film would follow the contours of the asperities and, under conditions of suppressed dilatancy, shear failure would be forced through the inter-asperital ice (see Figure 4.9a). However, inspection of Figure B.20 reveals that the adfreeze bond between ice and a plate of roughness 2.5μm failed at a stress of 6.0 kPa. This is inconsistent with the above model. Clearly, the shear plane is not being forced through inter-asperital pore ice. This suggests that the asperital pores are either filled with air or supercooled water. Thermodynamic considerations cannot account for the existence of such a large body of supercooled water at -1 ^{0}C. Moreover, it is highly probable that during sample preparation, air voids were trapped in the pores of the plate surface. Therefore, it is reasonable to assume that the area of ice through which shearing occurred was only a small fraction of the total shear plane area (Figure 4.9b).

Similar tests were conducted on frozen silt and frozen sand. The results (Figures B.21 and B.22) indicate that the adhesive shear strengths (greater than 17.8 kPa) exceed

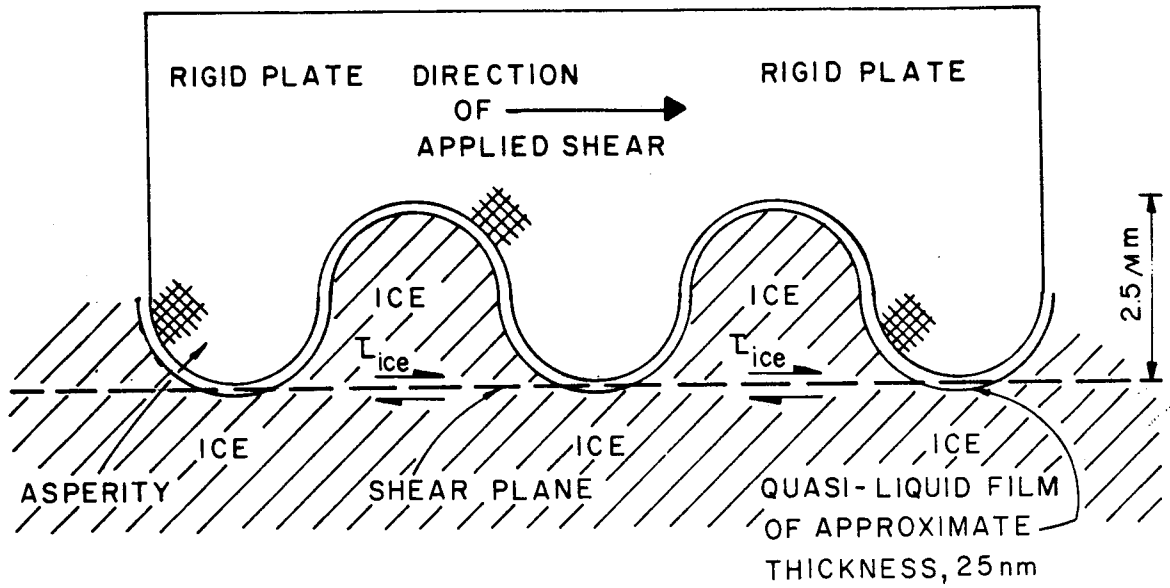

a) NO AIR VOIDS AT PLATE-ICE INTERFACE

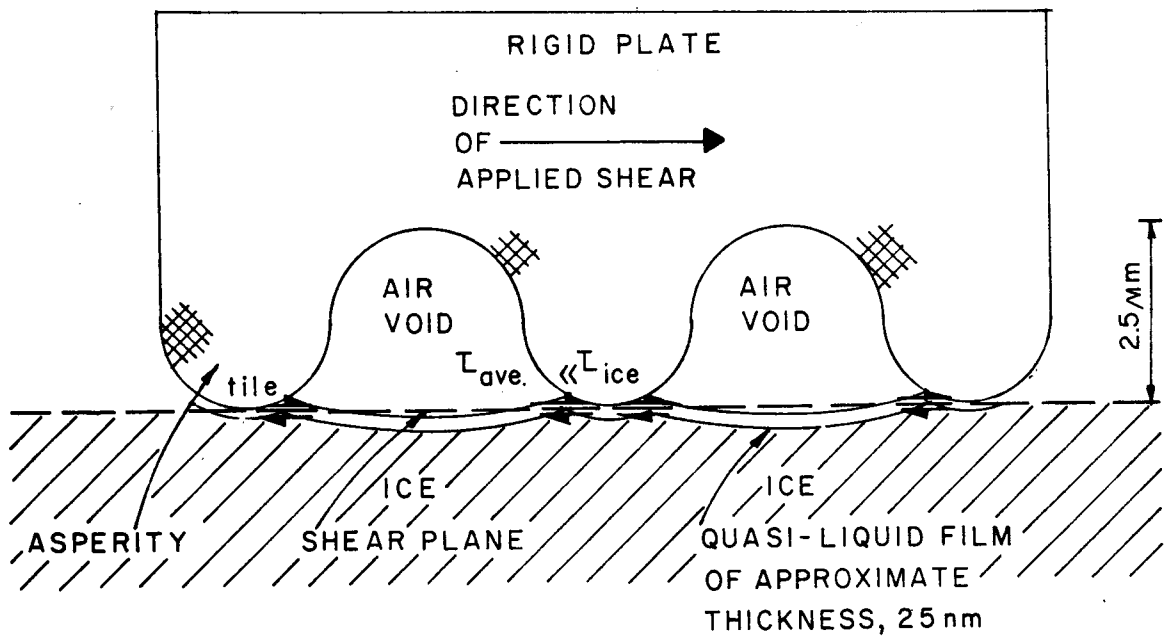

b) AIR VOIDS AT PLATE-ICE INTERFACE

Figure 4.9
Shear Failure Mechanisms Between a Smooth Plate (CLA = 2.5 μm) and Ice

that of ice. This may be explained using an extension of the model proposed for ice. The proposed failure mechanism for frozen soils is shown in Figure 4.10. The air voids still occupy the inter-asperital pores. However, the soil particles create an additional frictional resistance along the shear plane, thereby effecting a higher shear strength. This model is only applicable if the freezing front progresses from the soil to the plate during preparation. If the freezing front advances in the opposite direction, then a thin layer of ice may form at the plate-soil interface, and the failure mechanisms would be characteristic of ice (Figure 4.9b). Inspection of the plate-soil interfaces on completion of the tests, revealed that the freezing front had progressed from the soil during sample preparation.

In summary, the adhesive shear failure mechanism has been determined to be a function of the ice content at the interface and the local geometry of the asperties on the interface. It may be expected that a critical plate roughness exists, above which, ice will fill the pores and so effect an increased adhesive shear strength. In this light, the adfreeze strength of ice to a plate of roughness 125μm, was determined to be an excess of 21.3 kPa (Figure B.24) and is consistent with the above model.

It is emphasised that the proposed model is an oversimplification of the adhesion problem. However, it does provide a clear and rational explanation for the phenomena observed in this study.

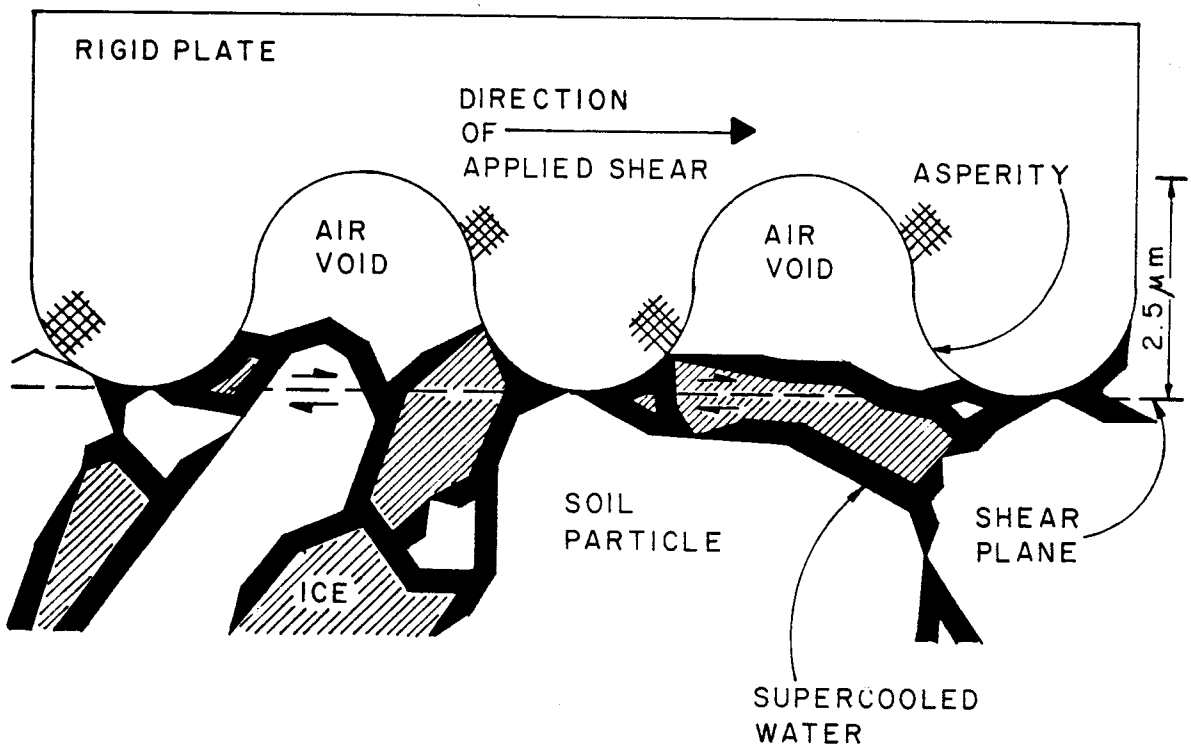

Figure 4.10
Shear Failure Mechanism Between a Smooth Plate (CLA = 2·5 μm) and Frozen Soil

4.6.3.2 Influence of Stress History on the Creep of Frozen Soils

Inspection of Figures B.1 to B.3 demonstrates that the creep characteristics of frozen sand and frozen silt are a function of loading history. Upon cycling the applied shear stress from 17.8 kPa to 25.0 kPa to 17.8 kPa, creep in both soil types were arrested. This implies that secondary creep is either very small or does not exist for these materials under the imposed test conditions.

An analogous test revealed that the creep rate of ice was unaffected by this loading cycle. This is consistent with the belief that long-term deformations in ice are better characterised by secondary creep.

4.6.3.3 Influence of Axial Stress on the Shear Creep of Frozen Soil

Inspection of Figures B.5 and B.6 reveals that horizontal shear strain rates for ice and frozen silt are unaffected by changes in applied axial stress. This supports the view that ice and frozen fine-grained soils behave in a frictionless manner under low stresses.

In contrast to this, the horizontal shear creep data for frozen sand (Figure B.7) suggest that ice-poor frozen sand behaves in a frictional manner under low stresses.

4.6.3.4 Influence of Frozen Bulk Density on the Creep of Frozen Soils

Figure B.1 presents creep data for ice over a period of 48 days. Inspection of these data indicate that steady-state creep conditions were reached after 5 days and continued throughout the test. Similar observations were noted in other creep tests on ice (Figures B.5 and B.24). Therefore, in this study the creep data of ice was analysed in terms of secondary creep.

The ice data is presented in terms of effective shear stress and effective shear strain rate (Odqvist (1966)) and is compared to the flow law for ice in Figure 4.11. The effective shear stress, σ_e , and the effective shear strain rate, $\dot{\varepsilon}_e$, reduce to

$$\sigma_e = (\sigma_{11}^2 + 3\tau_{12}^2)^{1/2} \qquad \text{.....4.6}$$

$$\dot{\varepsilon}_e = \left(\dot{\varepsilon}_{11}^2 + \frac{\dot{\gamma}_{12}^2}{2}\right)^{1/2} \qquad \text{.....4.7}$$

where τ_{12} and σ_{11} are the applied horizontal shear and vertical axial stresses, respectively, and $\dot{\gamma}_{12}$ and $\dot{\varepsilon}_{11}$ are the measured horizontal shear and vertical axial strain rates, respectively.

The agreement between these data and the flow law for polycrystalline ice is good.

The creep behaviour of frozen sand is depicted in

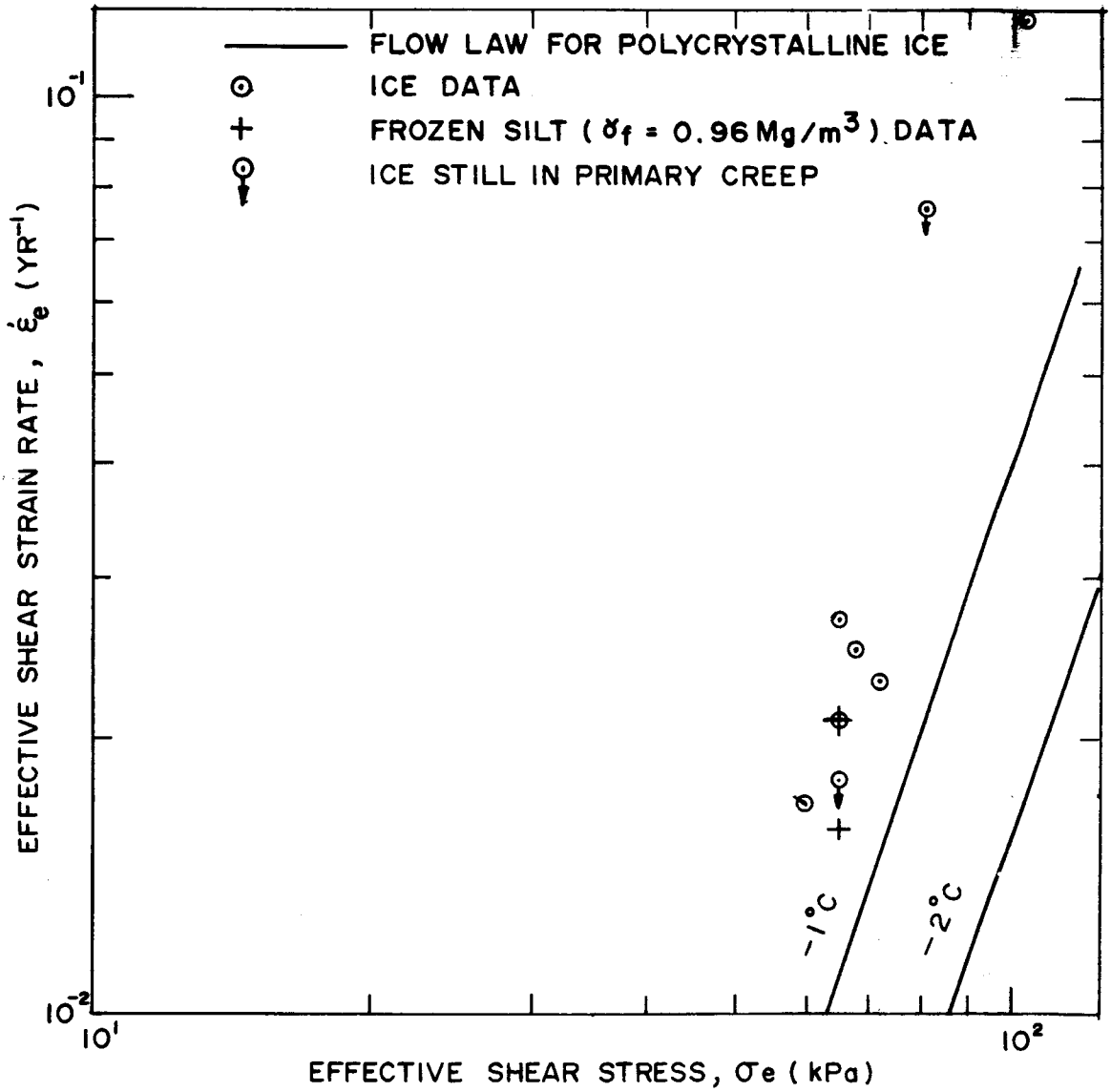

Figure 4.11
Summary of Creep Data for Ice and Silt 3

Figures B.3, B.7, B.22 and B.26. The results are consistent with the current philosophy that ice-poor sand is characterised by damped frictional creep. Comparison of Figures B.1 and B.3 reveal that frozen sand creeps faster than ice in the initial stage of primary creep. This observation was also noted in Figures B.5, B.7, B.20, B.22, B.24 and B.26 and is consistent with Tsytovich's philosophy of damped creep (Tsytovich (1975))

> "In the case of decaying creep of frozen soils, closure of microscopic cracks, size reduction of open cavities, and irreversible shears of particles relative to one another predominate."

Moreover, it can also be argued that in the initial period of damped creep, the load is supported to a large extent by the pore ice, thereby giving rise to higher creep rates than observed in polycrystalline ice. This high mobility of the pore ice is associated with re-orientation of the sand grains, resulting in a gradual stiffening of the sand matrix. In this way, the load is gradually transferred to the soil matrix, thereby strengthening the frozen soil.

The creep behaviour of frozen silt is strongly dependent upon the frozen bulk density (Figures B.13 to B.19). Inspection of Figures B.11, B.12, B.14, B.15 and B.19 reveals that the long-term creep of Silt 3 (bulk density = 0.96 Mg/m^3) is characterised by steady state creep. The secondary creep rates are comparable to those of ice (Figure 4.11). However, on increasing the frozen bulk density to

1.42 - 1.59 Mg/m^3 a considerable change in creep behaviour was observed (Figures B.2, B.4, B.6, B.8, B.10, B.12, B.13, B.15, B.17 and B.19). Secondary creep rates were considerably decreased (Table 4.1). This phenomenon is attributed to dispersion hardening of the ice matrix (Hooke et al. (1972)).

The creep of Silt 1 (bulk density = 1.76 to 1.89 Mg/m^3) is further complicated by an inter-connecting network of unfrozen water around the frozen soil particles. Inspection of Figures B.9, B.12, B.16, B.19, B.21, B.23, B.25 and B.27 reveals that creep in Silt 1 is more pronounced than similar tests on ice, and is dominated by transient processes even after 33 days of constant loading. This is attributed to time-dependent consolidation.

4.7 Summary

The simple shear test has proven to be a versatile apparatus for determining the creep characteristics of frozen soil. The following conclusions are inferred from this study

1. The adfreeze strength is conveniently determined using the simple shear apparatus described in this chapter.
2. The integrity of the adfreeze bond is maintained and slip does not occur if the stress applied at the interface is less than the adfreeze bond strength.
3. The adfreeze bond strength has been determined to be a function of the plate roughness and the nature of the

ice at the interface. A frozen soil-plate model has been proposed to describe the load transfer characteristics of very smooth plates (CLA less than 2.5μm). In practice piles are never this smooth and it is doubtful that the model has any practical contribution to piling. However, it is of interest to physicists and aeronautical engineers.

4. The short-term (0 to 45 days) deformation behaviour of polycrystalline ice in the low stress range (50 to 100 kPa) at -1 ^{0}C is characterised by a brief period (0 to 5 days) of primary creep and a prolonged period of apparent secondary creep (5 to 45 days). The observed creep rates are consistent with other published creep data for ice (Morgenstern et al (1979)).

5. The short-term deformation behavior of ice-poor frozen sand in the low stress range at -1 ^{0}C is characterised by damped creep.

6. There is no evidence in this study to suggest that in the low stress range secondary creep exists for frozen silts at -1 ^{0}C. However, creep is enhanced by consolidation processes at frozen bulk densities greater than 1.76 Mg/m^{3}.

CHAPTER 5

PILE DESIGN

5.1 Introduction

The design of a pile foundation requires that both carrying capacity and settlement be checked. Carrying capacity is assessed by consideration of adfreeze strengths. A settlement based design must ensure that pile creep displacements throughout the life of the structure are tolerable.

5.2 Bearing Capacity Design

Failure of a pile in frozen soil is associated with rupture of the adfreeze bond and tertiary creep of the soil beneath the pile tip. The strength properties of frozen soils are temperature and rate-dependent and thus, the interaction between mobilization of compressive support at the pile tip and tertiary creep of the adfreeze bond is complex. Therefore, bearing capacity design is based on allowable "pseudo" adfreeze strengths which are determined from long-term field and laboratory tests.

The long-term allowable adfreeze strength is primarily dependent upon ground temperature, the roughness of the pile and the soil type. A summary of adfreeze strengths is presented in Figure 5.1. It is observed that the adfreeze strength is inversely related to the ice content and

directly related to the roughness of the pile. In the limit, the adfreeze strength of very rough piles approaches the shear strength of frozen soil.

It was recognised in Chapter 4 that the adfreeze strength is a function of the area of ice located along the shear plane which in turn is a function of the pile roughness. It is proposed that the adfreeze strength of a frozen soil, τ_a, is related to the long-term shear strength, τ_{lt}, by the relation

$$\tau_a = m \tau_{lt} \qquad \text{.....5.1}$$

where m is primarily a roughness-dependent parameter.

The long-term shear strength of a frozen soil is comprised of both frictional ϕ_{lt} , and cohesive, c_{lt} , components and can be expressed by a modified Mohr-Coulomb failure theory

$$\tau_{lt} = c_{lt} + \sigma_n \tan \phi_{lt} \qquad \text{.....5.2}$$

where σ_n is the normal stress on the shear plane.

The normal stress on the adfreeze shear plane is typically less than 100 kPa, thus the frictional component is generally insignificant and may be neglected. Hence, Equation 5.1 reduces to

$$\tau_a = m c_{lt} \qquad \text{.....5.3}$$

A review of long-term cohesive strengths of frozen soils has been presented by Vialov in his classical publication, "Rheological Properties and Bearing Capacity of Frozen Soils" (Vialov (1959)). A summary of these data is presented in Table 5.1 which also includes the long-term cohesive strength of polycrystalline ice as determined by Voitkovskii (1960) . These data are also presented in Figure 5.2 which defines the variation of cohesion with temperature for the four soil types outlined in Table 5.1. Comparison of the ice data for the long-term cohesive and adfreeze strengths (Figure 5.1) reveals that 'm' is approximately equal to 0.7 for timber piles. This is consistent with long-term adfreeze strengths as determined by Vialov (1959). The long-term adfreeze strengths of steel and concrete piles are not as well defined; however, it is possible to infer 'm' values of 0.6 for both concrete (Johnston and Ladanyi (1972)) and steel (Crory (1963)) piles.

In summary, the long-term adfreeze strength may be directly related to the soil shear strength by means of a coefficient which is dependent only upon the pile type and installation method. The coefficient 'm' is defined in Table 5.2.

It is of interest to note that in the Soviet codes no distinction is made between timber and concrete piles; however the code does recommend that a reduction factor of 0.7 be applied to steel piles (National Research Council of Canada (1976)).

Temperature (°C)	Ice[1]	Ice-rich[2] silt	Varved[2] clay	Ice-poor[2] fine sand
-0.35		55	180	230
-1.15		100	260	270
-1.2	160			
-1.8	200			
-4.0	300			
-4.2		300	470	450

[1] Voitkovskii (1960)

[2] Vialov (1959)

Table 5.1 Summary of Long-term Cohesion for Frozen Soils (kPa)

Pile Type	m
Steel	0.6
Concrete	0.6
Timber (uncreosoted)	0.7
Corrugated Steel Pipe	1.0

Table 5.2 Summary of 'm' Coefficients

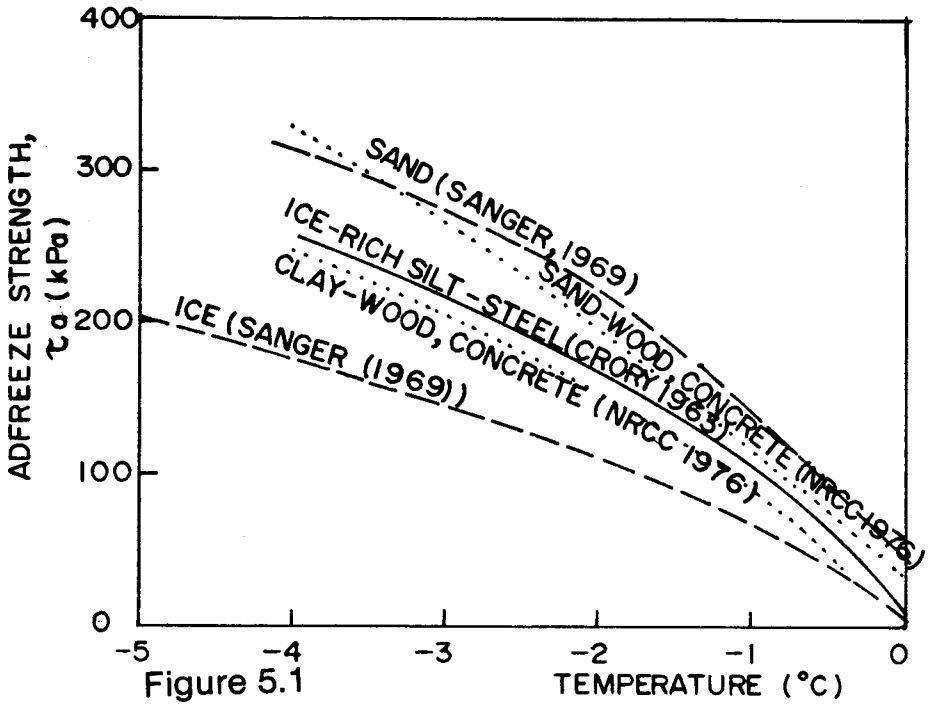

Figure 5.1
Published Adfreeze Strengths

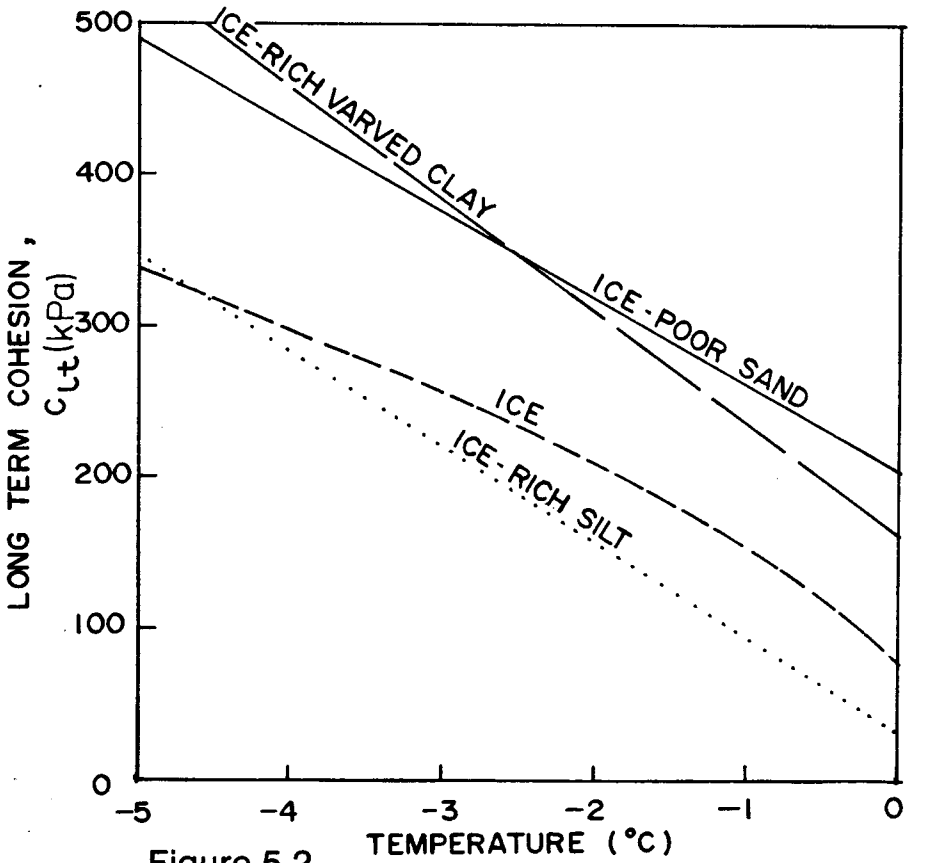

Figure 5.2
Long Term Cohesion of Frozen Soils

It is emphasised that the cohesion must be representative of the frozen soil condition immediately at the pile/frozen soil interface. In this way, Equation 5.3 indirectly incorporates the influence of pile emplacement on the allowable adfreeze strength. For example, when a steel pile is driven into ice-rich varved clay the soil structure remains intact and the cohesion of the varved clay may be used in the design. However, if the pile is frozen-in using a slurry mixed from the original excavated material, the varved structure of the soil around the pile is destroyed and the adfreeze strength should be reduced to that of a steel pile in ice-rich silt. Moreover, if a steel pile is frozen-in during winter moisture will migrate to the pile and a thin layer of ice will coat the surface of the pile. The adfreeze design should then be based on the cohesion of ice. If the pile is installed in summer the ice lenses form within the slurry and not at the pile/soil surface.

5.3 Settlement Design

5.3.1 Friction Piles

5.3.1.1 Ice and Ice-rich Fozen Soil

The deformation of the soil around a pile shaft may be idealised as shearing of concentric cylinders (see Figure 5.3). This approach has been verified analytically by Frank (1974) and Baguelin *et al.* (1975). Vialov (1959), Johnston and Ladanyi (1972) and Nixon and McRoberts (1976) have

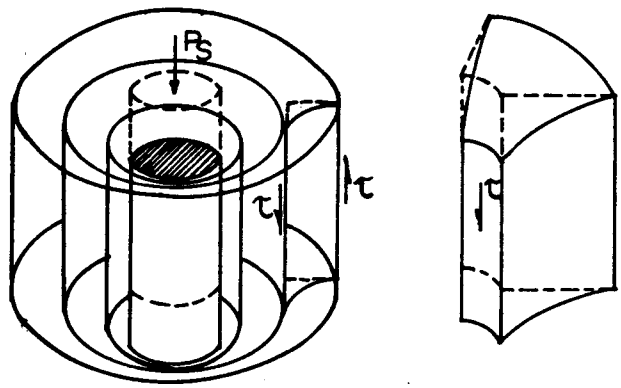

Figure 5.3
Analytical Model for Friction Piles

applied this analytical model to frozen soils. Accordingly, Johnston and Ladanyi (1972) have proposed that the creep of friction piles in ice may be predicted using

$$\frac{\dot{u}_a}{a} = \frac{3^{\frac{n+1}{2}} B \tau^n}{n-1} \qquad \text{.....5.4}$$

where $\dot{u}_a$ is the pile steady-state settlement rate (m/yr), a is the pile radius (m), τ is the average applied adfreeze load (kPa), and B and n are temperature dependent parameters, defined in Chapter 2.

The validity of the analysis is based on the following assumptions

1. The analysis is insensitive to changes in normal stress on the lateral surface of the pile.
2. There is no slip at the pile-soil interface.
3. Gravity forces are negligible.
4. The soil is homogeneous and isotropic and the properties are uniform with depth.

Some of these assumptions may be restrictive, and comments on their validity are necessary.

Assumption 1 is valid since it was shown in Chapter 2, that the long-term deformation behaviours of ice and ice-rich frozen soils are independent of normal stress. Assumption 2 is satisfied at low stress levels since it was confirmed in Chapter 4 that piles do not slip through frozen soil unless the applied adfreeze loading is greater than the adfreeze strength. Finally, geothermal gradients in

permafrost are typically greater than 30 m/^{0}C and thus, in most long pile configurations the temperature distribution may be assumed uniform with depth. However, if a non-uniform temperature-depth profile can be justified, then Nixon and McRoberts (1976) have shown how the analysis may be developed to account for depth-dependent soil properties. Similarly, radial inhomogeneity may be incorporated into the analysis by considering the soil as concentric homogeneous cylinders and integrating the strains across each region.

The above synthesis justifies the use of this analysis for the prediction of stresses and strains around a friction pile in frozen soils.

Therefore, the load carrying capacity, P_s of a friction pile of length L, may be determined from

$$P_s = \sum_{i,k}^{1} \left[2\pi a \left(\frac{\dot{u}_a}{a} \right)^{\frac{1}{n_i}} \ell_i \left(\frac{n_i - 1}{3^{\frac{n_i+1}{2}}} \right)^{\frac{1}{n_i}} \left(\frac{1}{B_i} \right)^{\frac{1}{n_i}} \right] \qquad \text{.....5.5}$$

where k is the number of soil layers.

It is noted that if the soil properties are not depth-dependent then Equation 5.5 reduces to

$$P_s = 2\pi a L \left(\frac{\dot{u}_a}{a} \right)^{\frac{1}{n}} \left(\frac{n - 1}{3^{\frac{n+1}{2}}} \right)^{\frac{1}{n}} \left(\frac{1}{B} \right)^{\frac{1}{n}} \qquad \text{.....5.6}$$

Equation 5.6 is conveniently summarised in graphic form for polycrystalline ice in Figure 5.4 which relates the normalised pile velocity, $\dot{u}_a/a$ to the ground temperature and the average applied shaft stress, τ .

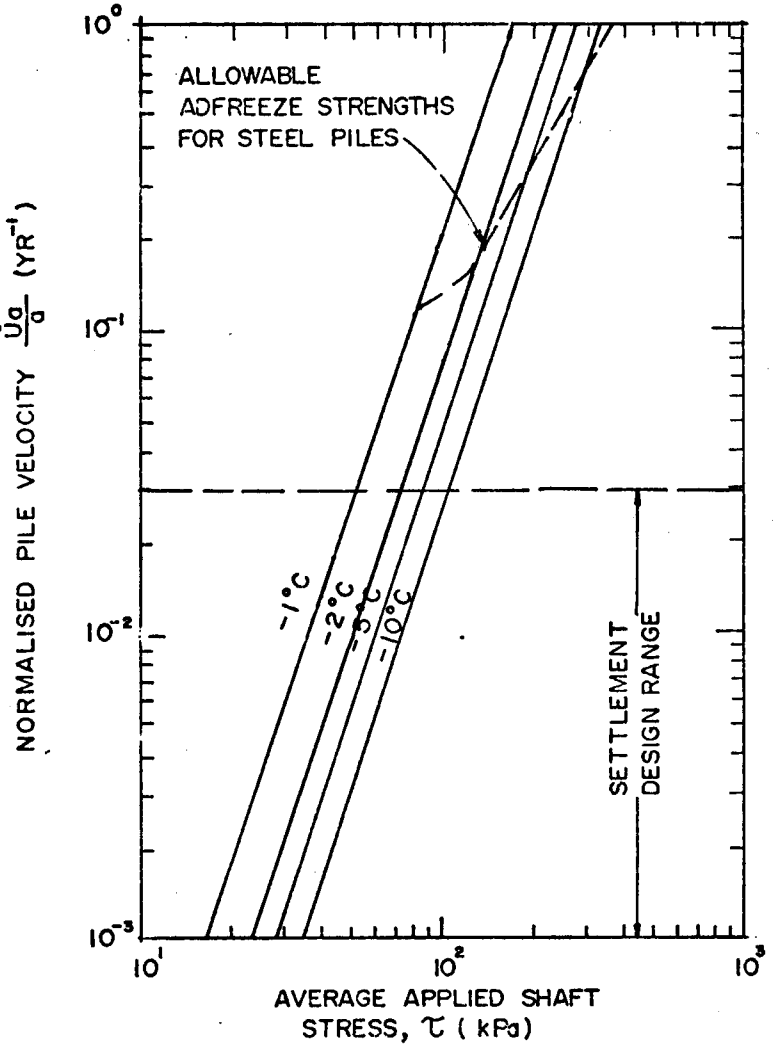

Figure 5.4 Design Chart for Friction Piles in Ice

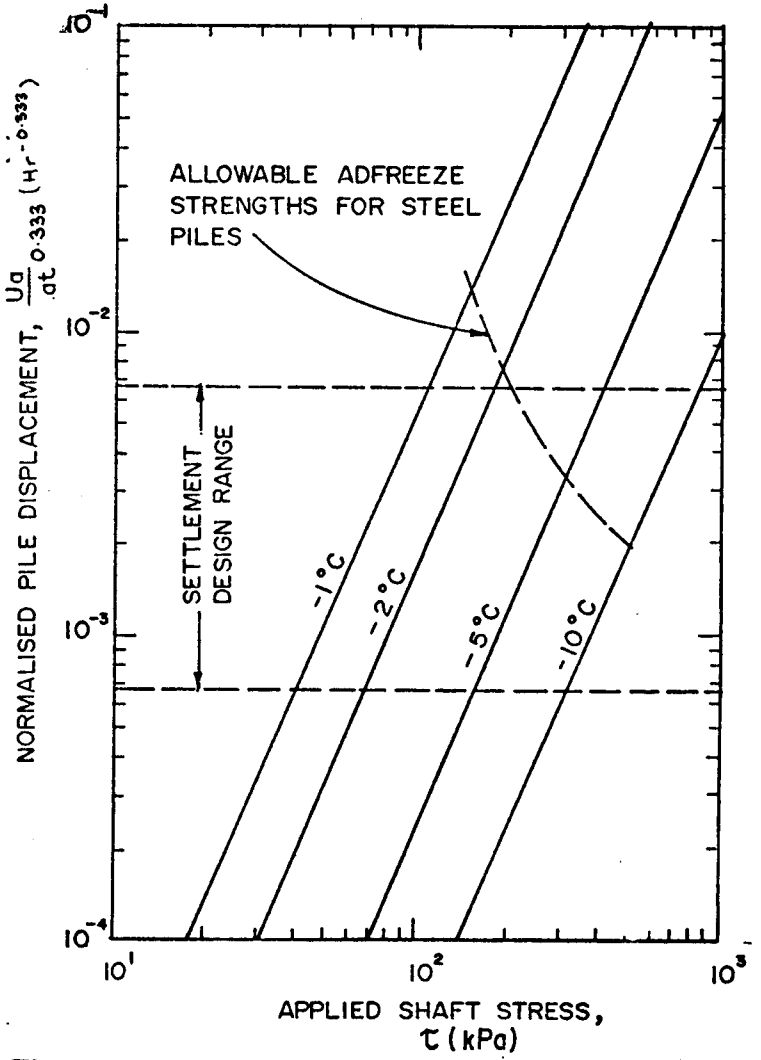

Figure 5.5 Design Chart for Friction Piles in Frozen Suffield Clay (γ_f = 1.76 Mg/m^3)

5.3.1.2 Ice-poor frozen soils

A constitutive relationship for frozen soils has been proposed in Equation 2.7. The ratio, $\frac{\sigma_1}{f\sigma_3}$ is typically less than 1.25 for most pile configurations. Therefore, better accuracy may be obtained by putting 'f' equal to 1. For the condition of simple shear Equation 2.7 now reduces to

$$\gamma = 3^{\frac{c+1}{2}} K \tau^c t^b \qquad \text{.....5.7}$$

where γ and τ are the shear strain and shear stress, respectively. Equation 5.7 is analagous to Equation 2.3 and so the normalised displacement, u_a/a, may be related to the applied shaft stress accordingly,

$$\frac{u_a}{a t^b} = \frac{3^{\frac{c+1}{2}} K \tau^c}{c-1} \qquad \text{.....5.8}$$

Normal stresses at depth on very long piles may have a significant influence on the pile creep. These high confining pressures may be incorporated into the analysis using the approach outlined by Johnston and Ladanyi (1972). Creep constants obtained from Table A.3 were substituted into Equation 5.8 to yield creep predictions for piles in frozen Suffield clay, Hanover silt and Ottawa sand. These predictions are summarised in graphical form in Figures 5.5 to 5.7, respectively. The load carrying capacity of a friction pile in an ice-poor frozen soil is thus given by

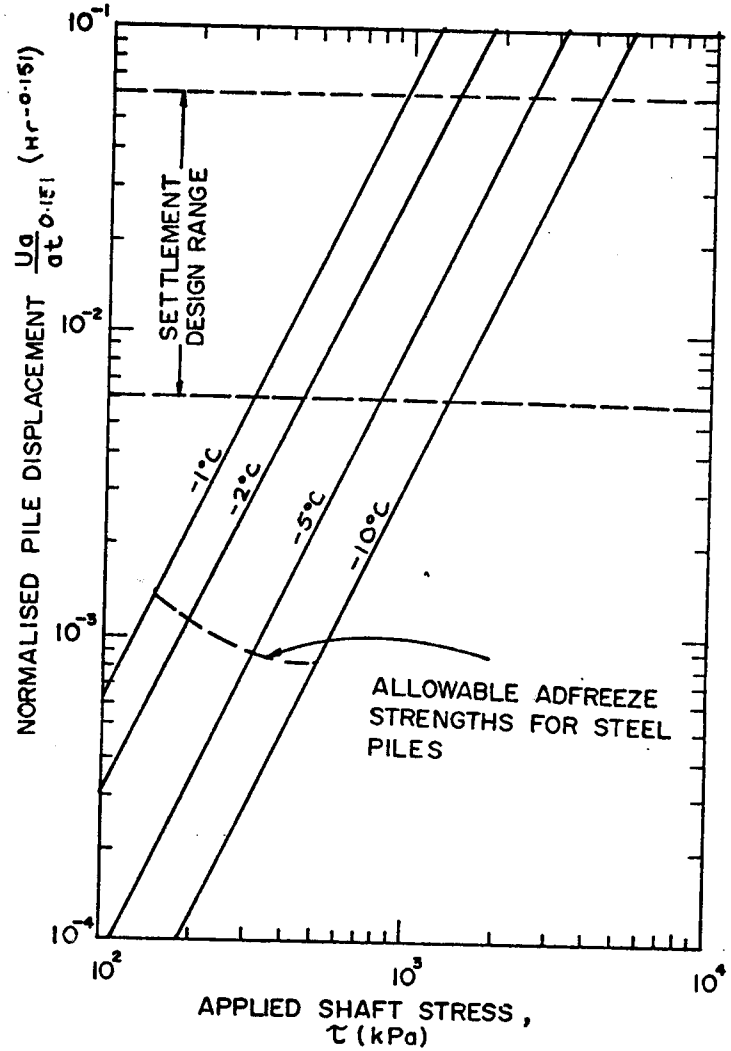

Figure 5.6 Design Chart for Friction Piles in Frozen Hanover Silt ($\gamma_f = 1.78$ Mg/m^3)

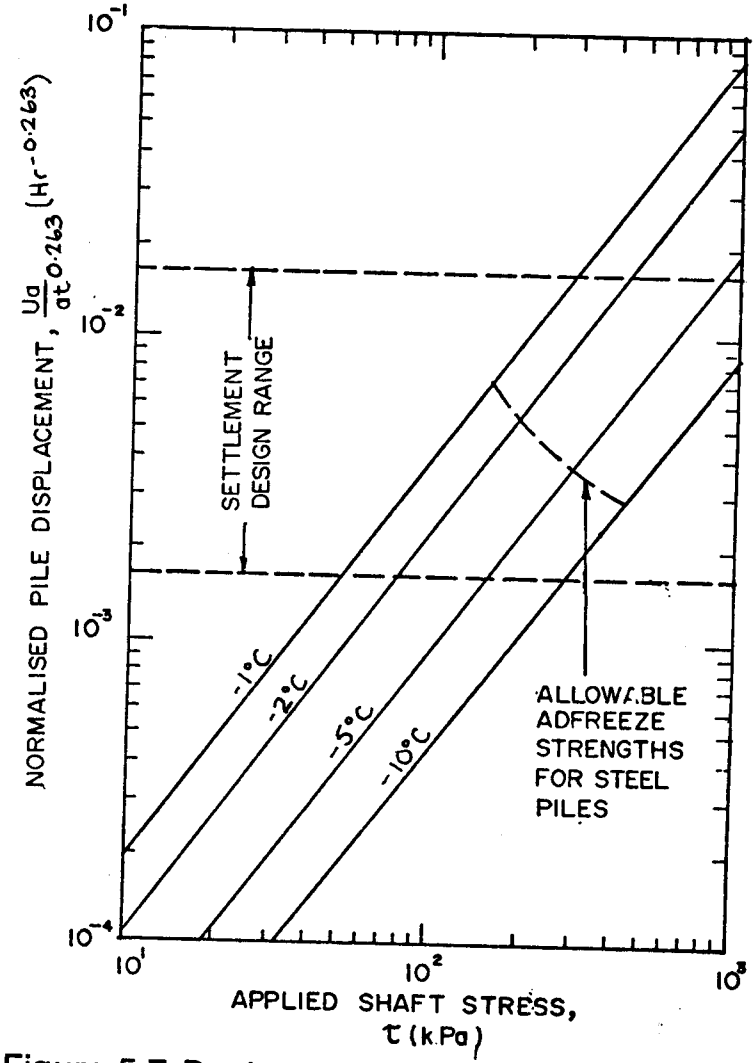

Figure 5.7 Design Chart for Friction Piles in Frozen Ottawa Sand ($\gamma_f = 2.00$ Mg/m^3)

$$P_s = 2\pi a L \left(\frac{u_a}{a t^b}\right)^{\frac{1}{c}} \left(\frac{c-1}{3^{\frac{c+1}{2}}}\right)^{\frac{1}{c}} \left(\frac{1}{K}\right)^{\frac{1}{c}} \qquad \text{.....5.9}$$

5.3.2 End-bearing Piles

5.3.2.1 ice and ice-rich frozen soils

Nixon and McRoberts (1976) simulated end-bearing using the following two models,

1. A circular footing on a viscous half-space.
2. An expanding spherical cavity in an infinite viscous media.

The two approaches have been compared to a finite element solution of the surface footing problem(Nixon (1978)). The results of this study are encouraging. It transpires that for a creep exponent of 3, the two models predict similar results and overestimate the creep strain as computed by the finite element analysis by a factor of 1.7. However, the first approach is only applicable to surface loads whereas, the expanding cavity model can similate creep behaviour at depth. Field and laboratory evidence (Vialov (1959) ;Ladanyi and Johnston (1974)) indicate that the deformation behaviour of frozen soil beneath a deep circular footing resembles that of an expanding spherical cavity of radius, a. In this light, the second model is a better representation of end-bearing.

The problem of an expanding spherical cavity in a non-linear viscous frictionless media and its limitations as applied to a deep circular footing have been discussed in

detail by Ladanyi and Johnston (1974) . Thus, the relation between the applied end-bearing pressure, σ_E and the resulting pile settlement rate is given by

$$\frac{\dot{u}_a}{a} = \frac{2}{3}\left(\left[1 - \frac{B}{2}\left(\frac{3}{2n}\sigma_E\right)^n\right]^{-3} - 1\right) \qquad \text{.....5.10}$$

This can be simplified and approximately expressed by

$$\frac{\dot{u}_a}{a} = B\left(\frac{3}{2n}\sigma_E\right)^n \qquad \text{.....5.11}$$

from which the end bearing load, P_E may be calculated

$$P_E = \left(\frac{1}{B}\frac{\dot{u}_a}{a}\right)^{\frac{1}{n}} \frac{2\pi a^2 n}{3} \qquad \text{.....5.12}$$

Equation 5.12 is conveniently summarised in graphical form for polycrystalline ice in Figure 5.8 which relates the normalised pile velocity to the ground temperature and the end-bearing pressure, σ_E .

5.3.2.2 Ice-poor soils

The analysis of end-bearing piles in ice-poor soils may be solved by introducing Equation 2.7 into the expanding cavity analysis. This is not a very difficult mathematical exercise, however, it has been found that the solution so obtained is too complicated for practical use. Hence, in this analysis 'f' will be assumed equal to unity. The acceptability of this has been discussed by Ladanyi and

Johnston (1974) who concluded that the assumption is not unreasonable in frozen soils. Hence, the time-dependent pressure-deformation relation is given by

$$\frac{u_a}{a t^b} = K \left(\frac{3}{2c} \sigma_E \right)^c \qquad \text{.....5.13}$$

Equation 5.13 is summarised in graphical form for frozen Suffield clay, Hanover silt and Ottawa sand in Figures 5.9 to 5.11, respectively. From Equation 5.13 the load carrying capacity of an end-bearing pile is given by

$$P_E = \left(\frac{1}{K} \frac{u_a}{a t^b} \right)^{\frac{1}{c}} \frac{2\pi a^2 c}{3} \qquad \text{.....5.14}$$

5.3.3 Combined End-bearing and Friction Piles

The non-linearity of Equations 2.3 and 2.7 preclude a closed solution to the pile problem. However, an approximate solution may be obtained by summing the shaft and tip components as determined from Equations 5.6 and 5.12 (ice and ice-rich frozen soils) and Equations 5.9 and 5.14 (ice-poor frozen soils). This approach assumes that the upper layer of soil will be deformed by the load transferred from the pile shaft and that the lower layer of soil will be deformed exclusively by the pile base load. Figure 5.12 shows the separate deformations. The deformation patterns along A^1-B^1 and A^2-B^2 will not be compatible and this will lead to some interaction between the upper and lower soil

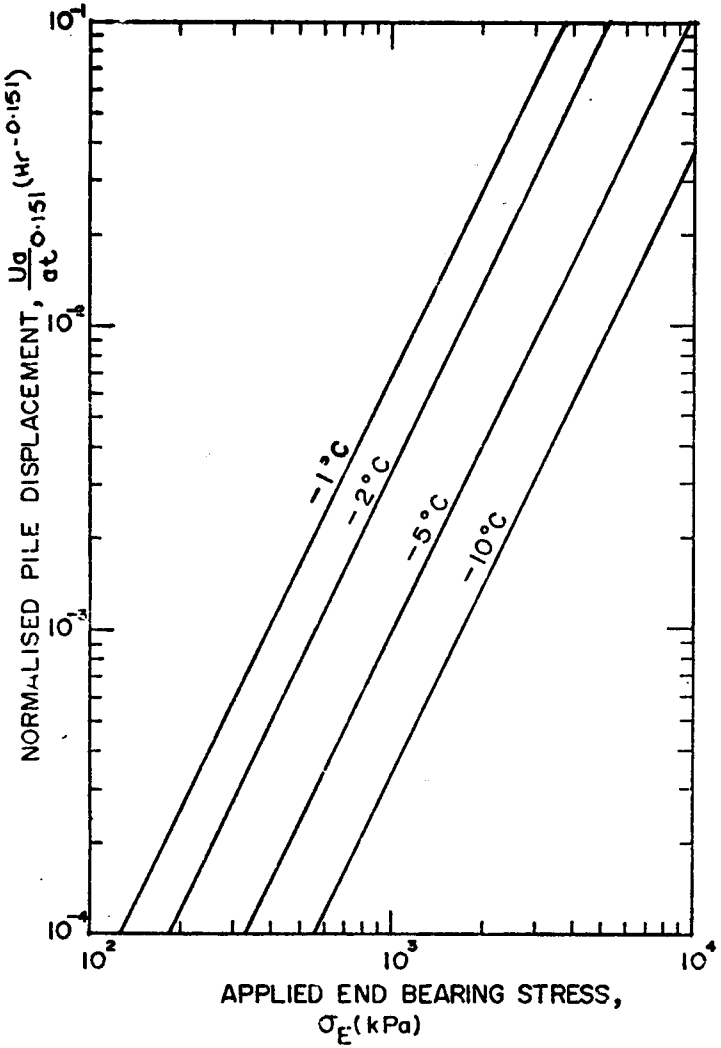

Figure 5.10 Design Chart for End Bearing Piles in Frozen Hanover Silt (γ_f = 1.78 Mg/m^3)

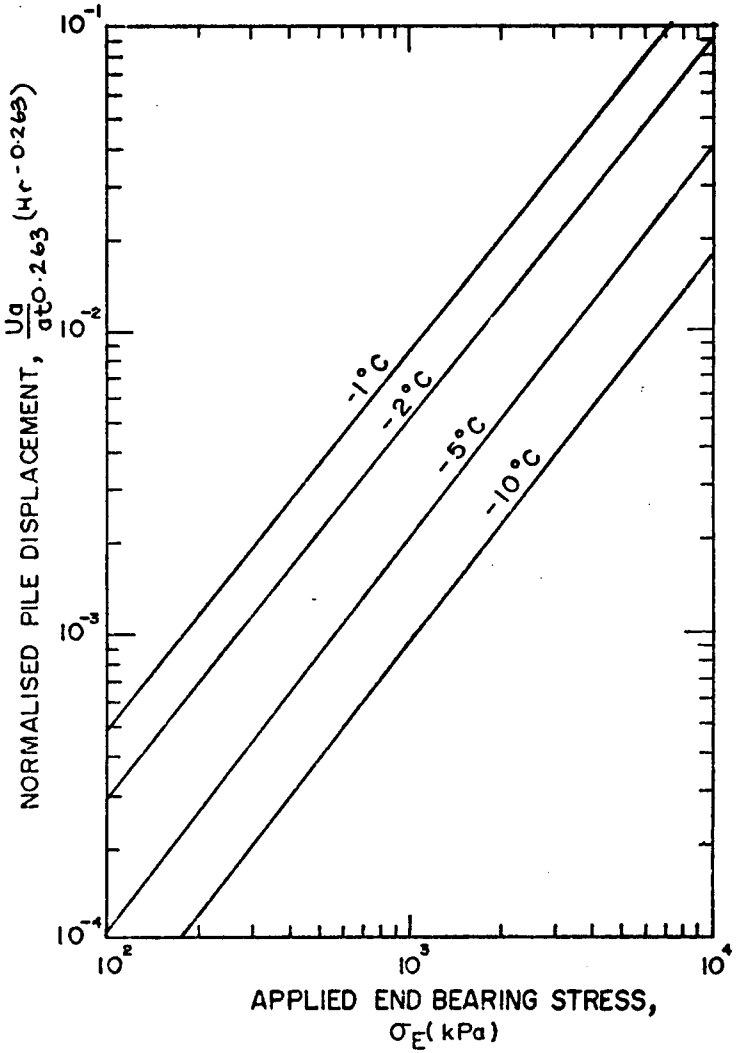

Figure 5.11 Design Chart for End Bearing Piles in Frozen Ottawa Sand (γ_f = 2.00 Mg/m^3)

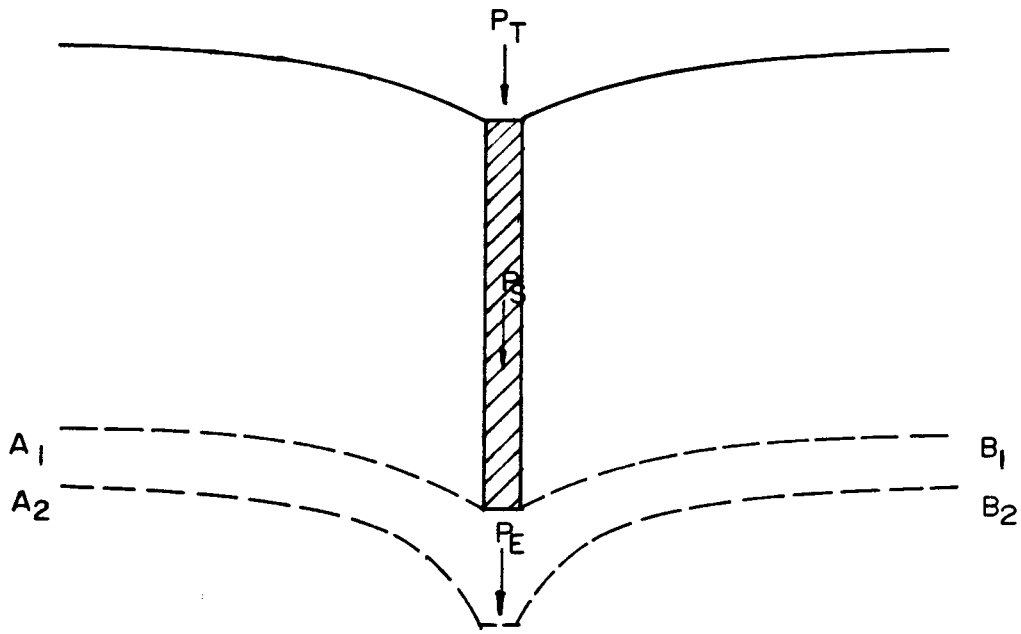

Figure 5.12

Uncoupling of Effects Due to Pile Shaft and Base (Randolf and Wroth (1978))

layers. This simplified approach is therefore only approximate, however, the acceptibility of this model has been checked against numerical solutions and verified by Randolph and Wroth (1978).

Therefore, the total pile load capacity in ice and ice-rich frozen soils, P may be determined from Figures 5.4 and 5.8 or if the temperature distribution is uniform with depth P_T may be calculated using,

$$P_T = 2\pi a \left(\frac{1}{B}\frac{\dot{u}_a}{a}\right)^{\frac{1}{n}}\left[\left(\frac{n-1}{3^{n+\frac{1}{2}}}\right)^{\frac{1}{n}} L + \frac{na}{3}\right] \qquad \ldots\ldots 5.15$$

The percentage of load borne at the pile tip in isothermal ice may be determined from Equations 5.5 and 5.15

$$\frac{P_E}{P_T} = \frac{\frac{na}{3}}{\left(\frac{n-1}{3^{n+\frac{1}{2}}}\right)^{\frac{1}{n}} L + \frac{na}{3}} \qquad \ldots\ldots 5.16$$

Thus, for a 0.2 m diameter pile of length 25 m installed in polycrystalline ice, the fraction of load supported in end-bearing is 0.5 % at -1 ^{o}C and 0.65 % at -10 ^{o}C.

Similarly, the total pile load capacity in ice-poor frozen soils is given by,

$$P_T = 2\pi a \left(\frac{1}{K}\frac{u_a}{a+b}\right)^{\frac{1}{c}}\left[\left(\frac{c-1}{3^{c+\frac{1}{2}}}\right)^{\frac{1}{c}} L + \frac{ca}{3}\right] \qquad \ldots\ldots 5.17$$

and the percentage of load borne at the pile tip in isothermal frozen ground is given by,

$$\frac{P_e}{P_T} = \frac{\frac{ca}{3}}{\left(\frac{c-1}{3^{c+1}}\right)^{\frac{1}{c}} L + \frac{ca}{3}} \qquad \text{.....5.18}$$

Thus, for a 0.2 m diameter pile of length 25 m installed in isothermal frozen Ottawa sand, the fraction of load supported in end-bearing is 1.1 %.

From the preceeding review it follows that pile end-bearing is negligible in homogeneous frozen soils.

5.4 A Review of Pile Creep Test Results in Permafrost

Pile creep in ice and ice-rich frozen soils and ice-poor frozen soils has been predicted using Equations 5.15 and 5.16, respectively. In order to evaluate the applicability of these predictions it is necessary to compare the predicted behaviour with actual deformation behaviour as obtained from pile load tests and documented case histories.

5.4.1 Criteria and Procedures for Analysing Pile Creep

The deformation behaviour of a loaded pile in permafrost is very sensitive to its environment. Therefore, in order to procure reliable representative creep rates from the test results it is essential to subject each set of data to a critical and rigorous review giving particular attention to the following details

1. Ground Conditions

   The deformation behaviour of frozen soil is strongly influenced by the ground conditions, in particular, the

ice content of the deposit and the ground temperature. Consequently, these variables must be adequately defined. In Chapter 2 it was recognised that the long-term deformation behaviour of ice and ice-rich frozen soils may be approximated by secondary creep while creep of ice-poor soils is characterised by damped creep. In this light, the data were categorised as either ice and ice-rich or ice-poor.

2. Pile Type and Emplacement Method

In order to take into account variations in pile geometry and backfill properties the concept of 'effective pile diameter' has been introduced. The effective pile diameter of a square pile is theoretically shown to be equal to the pile width in Appendix C. Similarly, the effective pile diameter of an H or rectangular pile of cross-sectional dimensions, l by b is equal to (l+b)/2. The effective pile diameter also depends upon the backfill properties. If a sand slurry is used the effective pile diameter is given by the average diameter of the drilled hole. In the following study the effective pile diameter was not always obvious. In such cases the effective pile diameter was set equal to average pile diameter.

3. Magnitude and Type of Loading

The scope of this review encompasses only the creep data of interest to foundation engineers and therefore, pile creep data was only included if the ensuing creep was

not characterised by tertiary creep.

The validity of using incremental load tests to determine static load pile creep has been assessed in Chapter 4, from which it emerged that ice-poor frozen soils are stress-path dependent. Thus, in this study, for ice-poor soils, only creep data during the first load increment were analysed.

Finally, the data were categorised as either friction pile data or end bearing pile data.

5.4.2 Outline of Pile Creep Tests

The earliest pile creep tests found in the North American literature were initiated by AFCEL at the Alaska Field Station. Crory (1963) reports that they produced little conclusive data.

In 1959 long-term load tests on three creosote-treated timber piles commenced at Pile Site C on the Alaska Field Station and have been reported by Madzula (1966) and Huck (1967). Unfortunately, the piles and their instrumentation were subject to frost-heave forces in the active layer. The outcome of this is reflected in the creep data presented by Huck which shows that the piles were heaving during the summer months. Therefore, these data are considered unreliable.

In 1966 six additional pile creep tests were conducted at Pile Site C. However, Huck (1967) indicates that the test loads exceeded the pile side shear capacities and thus slip

occurred at the pile-soil interface. Therefore, these tests were not analysed in this study.

Crory (1973) and Crory (1975) reported twenty-four hour incremental pile load tests undertaken by CRREL at Bethel Air Force Station and Moose and Spinach Creeks, Alaska. However, no detailed creep data has been released.

Morgenstern (1978) provided the author with pile creep test data for two piles in ice-rich silt. The piles were loaded incrementally at 72 hour intervals.

Johnston and Ladanyi (1972) published results of one incremental and ten static load pull-out tests at Thompson and Gillam, Manitoba. The ground conditions consisted of ice-rich silts and clays. Ground temperatures varied from -0.1 to -0.3 ^{o}C. The loads were very high and all of the piles at both sites were pulled out. Anchor GG2 was the only anchor to be tested in the stress range pertinent to this study.

Rowley et al. (1973) reported results of a twenty-four hour incremental pile load test on a timber pile in permafrost near Inuvik. The ground conditions consisted of ice and ice-rich frozen silt. The average ground temperature was -1.4 ^{o}C.

Frederking (1974) reported results of load tests on wooden piles frozen into lake ice at the NRC laboratories in Ottawa. Unfortunately, temperature control was very poor thus no attempt has been made to analyse these results.

A study of the Soviet literature reveals a comparative

wealth of pile creep data in frozen soils. Vialov (1959) reported that in 1950 an extensive pile load testing program was initiated in the underground chambers of the Igarka laboratory. The experiments consisted of pushing and pulling model wooden piles that were embedded in various types of frozen soil. Ground temperatures were maintained at -0.4 ^{0}C. Long-term static load tests were also conducted on similar model piles in ice at -0.4 ^{0}C (Vialov (1959)). In addition, the results of static pile load tests on full-scale concrete piles, driven into various types of frozen soils were also given. For these cases, the ground temperature varied from -0.2 to -1.0 ^{0}C.

Vialov (1973) summarised results of a long-term incremental load test on a square reinforced concrete pile in Mokhsogollokh, USSR. The foundation material was primarily ground ice. Temperatures were not reported; however, ground temperatures in the permafrost of the Mokhsogollokh area at a depth of 10 m are -2.0 ^{0}C (National Research Council of Canada (1976)).

The results of an incremental pile load test on a circular reinforced concrete pile, embedded mainly in ice at Yakutsk, USSR were also given. The test temperature was -2.3 ^{0}C.

Dokuchayev and Markin (1972) published the results of one incremental and static load test on square reinforced concrete piles in ice-rich silt. The ground temperature varied from -1.0 ^{0}C at the top of the pile, to -4.0 ^{0}C at

the tip.

Vialov (1978) reported results of very long-term (20 years) field punching tests in ice-rich frozen soil. The ground temperatures varied from -0.05 ^{0}C at the outset to -2.0 ^{0}C on completion of the tests.

Finally, Womick and LeGoullon (1975) have documented the behaviour of pile foundations for the Fairbanks Telemetry Station of European Space Research Organisation. The permafrost is comprised of bands of ice(up to 3 m thick) and ice-rich silts. The ground temperature at depth warmed slowly from -1.1 to -0.5 ^{0}C over a period of four years. Miller (1971) reported that the temperature data in the last three years may be in error. Therefore, only settlements incurred during the first two years have been included in this study.

5.4.3 Discussion of Pile Creep Test Data

The preceding review has extracted the reliable creep data and categorised them according to permafrost type. The ice-rich and ice-poor frozen soil data for piles are summarised in Tables 5.3 and 5.4, respectively and the ice-rich punching data are summarised in Table 5.5. It is convenient to discuss these data according to these categories.

5.4.3.1 Ice and Ice-rich Frozen Soils

It was concluded in Chapter 2 that the long-term

SOURCE	PILE TEST DESIGNATION	PILE TYPE	EFF. PILE DIAMETER (m)	SOIL TYPE	SOIL TEMPERATURE (°C)	APPLIED SHAFT STRESS (kPa)	NORMALISED PILE VELOCITY (yr^{-1})	TYPE OF LOADING	TEST DURATION (hr)
JOHNSTON AND LADANYI (1972)	GG2	GROUTED ROD	0.15	ICE-RICH VARVED CLAY	−1 to −0.3	120	3.4	STATIC	1500
ROWLEY AND WATSON (1973)	T12V	WOOD	0.46	ICE-RICH SILT	−1.1	30	4.6	INCREMENTAL	24
VIALOV (1959)	21	WOOD	0.035	ICE-RICH SILT	−0.4	90	0.63	INCREMENTAL	2420
						100	1.5		120
	13	CONCRETE	0.22	"	−0.2	55	3.5	STATIC	1000
	64	WOOD	0.035	MASSIVE ICE	−0.4	55	1.1	"	3000
	137	"	"	"	"	40	0.21	"	950
	184	"	"	"	"	100	2.3	"	650
	210	"	"	"	"	60	1.5	"	850
	212	"	"	"	"	40	0.031	"	9000
	218	"	"	"	"	40	0.20	"	3000
DOKUCHAYEV AND MARKIN (1971)	πDC2	CONCRETE	0.40	ICE-RICH SILT	−1 to −4	170	0.96	"	360
VIALOV (1973)	G1	CONCRETE	0.16	MASSIVE ICE	−2.3	50	0.010	INCREMENTAL	720
						100	0.086		
	SI	CONCRETE	0.25	"	−1 to −2	54	0.029	INCREMENTAL	2600
						65	0.058		
WOMICK AND LEGOULLON (1972)		STEEL	0.10	MASSIVE ICE	−1.0	62	0.10	STATIC	1750

Table 5.3 Summary of Pile Creep Test Data in Ice and Ice-rich Soils

Pile	Soil Type	Pile Diameter (m)	Temp-erature (°C)	Bulk Density (Mg/m^3)	Shaft Stress (kPa)	Test Duration (hr)	Pile Disp. at Time,t (mm)	Predicted Pile Disp at Time,t(mm) Suffield Clay[1]	Hanover Silt[1]	Ottawa Sand[2]	Manchester Fine Sand[2]
14	Varved Clay	0.035	-0.4	1.77	50	2800	0.3	0.35	0.009	0.19	0.089
16	Varved Clay	0.035	-0.4	1.77	110	800	0.19	1.5	0.036	0.39	0.32
24	V.Silty Snd	0.035	-0.4	1.91	130	1200	0.19	2.6	0.053	0.54	0.65
25	V.Silty Snd	0.035	-0.4	1.91	80	2000	0.05	0.97	0.021	0.33	0.25
					110	1400	0.27	1.8	0.039	0.45	0.46
26	Sandy Silt	0.035	-0.4	1.85	100	800	0.13	1.2	0.029	0.35	0.25
27	Sandy Silt	0.035	-0.4	1.85	60	1700	0.13	0.46	0.012	0.22	0.11
29	V.Sandy Slt	0.035	-0.4	1.9	100	1450	0.95	1.5	0.032	0.41	0.37
1	Sndy,Cly St	0.1	-0.3	?	70	2300	16.9	10.0	0.19	3.1	2.8
					30	130	0.75	1.1	0.024	0.51	0.054
12	Silty Clay	0.1	-0.15	?	10	400	1.0	0.16	0.004	0.19	0.008
22	Sndy,Sty Cl	0.1	-0.15	?	15	500	2.0	0.45	0.009	0.34	0.028
18	Snd+St+Cly	0.1	-0.4	?	50	900	3.25	5.5	0.079	1.5	0.58
13	Sty,Cly Snd	0.1	-0.7	?	75	1800	4.4	11.0	0.14	2.4	1.6
11	Snd+St+Cly	0.1	-0.9	?	100	8000	3.8	25.0	0.26	4.4	6.3

[1] Sayles(1968,1973)
[2] Sayles and Haines(1974)

Table 5.4 Summary of Pile Creep Data in Ice-poor Soils

Punch	Soil Type	Average Test Temperature (°C)	Net Applied Punch Load (kPa)	Observed Creep Rate, $\dot{u}_a/a$ (Yr^{-1})	Test Duration (Yr)
1	Silt and Sand	-0.05	80	0.0099	0.5
		-0.1	200	0.0101	6.0
		-0.15	200	0.0048	3.0
		-0.3	200	0.0013	3.0
		-0.7	200	0.0011	3.0
2	Silt and Sand	-0.1	200	0.023	0.46
		-0.2	325	0.016	0.3
		-0.32	325	0.0031	6.0
		-0.58	325	0.0035	5.0
		-0.7	325	0.0037	6.0
3	Clay, Silt and Sand	-0.12	350	0.045	0.5
		-0.2	350	0.020	0.4
		-0.48	350	0.0051	6.0
		-0.63	350	0.0056	4.0
		-0.79	350	0.0031	2.0
		-0.6	350	0.0031	2.0

Table 5.5 Summary of Punching Test Data (Vialov, 1978)

deformation behaviour of ice and ice-rich frozen soils may be approximately represented by steady-state creep and that the flow law for ice provides the upper limit to the flow law for ice-rich soil. In this light, the friction pile data have been interpreted as secondary creep and are presented in Figure 5.13 which relates the minimum recorded pile velocity to the average applied pile shaft stress. The tests were conducted for durations ranging from 24 to 26000 hours at -0.4 ^{0}C. At a given temperature, scatter in the data may be attributed to variations in duration of testing. At low stresses long durations are needed to establish approximately steady state conditions. From the data given by Vialov (1973) it can be seen that steady-state creep had been achieved after about 240 hours at a temperature of -2.3 ^{0}C, under an applied shear stress of 50 kPa. Long-term tests in ice at -0.4 ^{0}C (Vialov (1959)) resulted in steady-state conditions after 100 hours under an applied adfreeze loading of 100 kPa. In addition, the results of Dokuchayev and Markin (1972) indicated that steady-state conditions were established after 120 hours in ice-rich silt at an average ground temperature of -2.5 ^{0}C, under an average applied shaft stress of 170 kPa. This suggests that tests shorter than 250 hours are still dominated by transient creep and have been excluded from further analysis of steady state. To this extent, Figure 5.14 summarises the long-term creep data for ice and ice-rich frozen soil. Inspection of this figure reveals that the correlation is much improved but that the

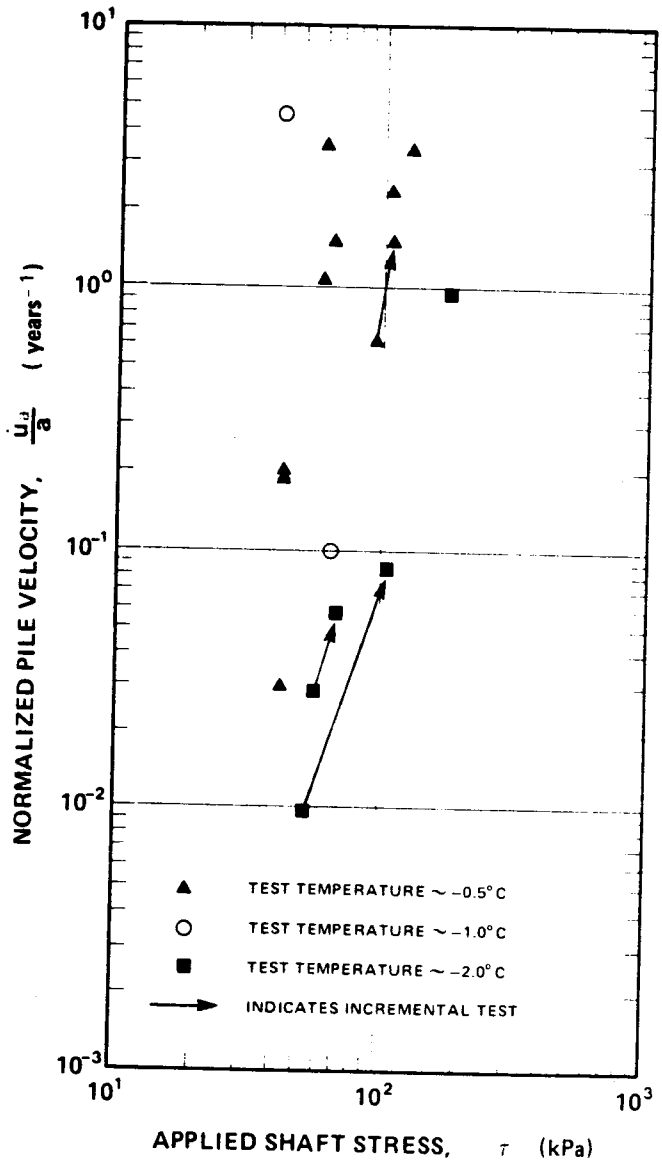

Figure 5.13

Summary of Reliable Pile Creep Data in Ice-Rich Frozen Soils

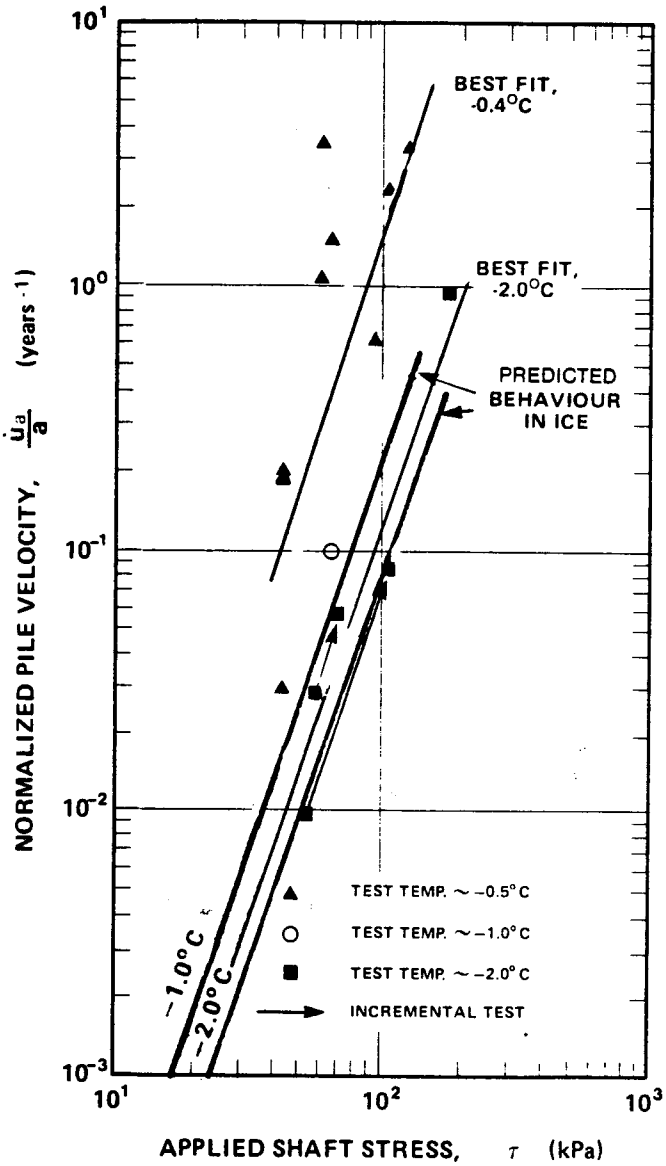

Figure 5.14

Summary of Long Term (> 250 hrs) Reliable Creep Data in Ice-Rich Soils

data are exclusively at -0.4 ^{0}C and -2.0^{0}C. Linear regression analyses have been performed at these two temperatures and the results are superimposed upon the data. The predicted pile velocities in ice are also shown in this figure. Comparison between predicted and observed pile creep is good, hence the available data support the application of the flow law for ice to pile design in ice and ice-rich frozen soils.

The end-bearing creep data in ice-rich frozen soils are presented in Table 5.5. The data is compared to the predicted behaviour in ice in Figure 5.15 which relates the normalised pile (punching) velocity to the applied end-bearing (punching) pressure. It is observed that the field creep rates are up to two orders of magnitude lower than the predicted behaviour in ice. Vialov (1978) reported minimal ice lensing at the test site. Thus, these data support the hypothesis outlined in Chapter 2 that creep rates in homogeneous ice lens-free, frozen silt (frozen bulk density = 1.77 Mg/m^{3}) are much lower than in ice. Further, it is observed that this discrepancy is reduced at temperatures very close to the melting point (-0.05 to -0.1 ^{0}C). This is attributed to the higher unfrozen water contents at these higher temperatures.

5.4.3 2 Ice-Poor Frozen Soils

The long-term deformation behaviour of ice-poor frozen soil is characterised by damped creep. The primary creep

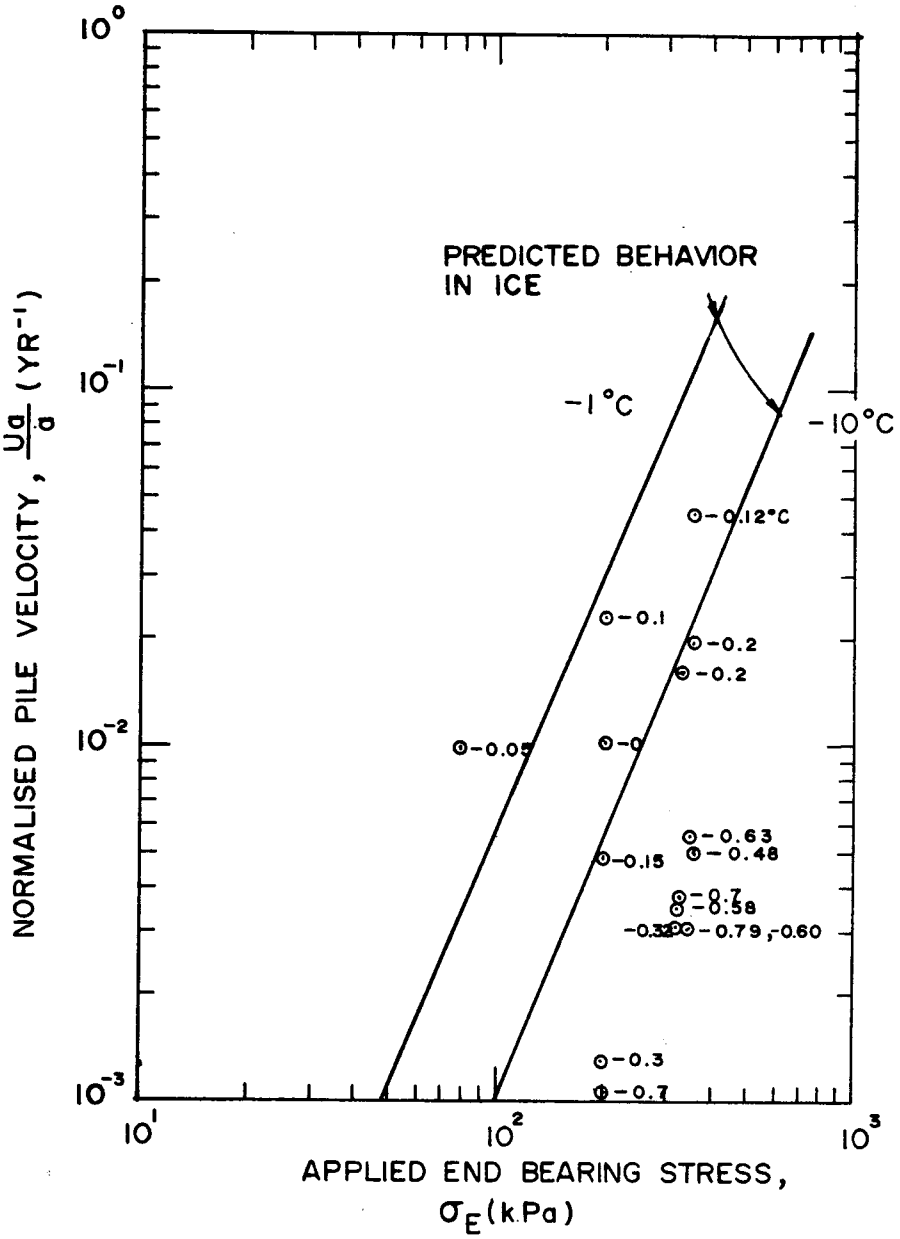

Figure 5.15

Summary of Punching Data in Ice-Rich Soils (Vialov (1978))

data for friction piles in ice-poor soils are summarised in Table 5.4. The data are presented in terms of the total normalised pile displacement, u_a/α, at the end of the test. Table 5.4 also includes the predicted normalised displacements for piles in frozen Suffield clay, Hanover silt, Ottawa sand and Manchester fine sand. It is observed that the predicted creep behaviour is consistent with actual behaviour, except for frozen fine-grained soils at temperatures very close to the melting point (−0.15 ^{0}C). At these temperatures observed settlements are greater than predicted settlements. This is attributed to a departure from the flow law (Equation 5.7) as a result of higher unfrozen water contents.

It is also observed that the pile creep data support the prediction that loose (as defined by density), ice-poor frozen silt is stiffer than ice-poor frozen sand. This behaviour was also inferred from results of pile load tests in ice-rich silt and ice-poor clay (Morgenstern (1978)) and from the results of the laboratory tests outlined in Chapter 4 where it was concluded that primary creep displacements in sand are greater than in silt. This behaviour is speculated as being attributable to the phenomenon of dispersion hardening in which silt-sized particles impede the movement of dislocations in ice, thereby inhibiting creep (Chapter 2).

It is demonstrated in Table 5.4 that the predicted and observed pile displacements are in good agreement but, in

order for the long-term behaviour to be accurately predicted, it is necessary to collate observed and predicted time exponents. Figure 5.16 summarises the time-displacement behaviour on a double logarithmic plot for pile tests in very sandy silt and clayey, silty sand (Vialov (1959)). The time exponents are determined to be 0.38 and 0.36, respectively. The corresponding predicted exponents are 0.39 and 0.37, repectively. Clearly, the data are in excellent agreement.

In summary, it is demonstrated that pile creep behaviour in ice-poor soils may be reliably predicted on the basis of laboratory creep data.

5.5 Summary

Two design approaches have been presented. The limiting strength design determines the embedment area such that the long-term adfreeze strength is not exceeded. The limiting settlement design determines the embedment area such that long-term creep settlements are tolerable within the life of the structure.

A critical and detailed analysis of the pile test data has confirmed the integrity of the proposed design techniques.

The relative importance of each design approach may be assessed by superimposing the allowable adfreeze strength curves for steel piles in ice, ice-poor clay, silt and sand on Figures 5.4 to 5.7, respectively. It is noted that in

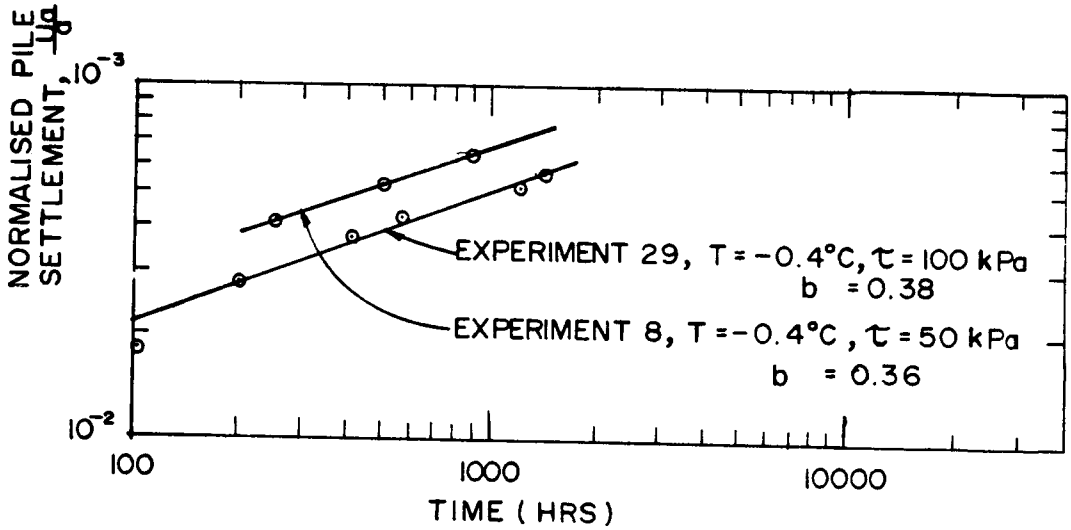

Figure 5.16

Summary of Pile Settlement/Time Data (Vialov (1959))

these figures the long-term adfreeze strength for steel piles is a function of temperature only. In this regard, the ordinate axis is meaningless.

Typically, the maximum allowable normalised pile velocity in ice and ice-rich frozen soils is 0.03 per year. This is represented as a horizontal line in Figure 5.4. Clearly, pile design in ice and ice-rich frozen soils is governed by settlement considerations.

Similarly, in ice-poor frozen soils adfreeze considerations will generally govern at colder temperatures. However, until more substantive data is available such a generalisation should not be used in practice; rather, it is recommended that the design be based on both settlement and adfreeze strength criteria.

5.6 Proposed Design Procedure

It is assumed that the pile type and emplacement method have been selected and that the ground conditions and loadings (Equations 3.2 and 3.3) have been defined. The proposed design guidelines are shown schematically in Figure 5.17 and described hereafter.

If competent bedrock is within practical piling distance of the ground surface then end-bearing piles are preferred and may be designed using temperate climate techniques. If this approach is either impractical or impossible then the piles must develop adequate bearing capacity in frozen or unfrozen soils.

Figure 5.17
Proposed Pile Design Procedure

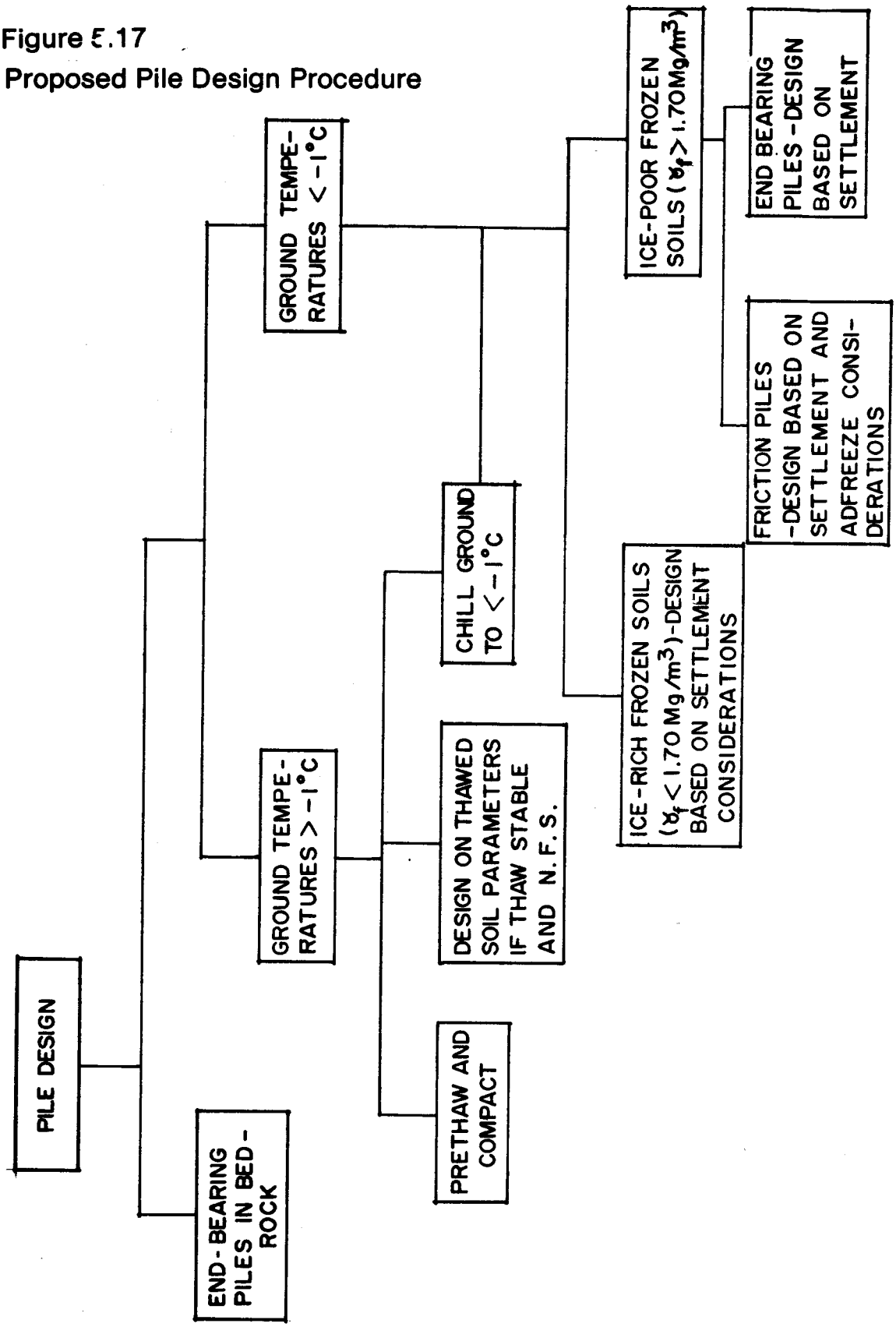

Settlement and strength properties of warm (greater than -1 ^{0}C) frozen soils are still poorly defined. Moreover, the thermal regime of such soils is in a delicate state of equilibrium. Thus, the presence of an impending structure and the changes induced by landscape modification will effect changes in the soil thermal regime, and in particular may cause some degradation of the permafrost. In this light, it is recommended that the embedment area be based only on temperatures colder than -1 ^{0}C. Therefore, in marginal permafrost areas where the ground temperature is warmer than -1 ^{0}C, special precautions must be taken and three design alternatives are available. First, if the permafrost is thaw-stable (i.e. clean coarse-grained frozen soils) then the design may be based on the unfrozen soil properties. Second, if the permafrost is thaw-unstable then the soil may be prethawed and compacted. In both cases there must be no crawl space between the structure and the ground surface. Third, the permafrost temperature may be lowered using artificial refrigeration. Pile design is then identical to that for cold permafrost.

If the ground temperature is colder than -1 ^{0}C, the following procedure is recommended. For piles installed in ice and ice-rich frozen soils (as a tentative guideline a soil is classified as ice-rich if its frozen bulk density, including segregated ice, is less than about 1.7 Mg/m^{3}) the embedment area is determined from Figure 5.4.

For piles installed in ice-poor frozen soils the design

may be based on either end-bearing or friction support but not both, because the relative displacement required to mobilise full end-bearing and full friction are not the same. The pile test results of Sivanbaev et al. (1977) support this statement. They reported results of incremental pile load tests on a wide range of pile-soil configurations and observed a distinct "plateau" effect in the load-settlement data. The authors also report that this has also been observed at several other locations in the USSR. The authors offer no explanation for this phenomenon; however, it is likely that this plateau effect corresponds to the delayed development of end-bearing beneath the pile tip.

For a friction pile the required embedment area is determined from both settlement and strength considerations. The allowable adfreeze strength may be estimated from Tables 5.1 and 5.2. It is emphasised that the allowable adfreeze strength must reflect the soil condition at the pile interface during operation. Thus, for slurried and steamed piles installed in winter it is recommended that the adfreeze strength be determined for piles in ice. Further, the adfreeze strength must be determined for the warmest soil conditions throughout the design life.

In order to satisfy the settlement criteria it is necessary to determine the flow law parameters as defined by Equation 2.7. If representative creep test data are not available then the embedment area may be inferred from the

design charts for ice-poor clay, silt and sand, presented in Figures 5.5 to 5.7, respectively. These charts are based on the results of tests on very loose frozen samples and thus, are considered to provide the upper limit for predicted creep displacements of piles in ice-poor clay, silt and sand at ground temperatures less than -1 ^{0}C, respectively.

The approaches are almost certainly conservative but this should not preclude the application of a factor of safety. It is recommended that the safety factor be applied to the embedment area. Its magnitude will depend upon the constuction control and, more importantly, the accuracy of the determined design parameters.

Finally, this chapter has only dealt with the support capacity aspect of design. There are many other aspects of design such as thermal considerations, estimation of downdrag loading during thawing and, of course, frost-heave loading during freezing. These concerns were reviewed in Chapter 3.

CHAPTER 6

ANALYTICAL STUDY OF PILE DRIVING IN PERMAFROST

6.1 Introduction

Direct driving is the preferred installation method. Both H piles and open-ended piles have been driven successfully in homogeneous fine-grained frozen soils using conventional impact driving equipment. However, serious setbacks have been encountered in dense coarse-grained frozen materials (Woodward-Lundgren (1971) and Crory (1973)). This prompted Woodward-Lundgren to undertake an extensive field piling program to determine the most efficient driving procedures. During the course of this study, 13 piles were driven into predrilled holes of diameter 0.7 times the pile diameter and 55 piles were driven directly into permafrost. It was determined that the success rates for driving directly into permafrost and into predrilled holes, in fine-grained frozen soils containing isolated gravel strata, were 35 % and 70 %, respectively. The authors anticipated that predrilling the holes to 85 % of the pile diameter would have ensured a success rate of 100 %. The authors concluded

> "Frequently both pipe and H piling were distorted during driving. The H pile exhibited particularly bad directional characteristics in that they frequently deflected perpendicular to the minor axis when an obstruction was encountered. Under similar

conditions pipe piling deformed radially near the tip but maintained direction"

As a result of this study Woodward-Lundgren concluded that driving piles to a prescibed depth, without predrilling, is not practical.

Davison et al. (1978) have observed that H piles will deform under sustained driving in dense frozen soils using hammer energies in excess of 22000 ft.lbs. However, they suggest that high driving stresses may be tolerated if the column axis is reinforced with steel angles welded to the web of the pile. Using this technique, the authors report that pile failure did not occur even when piles were driven at 3300 blows per metre using a Delmag D-22 (Rated Energy, 39800 ft.lbs). The authors conclude that this pile type may be satisfactorily driven in dense coarse-grained strata by predrilling a 0.1 to 0.15 m diameter pilot hole.

During impact driving most of the energy is expended in breaking down the soil structure, with only a small fraction transferred to the soil as thermal energy. Thus, only partial thawing of a very thin layer of soil occurs along the pile surface. During vibratory driving the pile undergos 10 to 20 vibrations a second and owing to the high frequency of each blow the energy cannot be diffused and concentrates in the soil in the immediate vicinity of the pile, thus effecting an increase in temperature and thawing of the soil. This thawed soil has been observed to be in excess of 0.1 metres (Vialov et al. (1969)).

In frozen fine-grained soils pile driving outpaces thawing and hence the pile point continually penetrates frozen ground (Vialov et al. (1969)). Further, as a result of frictional heat generated along the lateral surface of the pile, the adjacent soil is maintained in a thawed state thus minimising shaft resistance and thereby facilitating driving. This is supported in the field by Vialov et al. (1969) who observed that driving rates were invariant with depth and that liquefied soil is continually squeezed out at the ground surface during vibratory driving.

Huck and Hull (1971) report that the BRD-100 proved very successful in driving H and pipe piles into fine-grained frozen soils. They observed driving rates in massive ice of 1.0 m/min. However, difficulties were encountered when driving pipe piles into bouldery permafrost. The authors report that the boulders "plugged up" the bottom of the pipe and thus the pipes were driven essentially as displacement piles.

In coarse-grained frozen soils the pile advancement rate is commonly less than 10 cm/min (Vialov et al. (1969)) and driving does not outpace thawing. In such soils, driving is considerably facilitated by a reduction in soil strength following an increase in soil temperature.

It is anticipated that pile advancement by vibratory driving in dense granular frozen soils will only occur when the soil around the pile tip is thawed and the soil particles are able to undergo liquefaction. Thus, pile

advancement rates in these soils are expected to be less than for the identical soil in the thawed state.

Vialov et al. (1969) report that square reinforced concrete piles can be driven into heavy gravelly loam at a rate of 5 to 8 cm/min using the S-838 vibratory driver. They also report that driving is only marginally assisted by predrilling. However, it is likely that in gravelly frozen soils vibratory driving will result in less soil extrusion at the ground surface thus driving in such soils may be expedited by predrilling.

Despite the widespread success of using vibratory techniques to drive piles in the USSR and to advance boreholes in Canada and the USSR, piles are rarely driven in the vibratory mode in North American permafrost. The recent experience acquired in Alaska (Woodward-Lundgren (1971), Crory (1973), Crory (1975) and Davison et al. (1978)), with regard to impact driving, is largely responsible for the recent upsurge in impact pile driving in permafrost. However, there is still skepticism regarding vibratory driving in permafrost in North America. This exists as a result of the limited field experience and has been enhanced by mechanical problems experienced using conventional vibratory equipment in arctic environments (Woodward-Lundgren (1971)).

The intent of this chapter is to study pile driving using the wave equation analysis. The documented records for impact driving in frozen soils are analysed in order to

construct an appropriate soil model for use in the analysis. The extension to vibratory piling in permafrost is a complex thermal-vibration interaction problem and is beyond the scope of this thesis. However, an analytical approach to this dynamic problem is outlined at the end of this chapter.

6.2 Analysis of Impact Pile Driving Using the Wave Equation

Smith (1962) proposed that the stresses induced in a pile, being driven by an impact hammer, could be described as a wave or pulse travelling along the pile length. The theory for the one-dimensional wave equation has been summarised by Holloway (1975). The governing equation is

$$c^2 \frac{\partial^2 u}{\partial x^2} = \frac{\partial^2 u}{\partial t^2} \qquad \text{.....6.1}$$

where c is the velocity of wave propogation, u is the element displacement, x is the coordinate location of a point along the rod and t is the time. This has been analysed using a finite difference procedure by Smith (1962) and Bowles (1974), and more recently using a finite element procedure by Holloway (1975). The finite difference approach is simpler and has been adopted in this study.

A finite difference approximation to the above differential equation discretizes the physical problem into small segments. The pile is divided longitudinally into discrete masses, interconnected by springs. A complete description of the finite difference approximation is given

by Smith (1962) and Holloway (1975). In order to apply this procedure to the pile driving problem the physical characteristics of the hammer, capblock, pile cap and pile are handled in the same way as recommended by Smith (1962). Smith (1962) modeled the soil resistance by means of the elastic quake, Q, the ultimate ground resistance, $R_{ult}(t)$, and the viscous damping constant, J. These terms are defined in detail in his paper.

Frozen soils are visco-elastic, hence the ground resistance is a function of the time-to-failure. The ultimate strength/time-to-failure relationship for frozen soils, at very high strain rates, has been summarised in Chapter 2 and is given by Equation 2.8. Therefore, in order to determine the soil resistance acting on an element, i, the time-to-failure (or strain rate) of the adjacent soil must be known. This may be determined from the elastic quake and the element velocity, v_i,

$$t_{f_i} = \frac{Q}{v_i} \qquad \text{.....6.2}$$

Bowles (1974) demonstrated that for unfrozen soils the solution is only slightly sensitive to the selected value of quake and that satisfactory results are obtained if Q is selected between 2.5 and 3.8 mm. In this analysis the quake is assumed to be 2.5 mm.

A convenient simplifying assumption is to neglect shaft friction. This is a valid assumption for steel piles driven

into frozen clays, silts and sands, where the thawed slurry imposes negligible shaft resistance. This assumption is supported by field evidence which indicate that the blow counts are invariant with depth (Crory (1975)). Therefore, in this study shaft resistance has been neglected.

The ultimate ground resistance, R_{ult} , of a frictionless soil beneath a deep circular footing may be related to the soil unconfined compressive strength by the relation

$$R_{ult} = 2.57 \sigma_{cu} \qquad \text{.....6.3}$$

Thus, at any time, t, the soil resistance at the pile tip may be determined as a function of the velocity of the pile tip.

The laboratory results of high strain rate tests on frozen silts(Haynes et al. (1975) and Haynes and Karalius (1977)) indicate that for times-to-failure greater than approximately 0.4 seconds, the compressive strength is insensitive to the applied strain rate. This implies that when the pile tip velocity is less than 6 mm per sec, the soil resistance assumes a constant value, R'_{ult} . Therefore, during rebound of the pile tip the soil resistance is a linear function of R'_{ult}

$$R_{ult} = \left(\frac{D_n - D'_n}{Q}\right) R'_{ult} \qquad \text{.....6.4}$$

where D is the tip displacement and D^1 is the soil plastic displacement at the pile tip.

It is assumed that when $D < D^1$ the resistance at the pile tip is equal to zero. In other words, the pile tip cannot transmit tensile forces to the underlying frozen soil.

In summary, the analysis presented herein is identical to Smith's formulation, with the exception that a new soil model has been introduced. This analysis is most conveniently executed using a computer. A listing of the program is presented in Appendix D.

6.3 Parametric Studies

Since the selection of Q is somewhat arbitrary it is of interest to study the influence of Q in terms of the overall solution. Such a study was conducted for a 10.7 m 10BP57 steel pile driven into ice (temperature = 0 ^{o}C) using a Delmag D-12 driver. The pile details are summarised in Table 6.1. From the data of Hawkes and Mellor (1972) the compressive strength of ice is given by

$$\sigma_{cu} = (5300 - 665T)t_f^{(-0.265-0.013T)} \qquad \text{.....6.5}$$

where T is the temperature in degrees centigrade. Thus at 0 ^{o}C

$$\sigma_{cu} = 5300 t_f^{-0.265} \qquad \text{.....6.6}$$

Pile				Capblock			Pile Cap			Hammer
Stiffness (MN/m)	Length (m)	Area (cm^2)	Density (Mg/m^3)	Coeff. of Rest.	Stiffness (MN/m)	Weight (Mg)	Coeff. of Rest.	Stiffness (MN/m)	Weight (Mg)	Velocity (m/s)
698	10.67	108	7.86	0.5	358	2.5	1.0	358	0.34	6.26

Table 6.1 Pile and Pile-driver Details for Parametric Study

Source	Pile				Soil		
	Stiffness (MN/m)	Length (m)	Area (cm^2)	Density (Mg/m^3)	Soil Type	Bulk Density (Mg/m^3)	Temperature (°C)
Crory (1973)	698	5.33	68.3	7.86	Silty Sand	2.08	-1.7
Crory (1975)	698	10.67	108	7.86	Silt	1.58	-0.25

Table 6.2 Summary of Pile Driving Case Histories

The quake was varied from 0.25 to 4.0 mm. The results are presented in Figure 6.1. Inspection of this figure indicates that the calculated blowcount is only mildly sensitive to the quake.

The parametric study was extended to study the effect of ground temperature. The results are presented in Figures 6.2 and 6.3 which give the variation of blowcount with temperature and the variation of bearing stress with time since moment of impact, respectively. As expected, the maximum bearing stress increases with decreasing temperature from 230 MPa at -10 ^{0}C to 85 MPa at -1 ^{0}C.

Therefore, using the wave equation analysis it is possible to predict whether the pile tip will be damaged during driving. The wave equation may also be used to determine tensile stresses in a concrete pile thus providing a basis for designing the tensile reinforcement.

6.4 Comparison of Predicted Driving Behaviour With Actual Field Driving Records

Crory (1973) reported driving records for 8BP36 steel piles driven into frozen silty sand. Six piles were driven using a Delmag D-12 diesel hammer. The hammer had an overall weight of 5290 lbs, including a 2750 lb piston and a 754 lb anvil. Energy output per blow was 22600 ft.lbs. Cushion blocks were not used. Pile and pile driver details are summarised in Table 6.2. The actual blowcount was measured to be 72 blows/m. The predicted blowcounts are 29 and 39

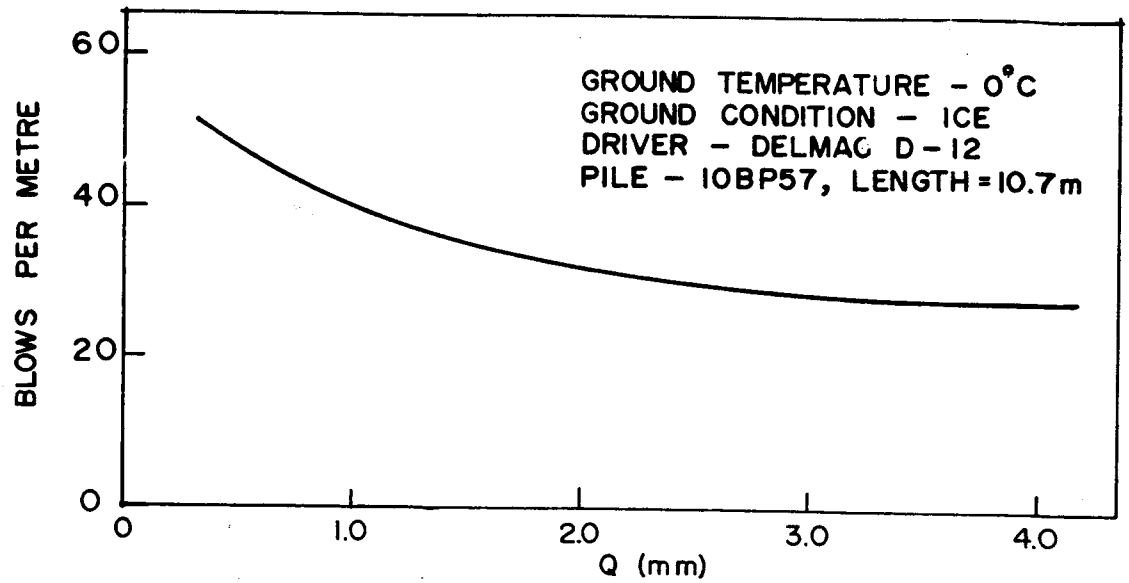

Figure 6.1
Blow Count Versus Quake

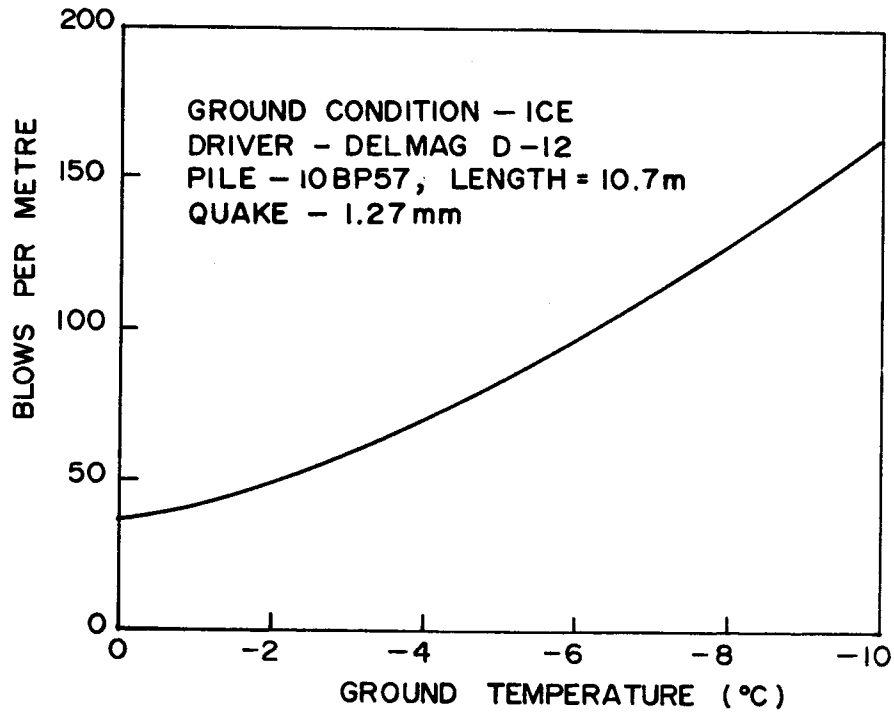

Figure 6.2
Blow Count Versus Ground Temperature

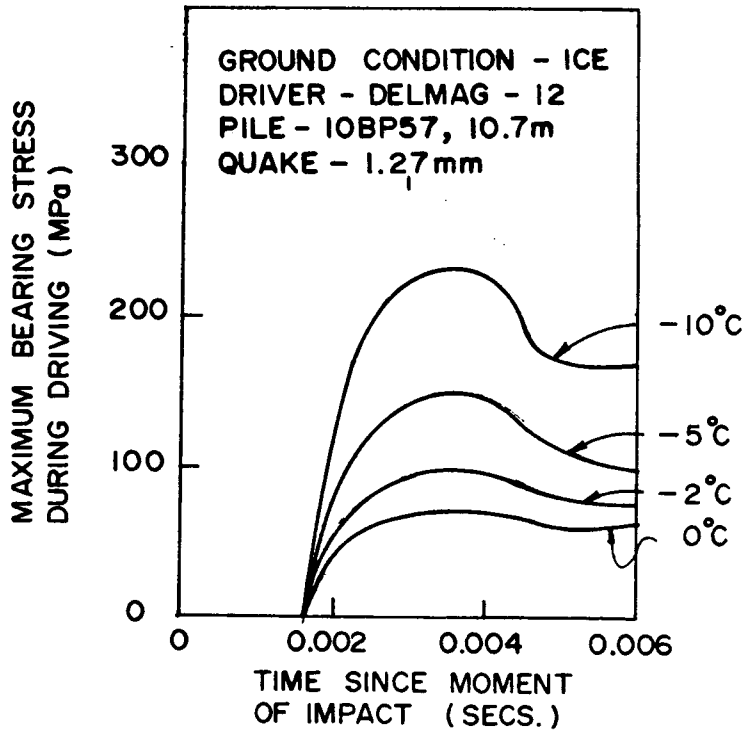

Figure 6.3
Maximum Bearing Stress Versus Temperature

blows/m in ice-poor silt and ice, respectively.

Crory (1975) reported driving records for 10BP57 steel piles driven in ice-rich silt. Eight bridge foundation piles were driven with a Delmag D-12 diesel hammer. The hammer specifications for this hammer were given in the preceding paragraph. Pile and pile driver details are summarised in Table 6.2. The average blowcount was measured to be 46 blows per m. The predicted blowcounts are 36 and 62 blows/m in ice-poor silt and ice, respectively.

The agreement between predicted and observed behaviour is excellent, thereby endorsing the accuracy of the proposed analysis.

6.5 Overview

The strength behaviour of frozen soil is strongly time-dependent and at present, the dependence of soil strength on the strain rate in the stress fracture range is poorly defined. Therefore, it is not possible to determine allowable bearing capacities on the basis of driving records.

A soil model has been proposed for use in the wave equation analysis. This model incorporates time-dependent fracture strength behaviour. It has been demonstrated that an accurate estimate of the blowcount can be obtained by introducing this model into the wave equation analysis. The wave equation also provides a means of estimating the maximum compressive and tensile stresses in the pile during

driving.

It transpires that the ground temperature is not as important a variable in influencing pile driveability as has been suggested in the literature. The only significant influence that ground temperature has on pile driving is to alter the penetration rate during driving.

The wave equation theory may be extended to analyse vibratory pile driving. Rockefellor (1967) pursued this approach to determine resonant piling frequencies in unfrozen soils. It seems reasonable to assume that this type of approach could be used in fine- and medium-grained frozen soils where pile penetration rates are high and soil thermal changes may be neglected. However, in coarse-grained frozen soils pile penetration rates are low and appreciable ground temperature changes occur as the thermal energy accumulates around the pile. Thus, the pile is slowly driven through unfrozen soil. Clearly, this is a complex thermal-resonance problem.

Finally, on the basis of the evidence presented in this chapter, there is no reason to suggest that piles cannot be practically vibrated through even the densest of frozen soils.

CHAPTER 7

CAST-IN-PLACE CONCRETE PILES IN PERMAFROST

7.1 Introduction

Cast-in-place concrete piles offer two major advantages over slurried and driven piles. First, appreciable end-bearing support may be realised by a belled pile. Second, installation of cast-in-place piles can be effectively controlled to produce a smooth-flowing, efficient piling program which is of prime concern in major piling operations.

However, cast-in-place piles have seldom been used in permafrost regions. The problems of setting and strength gain of the concrete and of thawing and refreezing of the surrounding frozen ground, as well as frost-heaving of the piles in the active layer, have discouraged design engineers from using concrete piles. However, the frost heave problem may be circumvented by isolating the pile through the active layer and the development of gypsum-based oil-well and calcium fluoroaluminate portland cements has overcome many of the shortcomings of cementing in permafrost. The intent of this chapter is to assess the suitability of cements for northern construction and so define the use of cast-in-place concrete piles in permafrost.

7.2 A Review of Arctic Cements

Cements vary due to the raw materials used, the percentage composition of chemical compounds and particle-fineness. Some cements are designed with specific properties for special construction tasks. Cements produced by different manufacturers may have widely different workabilities, strengths, setting characteristics and durability properties.

In order that a cement may be successfully applied in cold environments one basic criterion must be satisfied. The mixing water in the cement must not freeze prior to curing. There are essentially three ways of overcoming this problem. First, the temperature of the cement may be artificially maintained above 0 ^{0}C using external heat sources. This is expensive and is impractical for sub-surface cementing in frozen soils. Second, the heat of hydration may be utilised to maintain the temperature of the cement above 0 ^{0}C. Third, sodium or calcium chloride may be added to the cement to prevent freezing of the mixing water.

At present, there are only three types of cement that satisfy these conditions. Calcium aluminate and calcium fluoroaluminate cements utilise their high heats of hydration to prevent freezing, and gypsum-based oil-well cements contain salts to depress the freezing point of the mixing water.

Laboratory testing has shown that calcium aluminate cements deteriorate when subjected to continuous freeze-thaw

cycles (Cunningham et al. (1972)). Thus, high-alumina cements are unsuitable for permafrost cementing.

Calcium fluoraluminate or regulated-set cement, "reg-set" for short, is a recent development of the Portland Cement Association. Houston and Hoff (1975) describe it thus,

> "It is not a mixture of cements or an admixture, but it is a portland cement with some new ingredients blended in the kiln. The principle difference between reg-set and ordinary portland cement is that regulated-set cement contains a new ingredient, calcium fluoraluminate, which provides very high early strength. Associated with the development of this high early strength is the liberation of large quantities of heat."

The high heat of hydration enables the cement to gain its initial set within a few hours and at ambient temperatures as low as -9.4 ^{0}C. Unfortunately, the National Gypsum Company has halted production of this cement and at the time of writing (June, 1979) it is manufactured only in Japan and Germany.

Gypsum portland cement blends offer an effective cement mixture for cementing oil wells in permafrost. It is available under the trade names, Permafrost cement, Arctic set and Cold set. Cunningham et al. (1972) describe it thus

> "Permafrost cement is a blende of controlled set gypsum cement, API Class G cement, salt, a

dispersant and chemical additives to control thickening time."

A sixty percent gypsum and forty percent API class G blend is commonly used. Gypsum provides early strength, even at low temperatures, while the class G constituent gives additional later strength. The salt prevents the mixing water from freezing prior to curing.

In summary, there is potential for both permafrost cement and "reg-set" cement for use in sub-surface concreting in frozen soils. However, as mentioned previously reg-set is no longer produced in North America. Therefore, the remainder of this chapter will explore the possibility of using permafrost cement as a binder for structural concrete for cast-in-place piling.

7.3 Requirements for a Successful Cement for Use in Constructing Cast-in-Place Concrete Piles in Permafrost

The following criteria must be satisfied in order that a cement may be used successfully to construct cast-in-place concrete piles.

1. The concrete must be able to set at below-zero temperatures.
2. The mixing water must not freeze prior to curing.
3. The concrete must develop adequate compressive strength.
4. The heat of hydration must not cause excessive thermal disturbance to the permafrost.
5. The concrete must be stable to repeated freeze-thaw

cycles.

6. Adequate bond strength must develop between the concrete and the permafrost.

7.4 Evaluation of the Use of Permafrost Cement to Construct Cast-in-Place Concrete Piles

Permafrost cement was designed specifically to meet the needs of the petroleum industry. There is no documented evidence that this cement has been used in structural concrete.

7.4.1 Setting Characteristics

Maier et al. (1970) have confirmed that this cement will hydrate satisfactorily, without freezing, at temperatures as low as 15 ^{0}F (-10 ^{0}C).

7.4.2 Determination of Compressive Strengths of Permafrost Cement Concrete

A laboratory test program was established to evaluate the most suitable design mix for cold weather concreting. The aggregate consisted of standard concrete sand.

The experimental work in this section was accomplished in two phases. Phase 1 involved the evaluation of 12 concrete mixes made at varying water/cement ratios (0.4, 0.5, and 0.6) and varying sand/cement ratios (3.33, 4.0, 4.86, and 6.0). A test specimen (7.62 cm diameter by 15.2 cm long) was prepared from each mixture. Slurry temperatures varied between 3 ^{0}C and 8 ^{0}C. A thermistor was installed in

the centre of each cylinder and temperature was monitored during the first 24 hours of curing.

Temperature-time curing curves are summarised in Figures 7.1 to 7.4. The following conclusions may be inferred from these data,

1. Initial set was achieved after 4 to 6 hours.
2. Heat of hydration effected temperature rises of 1.4, 2.1, 2.5 and 4.0 ^{0}C for sand/cement ratios of 6.0, 4.86, 4.0 and 3.33, respectively.
3. For a given sand/cement ratio the heat of hydration was approximately insensitive to variations in the water/cement ratio.

The unconfined compressive strength of each cylinder was determined after seven days. The results are presented in Table 7.1.

The compressive strength and workability of the concrete mixtures were used as indicators to determine the mixtures most suitable for cast-in-place concrete piling. The following 2 water/cement/sand ratios (by weight) were selected, 0.45/1/2.75 and 0.45/1/3.0.

Phase II involved a more rigorous determination of design strengths for the 2 selected mixes. Three specimens (7.62 cm diameter by 15.2 cm long) were made from each slurry. The cylinders were cured at a temperature of -3 ^{0}C. Compressive strengths were determined after 7 days and are summarised in Table 7.2. The mean 7-day compressive strengths, corresponding to sand/cement ratios of 2.75 and

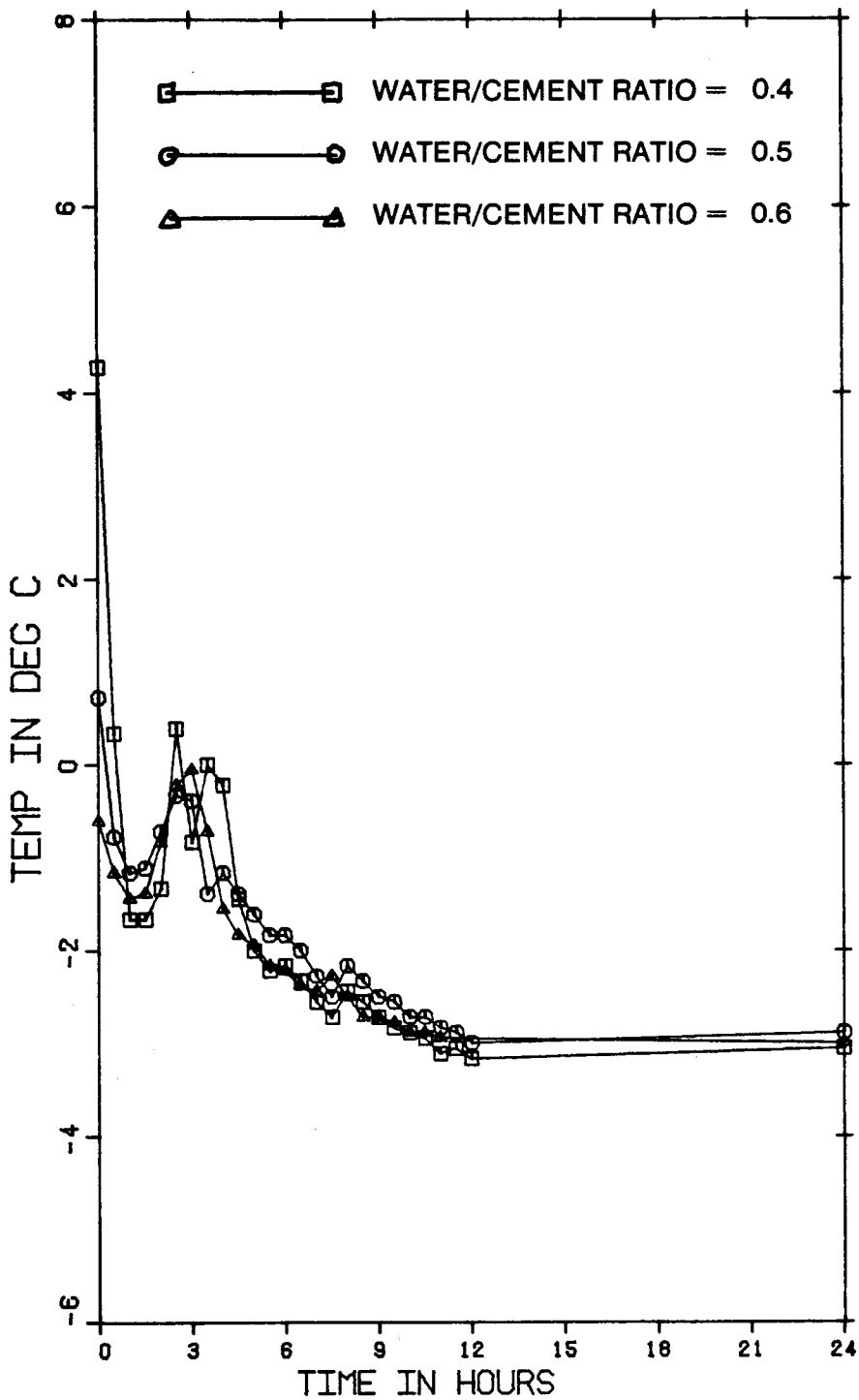

Figure 7.1

CURING CURVES FOR A CEMENT:SAND RATIO OF 1:6

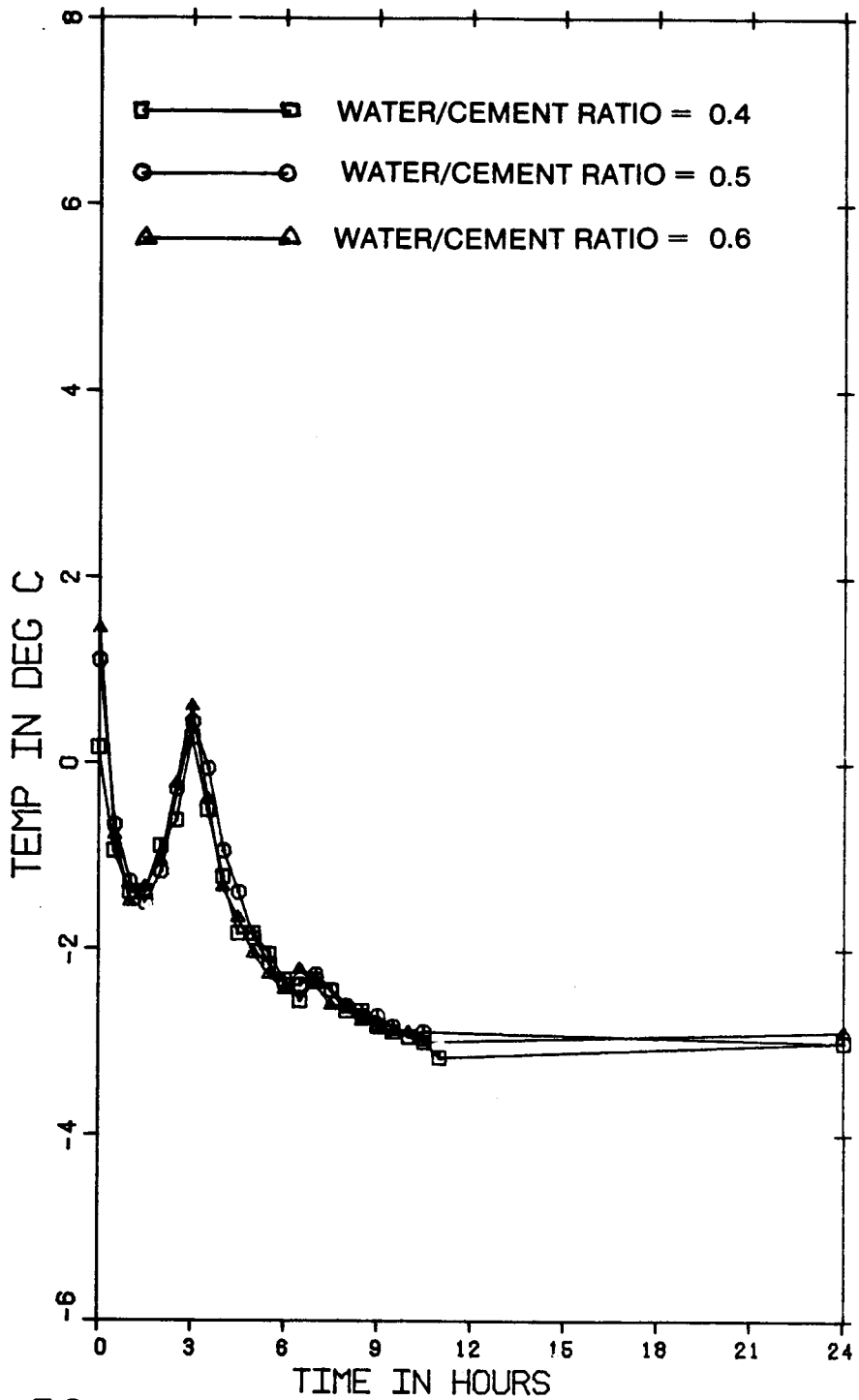

Figure 7.2

CURING CURVES FOR A CEMENT:SAND RATIO OF 1:4.86

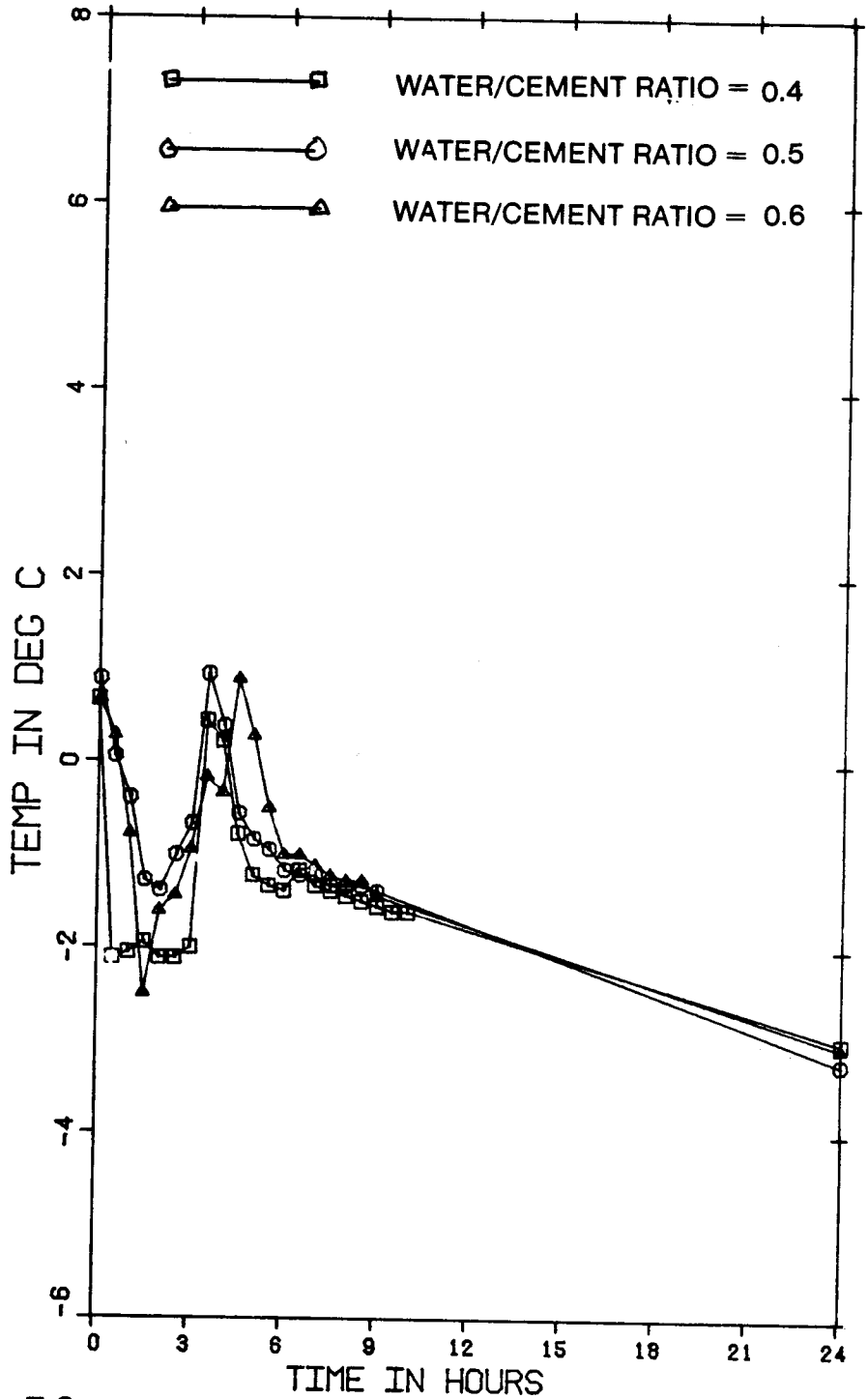

Figure 7.3

CURING CURVES FOR A CEMENT:SAND RATIO OF 1:4

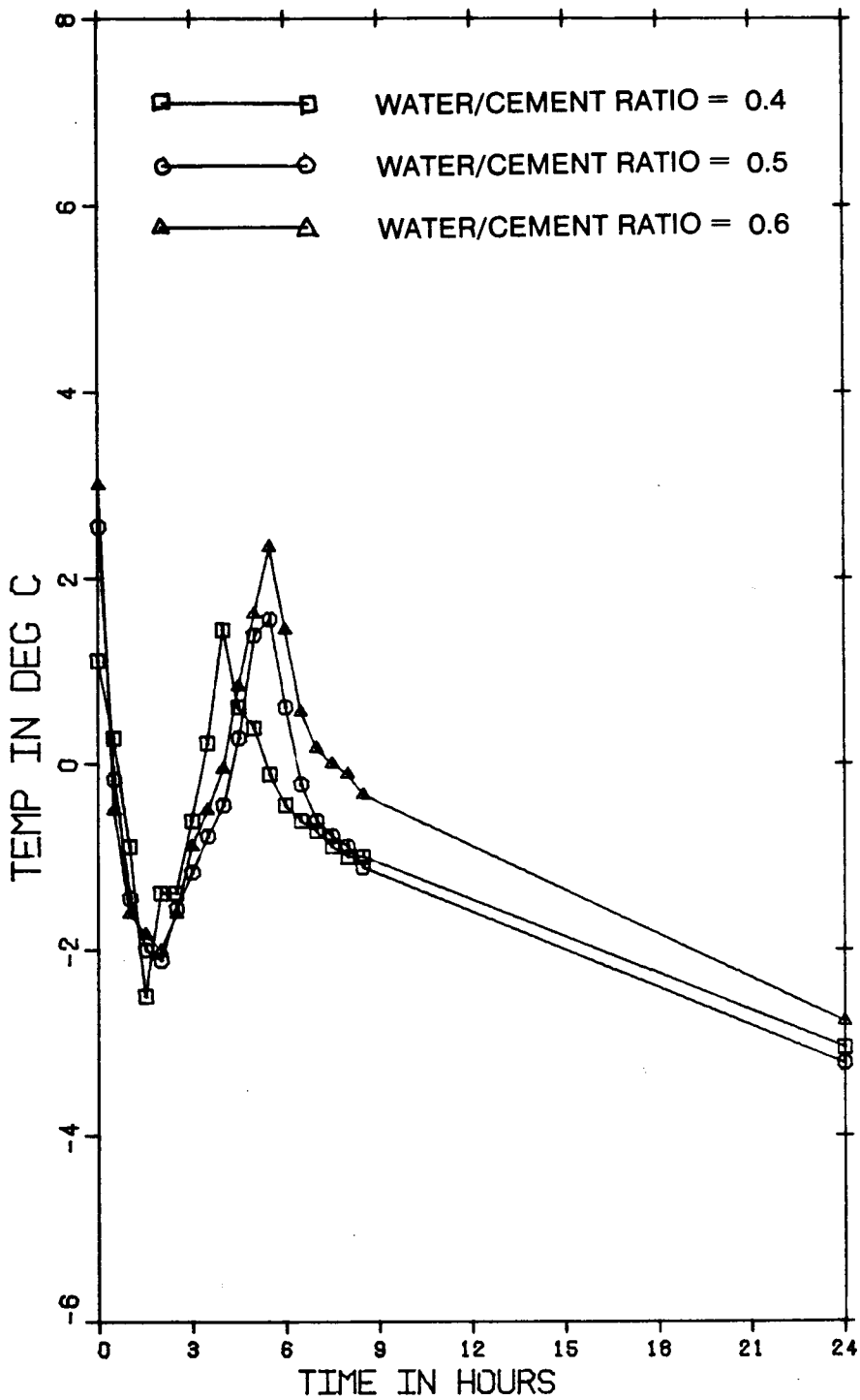

Figure 7.4

CURING CURVES FOR A CEMENT:SAND RATIO OF 1:3.33

Sample Number	Water/Cement Ratio (gm/gm)	Cement/Sand Ratio (gm/gm)	Bulk Density (Mg/m^3)	Compressive Strength (MPa)	Comments
1	0.4	0.17	1.87	2.47	Very dry mix, porous
2	0.5	0.17	1.96	3.38	Very dry mix, porous
3	0.6	0.17	2.06	4.04	Dry mix, porous
4	0.4	0.21	2.01	5.55	Dry mix, porous
5	0.5	0.21	2.08	6.54	Medium dry mix, porous
6	0.6	0.21	1.96	4.43	Medium dry mix, many air bubbles
7	0.4	0.25	2.15	8.53	Medium dry mix, a few air bubbles
8	0.5	0.25	1.99	6.68	Good consistency, many air bubbles
9	0.6	0.25	1.94	3.65	Wet mix, many air bubbles
10	0.4	0.33	2.13	8.98	Good consistency, a few air bubbles
11	0.5	0.33	1.97	6.55	Wet mix, many air bubbles
12	0.6	0.33	1.88	2.84	Wet mix, many air bubbles

Table 7.1 Summary of 7-day Cylinder Compressive Strengths - Phase 1

Sample Number	Water/Cement Ratio (gm/gm)	Sand/Cement Ratio (gm/gm)	Bulk Density (Mg/m^3)	Slump (cm)	Compressive Strength (MPa)
2-1a	0.43	3.0	2.06	18	9.54
2-1b	0.43	3.0	2.06	18	9.14
2-1c	0.43	3.0	2.09	18	10.04
2-2a	0.44	2.75	2.09	9	11.8
2-2b	0.44	2.75	2.09	9	12.2
2-2c	0.44	2.75	2.08	9	12.3

Table 7.2 Summary of 7-day Cylinder Compressive Strengths - Phase 2

3.0, were found to be 12.1 and 9.57 MPa, respectively.

7.4.3 The Effect of Cement Hydration on the Thermal Regime of the Permafrost

The heat of hydration of permafrost cement is specified to be 10000 cal/kg (Inland-Halliburton (1978)). The calculations outlined in Appendix E demonstrate that during curing the thawed annulus around a 0.5 m diameter permafrost cement concrete pile cast in ice will not exceed 9 mm. The analysis ignores sensible heat and is, therefore, conservative. Similarly, the thawed annulus around a 0.5 m diameter pile in permafrost (comprised of 20 % ice by total weight) was found to be less than 20 mm.

The results indicate that curing of permafrost cement concrete in frozen soils will not be detrimental to the thermal stability of the surrounding permafrost.

7.4.4 The Effect of Repeated Freeze-Thaw Cycles on the Compressive Strength of "Permafrost Cement" Concrete

The stability of permafrost cement to repeated freeze-thaw cycles has been investigated by Anderson (1971a) . Compressive strengths were periodically determined throughout the test period (26 days). Anderson (1971a) concluded

> "...Permafrost cement appears most durable...no cracking of the samples occurred and there was a general increase in compressive strength throughout

the test period."

7.4.5 Evaluation of the Adfreeze Bond Between Permafrost Cement Concrete and Permafrost

There are two issues that must be examined in relation to the development of adequate bond strength between permafrost cement concrete and frozen soil.

The first concern entails studying the influence of salt, intrinsic in the cement, on the adfreeze bond. This issue has been addressed by Halliburton Services Limited who have conducted pull-out tests on cement columns cured in ice (Anderson (1971b)) and frozen sand and gravel (Anderson (1971c)). Adfreeze strengths were reported to vary from 21 to 1990 kPa for ice and from 1740 to 2830 kPa for frozen sand and gravel. Ambient temperatures and loading rates were not given. However, it is probable that the samples were tested immediately after removal from the curing environment and thus, the temperature at the cement-soil (ice) interface would be similar to the temperature at which they were cured which was reported to be -6.7 ^{0}C.

Ambient temperatures in the field are typically warmer than -5 ^{0}C and therefore, this study is not representative of many field conditions. The influence of salt on the adfreeze bond strength is very sensitive to temperature and in warm permafrost salt contamination of the frozen soil, adjacent to the cement, will prevent complete freezeback thereby reducing the adfreeze bond strength.

Second, the possibility of mixing of the freshly placed

concrete mixing with the soil, during curing, must be examined as this may result in weakened concrete at the pile/soil interface.

A simple laboratory test program was undertaken to study the above concerns. A rectangular column (7.5 cm by 5 cm by 45 cm) of permafrost cement concrete was mixed at a water cement ratio of 0.44 and a sand/cement ratio of 2.75 and allowed to cure while in contact with one face of a vertical rectagular column (7.5 cm by 10 cm by 45 cm) of pseudo-layered frozen soil comprising of 20 cm of frozen sand (moisture content = 20 %), overlying 5 cm of ice, overlying 20 cm of frozen silt (moisture content = 70 %). Prior to placement of the concrete slurry the vertical face of the frozen soil was carefully trimmed to produce a uniformly smooth contact surface. The initial temperatures of the concrete slurry and frozen soil were 5 ^{0}C and -3 ^{0}C, respectively. The specimen was allowed to cure at -3 ^{0}C and after 3 days the interfaces were inspected. It was observed that the simulated permafrost had not completely frozen back to the concrete surface. The concrete and frozen soil were separated by a 2 mm zone of unfrozen saline soil. Therefore, it is concluded that salt does diffuse into the surrounding permafrost, thereby contaminating the pore water and thus preventing complete freezeback. This diffusion process probably occurs during the pre-hydration period when the mixing water is free to migrate into the thin zone of thawed soil which is produced when the concrete slurry placement

temperature is above 0 ^{0}C.

There was no evidence of contamination of the concrete by the thawed materials. In fact, no visible soil sloughing had taken place even adjacent to the ice-silt and ice-sand interfaces.

7.5 Discussion

The preceding brief review has shown that permafrost cement concrete will set and cure at below zero temperatures and develop adequate compressive strength to support structural loads. The concrete is also stable to freeze-thaw cycling and is not detrimental to the thermal stability of the permafrost.

However, the laboratory testing program has demonstrated that the cement does have an adverse effect on the adfreeze bond strength between the concrete and permafrost. A thawed zone of saline soil was observed at -3 ^{0}C around the permafrost cement concrete. The significance of this contamination is unclear. However, it is speculated that in cold permafrost (less than -6.7 ^{0}C), the thickness of this unfrozen saline film is decreased and under such conditions the pile may be capable of transferring structural loads to the frozen soil. Furthermore, the degree to which the thawed zone controls the adfreeze strength would certainly be reduced as the roughness of the pile is increased.

Clearly, a comprehensive field study of this salt contamination problem must define allowable adfreeze strengths before this construction method can be considered as a viable piling alternative. However, it does appear from this preliminary study that the cement does have potential for use as a construction material for belled and tapered piles and footings placed directly on frozen ground. The governing factor in such cases will be the concrete strength.

CHAPTER 8

INTERPRETATION OF PILE CREEP TESTS

8.1 Introduction

There are several issues that complicate the interpretation of field pile creep data. The major concern relates to the reliability of predicting long-term behaviour from short-term pile creep tests. This concern is particularly apparent when testing frozen-in timber piles since Nixon and McRoberts (1976) have suggested that pile compressibility will considerably influence the short-term primary creep response at temperatures lower than -2 ^{o}C. Further, the phase change expansion of the pore water during freeze-back of the slurry, may effect considerable pressure buildup along the embedded portion of the pile. Hence, in frictional frozen soils (ice-poor) these high lateral pressures may inhibit short-term pile creep. Finally, despite the widespread use of incremental testing, no definitive statement has been issued with regard to the effect of stress history on the creep of frozen soils.

Clearly, the above problems pose serious considerations for design engineers. The intent of this chapter is to clarify these concerns.

8.2 The Relationship Between Long-term and Short-term Creep Behaviour of Frozen Soils

The creep behaviour of ice-poor frozen soils may be described in terms of Equation 2.5. The validity of this relationship has been confirmed throughout the time range, 40 to 2000 hours (Sayles (1968) , Sayles (1973) and Sayles and Haines (1974)). Thus, extrapolation of short-term data (less than 250 hours) in ice-poor frozen soils is expected to yield satisfactory predictions for the long-term behaviour.

The interpretation of short-term creep data of ice-rich frozen soils is more complicated. Long-term creep in such soils is dominated by secondary creep, while the short-term behaviour is characterised by primary creep. Thus, in order to secure accurate predictions of long-term behaviour, it is necessary to extrapolate from steady-state creep not damped creep conditions.

The duration of primary creep is a function of the "mobility" of the creep mechanisms. In other words, the more active the creep mechanisms the shorter the duration of primary creep. Therefore, it is inferred that secondary creep will commence more quickly at higher stresses and warmer temperatures. This concept is supported by laboratory creep tests on polycrystalline ice. Colbeck and Evans (1973) reported that steady-state creep was observed after approximately one day of testing at -0.01 ^{0}C, under a uniaxial loading of 58 kPa. Similarly, Mellor and Testa

(1969) reported steady-state creep after approximately 12 days, at -2.06 ^{0}C, under a uniaxial loading of 43 kPa. Further, it was observed in the laboratory creep tests on polycrystalline ice (outlined in Chapter 4) that secondary creep was achieved after approximately 5 days at a temperature of -0.8 ^{0}C, under a shear loading of 19 kPa.

Clearly, extrapolation of short-term data (less than 5 days) at temperatures lower than -1 ^{0}C will considerably overestimate the long-term behaviour.

Woodward-Clyde (1976) extended this idea to piles in frozen soils and argued that a critical pile displacement must be attained before secondary creep may be realised. They observed that this critical pile displacement varied from 2.5 cm to 3.8 cm. However, their observations are inconclusive because of the high test loads and short-term incremental testing procedure. Further, if a critical displacement does exist it will surely depend on the ice content and the pile geometry.

Roggensack (1977) suggests that the extrapolation question may be circumvented by employing a simple power law to describe the transient creep of frozen ice-rich soils,

$$\dot{\varepsilon} = At^{a} + B \qquad \text{.....8.1}$$

He observed that the time exponent, a, varied from -0.2 to -1.1 and could be tentatively related to the applied deviatoric stress for a given temperature by the following

relationship

$$a = -6.0\,(\sigma_1 - \sigma_3)^{-0.50} \qquad \text{.....8.2}$$

In this way, the total transient strain may be segregated into primary and secondary components. Equation 8.2 is analogous to Andrade's law (a = -2/3) which Glen (1955) used to phenomenologically describe the transient creep of polycrystalline ice.

The constants A and a must be established from high quality controlled isothermal long-term creep tests. Such an undertaking would involve an enormous amount of experimental testing.

Hence, at this time the only reliable means of securing representative secondary creep data is to conduct long-term, isothermal creep tests.

8.3 The Effect of Pile Compressibility on the Short-term Creep Behaviour of Piles in Ice-rich Frozen Soils

Nixon and McRoberts (1976) extended the simple shear analysis of friction piles to account for pile compressibility and concluded that the time required to establish uniform shaft stress conditions and a steady settlement rate may vary from 1 day to as much as one year, depending primarily on the ground temperature.

Their analysis was based on the flow law for ice. In reality the short-term behaviour of ice-rich frozen soils is

governed by primary creep and thus, their analysis overestimates the time required to establish steady state conditions.

Primary creep data for polycrystalline ice (Glen (1955)) and (Mellor and Testa (1969)) are summarised in Figure 8.1. It is observed that this data may be described in terms of Equation 2.5. There are insufficient data to determine the complete dependence of strain on stress, temperature and time. However, the stress exponent 'c' may be inferred from Table A.3 to be approximately equal to 2.0. Thus, the primary creep law for ice may be expressed as follows,

$$\varepsilon_e = \left[\frac{1}{1.38(\theta+1)^{0.77}}\right]^2 \sigma_e^2 \, t^{0.37} \qquad \text{.....8.3}$$

Hence, for a rigid friction pile in polycrystalline ice the short-term pile velocity is given by,

$$\dot{u}_a = D(z,t)\,\tau^2 \qquad \text{.....8.4}$$

where,

$$D(z,t) = 0.37\,a\,t^{-0.63}\left[\frac{1.652}{(\theta+1)^{0.77}}\right]^2 \qquad \text{.....8.5}$$

Furth r, the short-term pile velocity of a compressible pile (Nixon and McRoberts (1976)) in polycrystalline ice is given by,

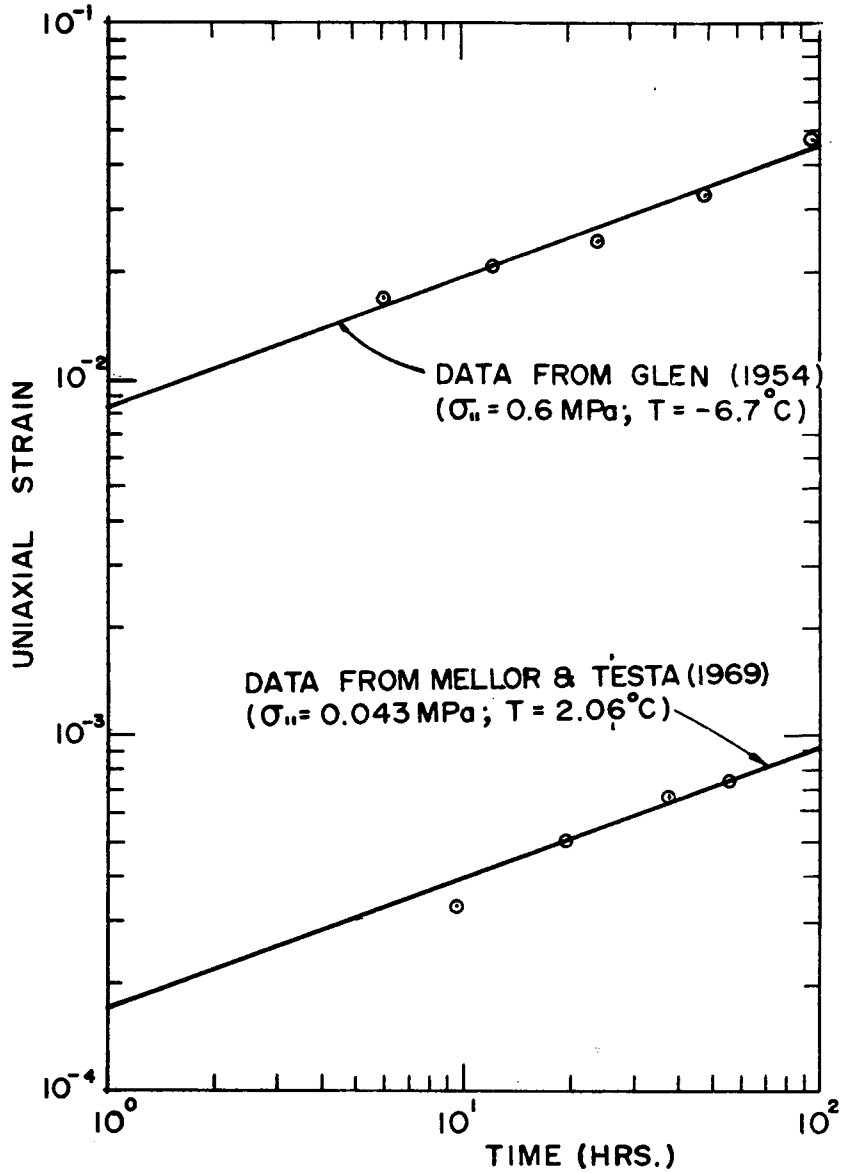

Figure 8.1
Primary Creep of Polycrystalline Ice

$$\dot{u}_a = D(z,t)\left(\frac{aE}{2}\right)^2\left(\frac{\partial^2 u}{\partial z^2}\right)^2 \qquad \text{.....8.6}$$

where E is the pile compressibility (MPa).

Equation 8.6 is mildly non-linear and may be solved using an explicit finite difference procedure. A listing of this program is presented in Appendix F.

The results of this analysis are presented in Figures 8.2, 8.3 and 8.4 for a pile length of 6.0 m and a pile diameter of 0.3 m. A pile modulus of 10 000 MPa was used, which is representative of a timber pile. The pile adfreeze loading was chosen to be 31.25 kPa. The results indicate steady state equilibrium conditions are achieved much more quickly than predicted using a secondary creep model (Nixon and McRoberts (1976)). Figure 8.2 shows that the pile is approximately 75 % compressed after 5 hours at -2 ^{0}C and after 75 hours at -5 ^{0}C. In comparison, Nixon and McRoberts (1976) calculated that a similar pile would be 75 % compressed after approximately 7200 hours at -5 ^{0}C. Figures 8.3 and 8.4 show the variation of pile displacement and shear stress distribution, respectively, with depth and time at -5 ^{0}C. It is noted that the bottom of the pile starts to deform after only 2 hours, thereby demonstrating the high mobility of the frozen soil in response to a loaded compressible pile. These predictions are consistent with field pile tests (ground temperature -0.3 ^{0}C) where it was observed that strain-gauge instrumented piles were compressed after only 2 hours of loading (Morgenstern

Figure 8.2
Settlement of a Compressible Pile in Ice-Rich Soil

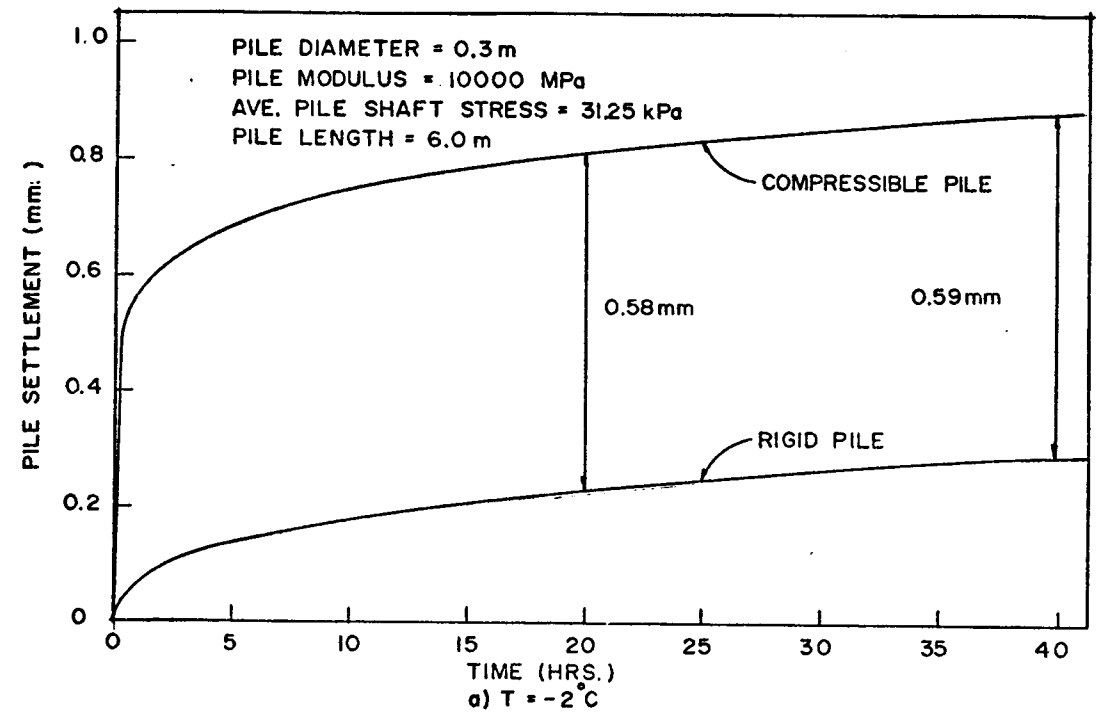

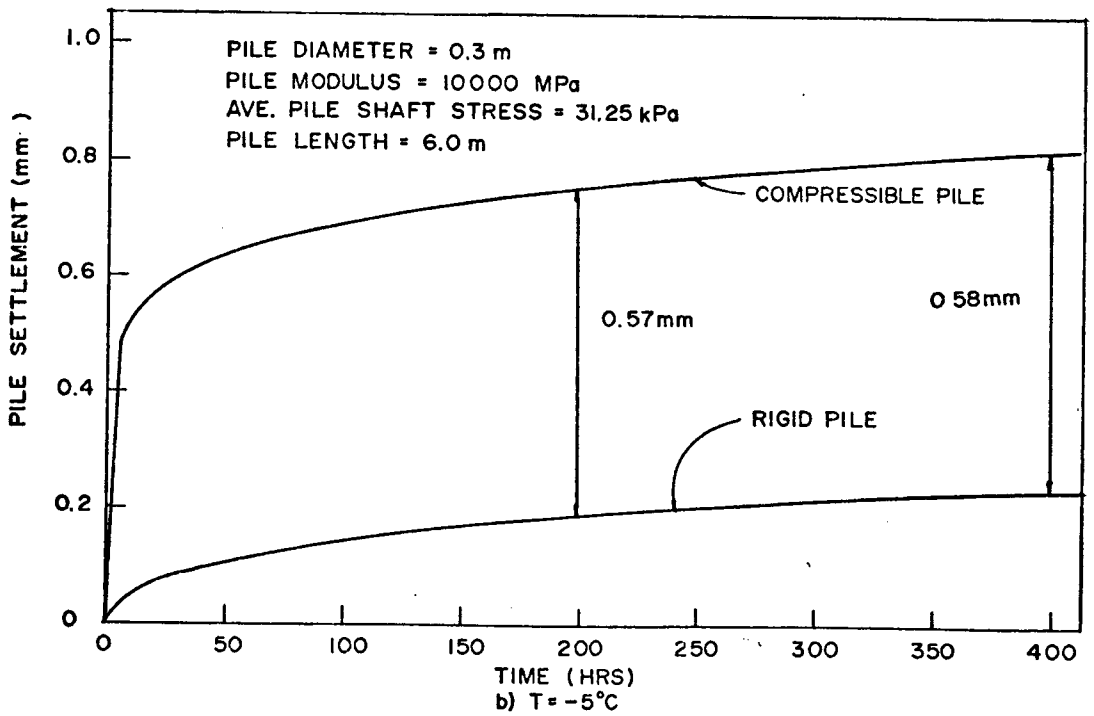

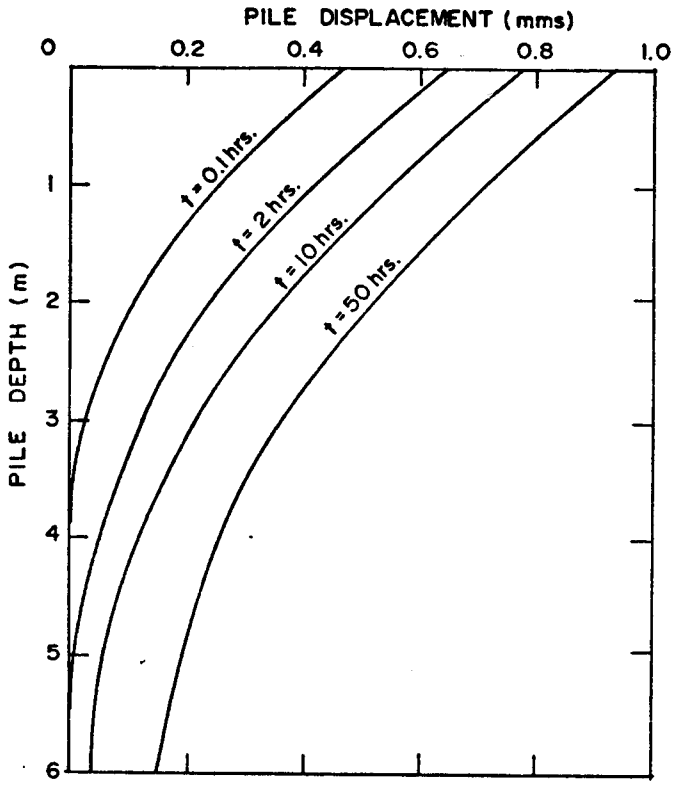

Figure 8.3
Pile Displacement Versus Time for a Pile in Ice-Rich Soil (T = −2°C)

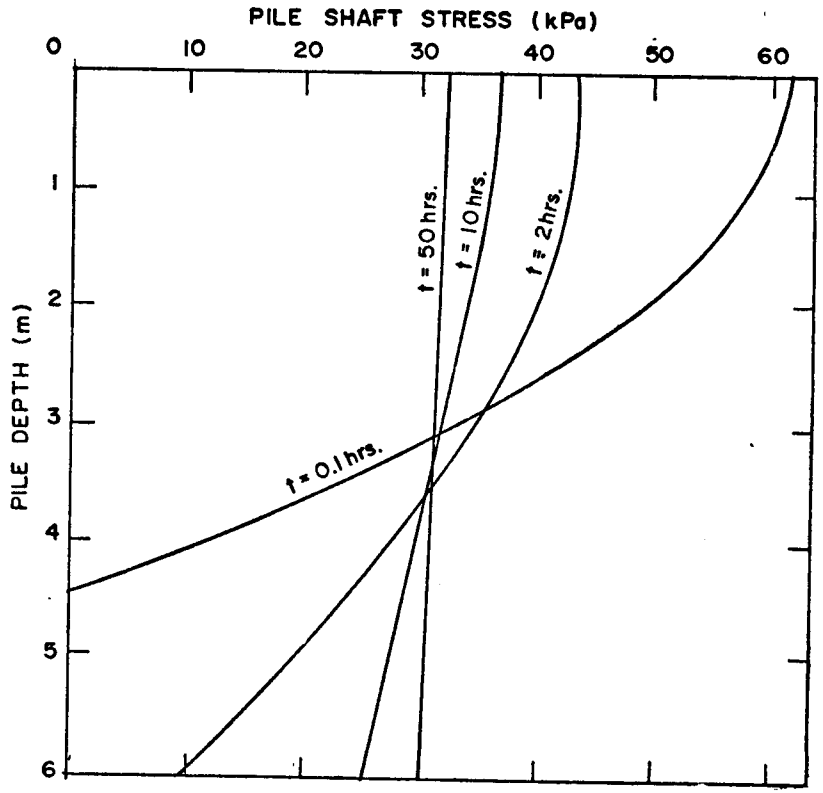

Figure 8.4
Shaft Stress Distribution Versus Time for a Pile in Ice-Rich Soil (T = −2°C)

(1978)).

The pile shear stresses immediately after loading are considerably higher than 31.25 kPa in the upper zone of the pile. The analysis suggests that the adfreeze bond around the upper portion of the pile will fail at very early times. The stress-transfer mechanism on this portion of the pile is highly transient and quite complex thereby precluding theoretical analysis at this time. However, it is anticipated that the strain rate in this portion of the pile would be very high and thus mobilise very high adfreeze strengths. In this light, the adfreeze failure zone is expected to be insignificant.

8.4 The Effect of Freezeback Pressures on the Short-term Deformation Behaviour of Frozen-in Piles

Frozen-in piles cannot be loaded until complete freezeback has occurred. Freezeback times vary from 2 days at -3 ^{0}C to 10 or more days at -1 ^{0}C. In winter considerable freezeback pressures may be generated around the pile. Under such conditions, the upper zone of slurry freezes within hours and the remainder of the slurry is forced to freeze under closed drainage conditions. These pressures slowly dissipate with time as the surrounding permafrost undergos stress relaxation. In Chapter 5 it was recognised that the horizontal overburden stresses imposed on the lateral surface of a pile in ice-rich soil may be neglected in pile design. However, the behaviours of ice-poor soils are

noticeably frictional (Sayles (1973)) and at higher confining stresses (greater than 250 kPa) the lateral pressures should not be ignored. This is of no real consequence in pile design, since the conservative influence of high confining pressures may be safely neglected. However, this phenomenon may have serious implications to pile test-based designs, where short-term, confined creep is more subdued than long-term unconfined creep. Clearly, it is important to study the relaxation of pressures around a frozen-in pile.

Davis (1960) solved the problem of relaxation of a hollow cylinder, in which a state of plane-strain exists. The axial strain vanishes and the material is assumed incompressible. At time t=0, the inner radius, r=a, is enlarged a small amount, ρ_a . This enlargement is maintained constant with time. Thus, as the viscous cylinder relaxes, the elastic strain is slowly converted to plastic strain.

The sum and difference of stress, s and S, respectively are given by

$$s = \sigma_\theta + \sigma_r \; ; \; S = \sigma_\theta - \sigma_r \qquad \text{.....8.7}$$

The initial purely elastic state of stress is expressed by the Lame formulas,

$$S_i = \frac{2a^2b^2}{(b^2-a^2)r^2} p_i \qquad \text{.....8.8}$$

$$S_i = \frac{2a^2}{b^2-a^2} p_i \qquad \text{.....8.9}$$

creating the radial displacement,

$$\rho_a = \frac{S_i r^2}{4Ga} \qquad \text{.....8.10}$$

where b is the external cylinder radius, p_i is the initial applied internal pressure and G is the shear modulus.

The radial velocity w=0 vanishes throughout the cylinder and hence the total rates of strain $\dot{\varepsilon}_\theta$ and $\dot{\varepsilon}_r$ must vanish at all times t. For a primary creep law of the form of Equation 2.5 this condition may be stated as follows

$$\frac{1}{4G}\frac{dS}{dt} + B(t)\left(\frac{\sqrt{3}}{2}\right)^{c+1} S^c = 0 \qquad \text{.....8.11}$$

where,

$$B(t) = K b t^{b-1} \qquad \text{.....8.12}$$

Therefore,

$$\frac{S^{1-c}}{1-c} = -4Gt^b K\left(\frac{\sqrt{3}}{2}\right)^{c+1} + \psi \qquad \text{.....8.13}$$

After integration, and applying the initial boundary condition that at time t=0, S=S , it transpires that,

$$S = \frac{S_i}{\left[1 + (c-1)GK2^{1-c}3^{\frac{c+1}{2}} S_i^{c-1} t^b\right]^{\frac{1}{c-1}}} \qquad \text{.....8.14}$$

The second unknown, 's', is prescribed through the equilibrium equation,

$$r^2 \frac{\partial s}{\partial r} = \frac{\partial}{\partial r}(r^2 S) \qquad \text{.....8.15}$$

Now, from Equation 8.14,

$$\frac{\partial}{\partial r}(r^2 S) = \frac{2DEr}{\left(r^{2(c-1)} + D\right)^{\frac{c}{c-1}}} \qquad \text{.....8.16}$$

where,

$$E = 4Ga\rho_a \qquad \text{.....8.17}$$

and

$$D = (c-1)GK2^{1-c}3^{\frac{c+1}{2}}E^{c-1}t^b \qquad \text{.....8.18}$$

Therefore

$$s = 2DE\int \frac{dr}{r\left(r^{2(c-1)} + D\right)^{\frac{c}{c-1}}} + f(t) \qquad \text{.....8.19}$$

The integral may be evaluated in closed form when 1/(c-1) is an integer. Thus, for frozen Hanover silt 'c' is approximately equal to 2 and Equation 8.16 becomes,

$$s = 2E\left[\frac{1}{r^2 + D} + \frac{1}{D}\log\left(\frac{r^2}{r^2+D}\right)\right] + S_b \qquad \text{.....8.20}$$

where s_b is the value of s at r=b.

Thus, from Equations 8.14 and 8.20 the radial stress, σ_r is given by,

$$\sigma_r = \frac{s - S}{2} \qquad \ldots\ldots 8.21$$

This problem has been solved for a 0.15 m diameter pile installed in a 0.25 m diameter hole. The ground conditions were assumed to consist of frozen ice-poor Hanover Silt at temperatures of -1 ^{0}C and -5 ^{0}C. The soil shear modulus was estimated to be 500 MPa (Kaplar (1969)). The moisture content and frozen bulk density of the slurry are assumed to be 15 % and 2.11 Mg/m^3, respectively. The maximum radial enlargement of the hole as a result of phase change of the mixing water is computed to be 1 mm.

Figure 8.5 shows the effect of ground temperature on the relaxation of radial stress at the slurry-permafrost interface. It is observed that at -1 ^{0}C the excess radial stress dissipates quickly and after 500 hours is equal to 150 kPa. However, at -5 ^{0}C the permafrost relaxes more slowly and after 500 hours the radial stress is equal to 350 kPa.

Figure 8.6 summarises the relaxation of radial stresses away from the pile in frozen silt at a temperature of -5 ^{0}C. The analysis shows that the effect of the imposed freezeback pressures is negligible at soil radii in excess of 3.0 m.

It is assumed that the slurry freezes under a closed

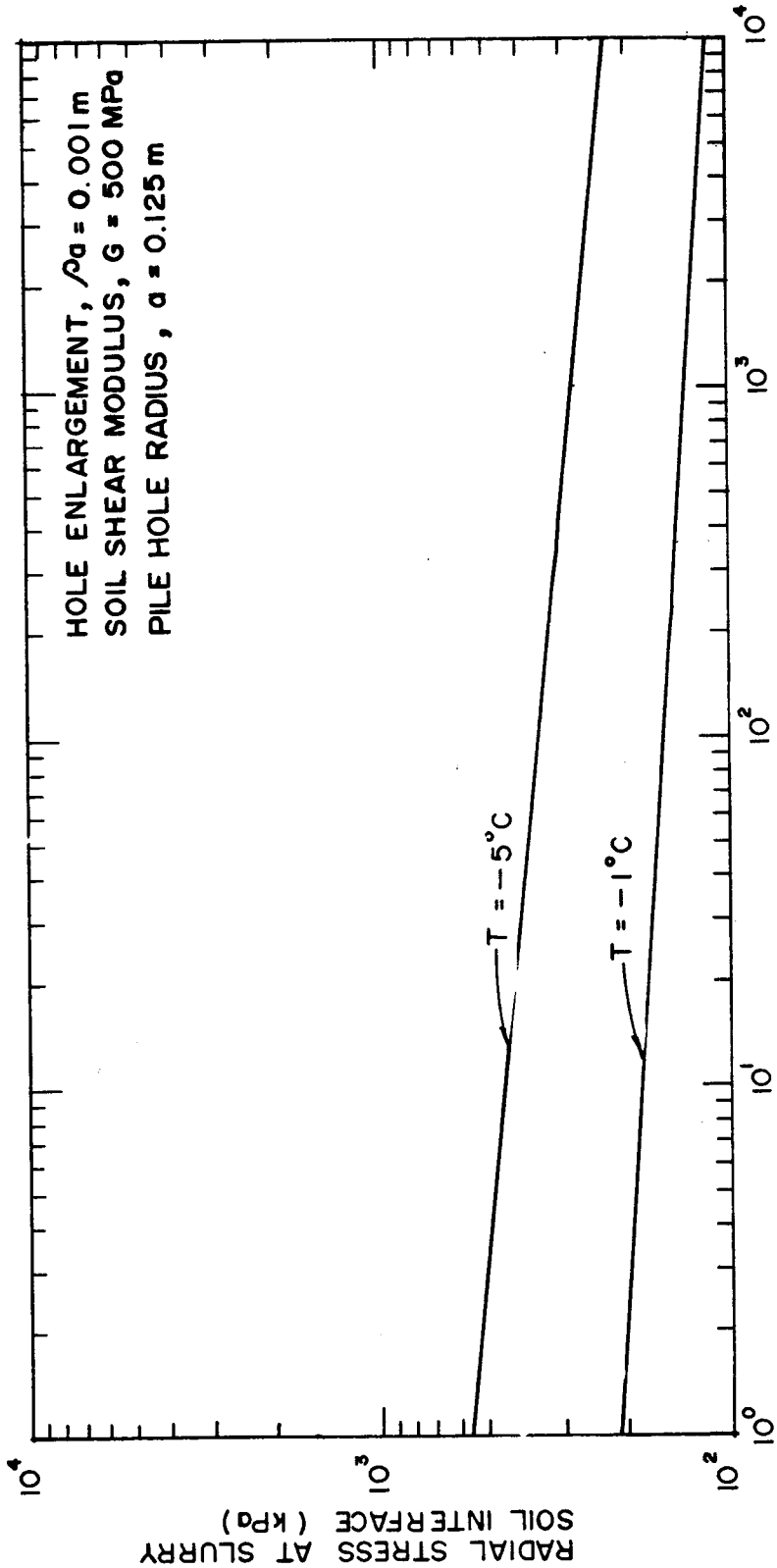

Figure 8.5
Radial Stress Relaxation at the Pile/Soil Interface for a Frozen-In Pile

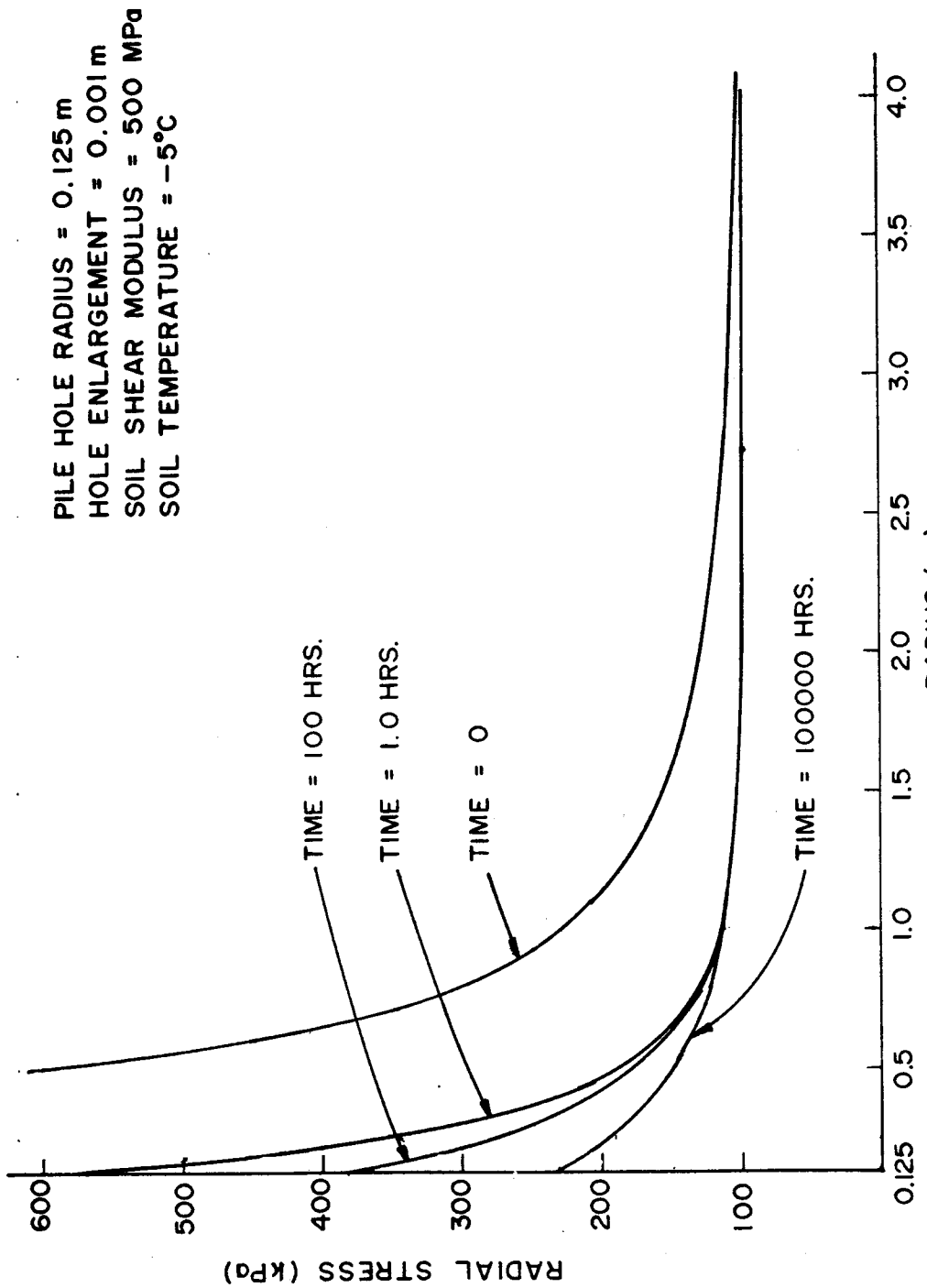

Figure 8.6
Radial Stress Relaxation Around a Frozen-In Pile

system, and that relaxation occurs only laterally. In reality, the slurry freezes initially in an open system, and thus, freezeback pressures will not be as high as computed. Further, radial stress dissipation will be facilitated by vertical stress relaxation. Also, the permafrost immediately surrounding the pile will be warmed by the slurry and thus the effective relaxation temperature will be higher than the original ground temperature.

Therefore, the analysis is certainly conservative. Even so, the results still confirm that excess stresses dissipate very quickly. At warm temperatures (greater than -2 ^{0}C) Sanger (1969) recommends a safe freezeback time of at least 10 days. It is demonstrated in Figure 8.5 that during this time, radial stresses will have decayed to 155 kPa at -1 ^{0}C. Thus, in warm permafrost the residual freezeback pressures will have only a marginal influence on the short-term behaviour. However, in cold permafrost it is recommended that the excess stresses be allowed to dissipate, prior to test loading. At a ground temperature of -5 ^{0}C this will require an equilibration period of approximately 40 days.

8.5 The Use of Incremental Loading in Pile Tests

Incremental load testing has received widespread use in the Arctic. The technique enables a considerable quantity of creep data to be collected from one pile test.

In Chapter 2 it was outlined that the duration of transient creep in ice-rich frozen soils is a complex

function of the segregated ice structure, the bulk density and grain size of the mineral soil, and the ground temperature. In light of this, it is very difficult, at this time, to recommend test guidelines which will ensure that secondary creep will be achieved during the duration of the test. Rather, it is recommended that each load increment be applied for as long as possible or until steady-state creep is achieved. In this way, the creep rate at the end of each increment will provide a conservative estimate of the secondary creep rate.

Incremental testing is best suited to positive load increments. If negative load increments are applied steady-state conditions may be considerably delayed as the ice structure undergos relaxation.

Ice-poor frozen soils are characterised by primary creep thus, interpretation of short-term incremental load tests is complicated by the influence of stress history. However, it may be reasoned that for positive load increments of the same duration the applied load at any given time tends to dominate the creep behaviour of the soil compared to prior, lesser loads and that this dominance becomes greater as time passes. That is, the long-term primary creep settlement of an incrementally loaded pile is approximately independent of stress history and depends only upon the magnitude of the final load. Consequently, the long-term primary creep settlement of a statically-loaded pile is expected to be essentially identical to the

long-term settlement of an incrementally loaded pile provided, of course, that the final total incremental load is identical to the static load.

It is demonstrated earlier in this chapter that long-term primary creep settlements may be safely projected from short-term static creep data. Therefore, the governing factor in defining a satisfactory duration of the load increment is dependent only upon stress history considerations, that is, the incremental load duration must be selected such that the influence of prior lesser loads on the current creep behaviour is negligible.

Unfortunately, the absence of high-quality incremental test data renders it very difficult to estimate satisfactory load increment durations. Hence, at this time it is not possible to provide guidelines for carrying out incremental tests on frozen soils. However, some interesting inferences concerning interpretation of incremental tests may be drawn from the predictions of the various material hardening theories.

Incremental creep curves may be reconstructed from static creep curves using a number of graphical or theoretical constructions. A common technique is based on the strain-hardening law (Hult (1966)). This method was used in this thesis to construct the incremental creep curve for uniaxial incremental loading of frozen Ottawa Sand at a temperature of -1 ^{0}C. The predicted incremental creep is compared to the static creep curves in Figure 8.7.

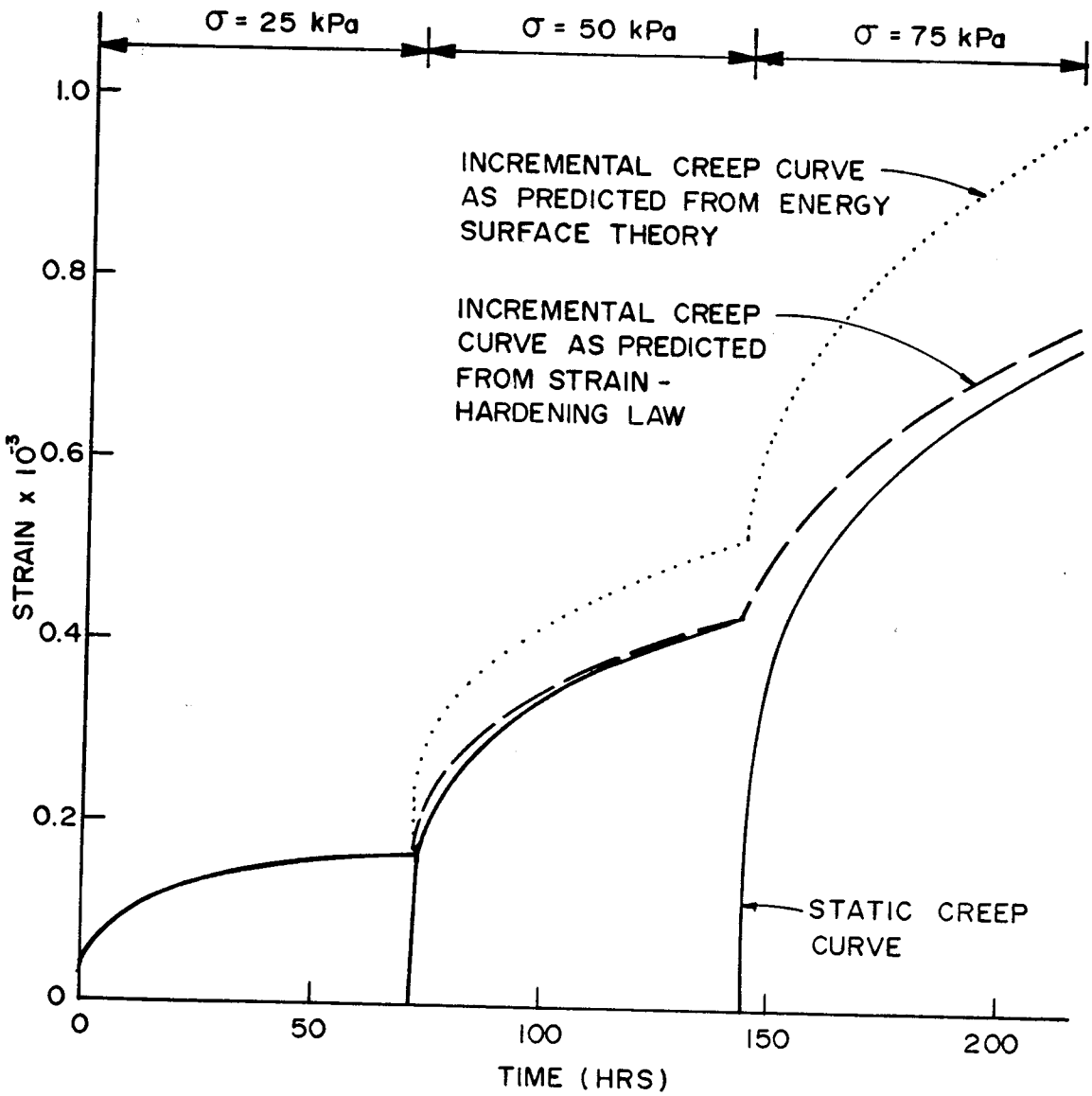

Figure 8.7
Predicted Incremental Creep Curves

A more rational procedure, perhaps, is to approach the problem in terms of strain energy. The uniaxial strain rate is expressed as a function of applied uniaxial strain energy. This relationship is summarised in graphical form in Figure 8.8. The stress contours are defined as energy surfaces (O'Connor and Mitchell (1978)). This figure may now be used to predict the creep displacements during an incremental load test. The proposed stress data is shown schematically in Figure 8.8 and corresponds to uniaxial loads applied incrementally at 72 hour intervals. The resulting incremental strain-time curve is deduced from this figure and is included in Figure 8.7 for comparison with the strain-hardening law predictions.

It is observed that there is a large discrepancy in the predicted short-term strain behaviour for the two methods. However, this is only a secondary concern because in the long-term the predictions will converge and the discrepancies will be insignificant. The primary concern however, is that the predicted time exponent, (b in Equation 2.5), at the end of the load increment, is comparable to the actual exponent obtained from a static load test. If this were not so the long-term predictions would be grossly in error. This issue is conveniently evaluated in Figure 8.9 which summarises the strain-time curves on a double logarithmic plot.

It is observed that the strain-time curves for the second and subsequent load increments are curved. This

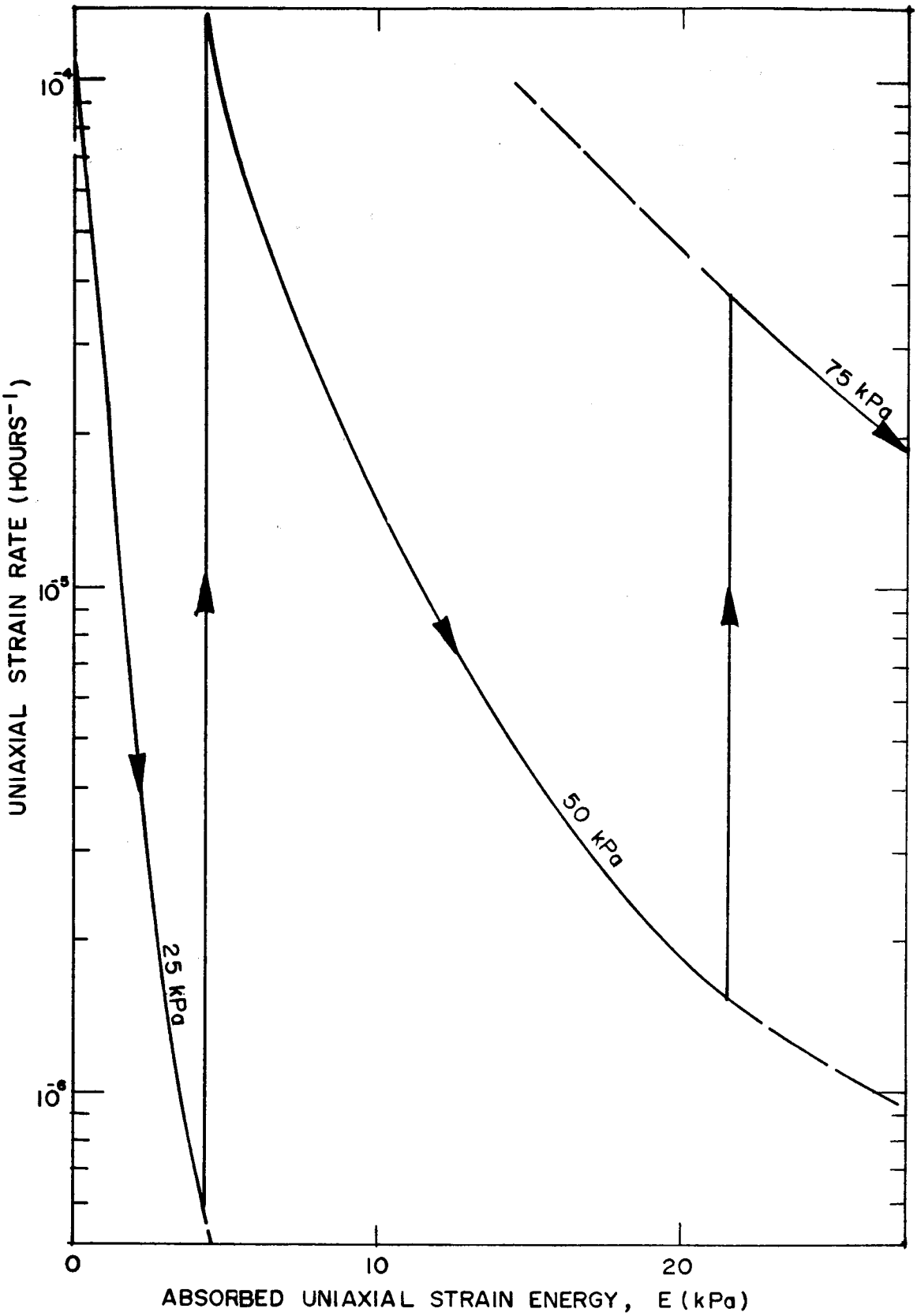

Figure 8.8

Energy Surface Diagram for Frozen Ottawa Sand (T = −1°C)

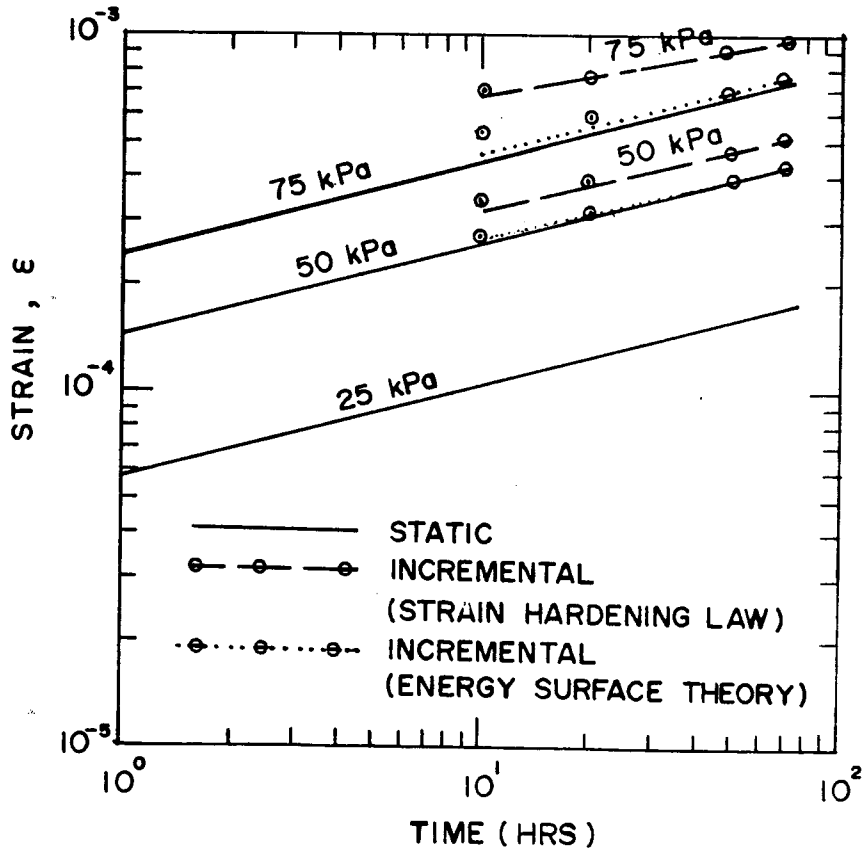

Figure 8.9
Predicted Creep of Frozen Ottawa Sand During Load Increments of 25, 50 and 75 kPa

non-linearity is attributable to stress history effects; in the long-term the curves will become parallel to the actual static strain-time curve. However, if this non-linearity were ignored and the data were interpretated as straight lines, the energy surface and strain-hardening theories would predict time exponents of 0.19 and 0.25, respectively. The reader is reminded that the actual static time exponent is 0.26. In effect, this means that if the 72 hour incremental creep curves were extrapolated according to a simple power law then the long-term (30 year) pile displacements in frozen Ottawa sand would be underestimated by as much as 25 %. This potential error, however, may be incorporated in the factor of safety. Further, the error may be minimised by selecting large load increments and applying the loads for longer periods of time.

8.6 Overview

Long-term creep behaviour may be reliably predicted from short-term load tests. The degree of accuracy of prediction will depend primarily upon test control, and the duration of the applied load. Adequate test control implies,

1. Ground temperatures remain steady throughout the test period.
2. The pile is isolated from external forces in the active layer (e.g. frost heave and downdrag forces).
3. The soil and ice conditions and the ground temperature are adequately defined.

4. Instrumentation is accurate and capable of adequately monitoring the predicted behaviour.
5. Pile installation is implemented using high quality-control construction techniques.

Further, for the specific problem of frozen-in piles installed in winter, it is recommended that the pile be allowed to stand for at least 50 days, prior to testing, unless precautions are taken to relieve the freezeback pressures (i.e. by actively controlling freezeback or by backfilling in stages). This practice will ensure that in-situ lateral earth stresses will be representative of the long-term.

The recommended duration of applied loading depends upon the ice content and the proposed stress path (i.e. incremental or static loading). For static and incremental load tests in ice-rich frozen soils it is recommended that constant loading be applied either until steady state conditions are attained or for as long as possible and in any event for a minimum period of 6 days.

For static load tests in ice-poor frozen soils, it is recommended that the load be applied for a minimum period of 72 hours and that only the data after 48 hours be analysed. This allows time for the pile to undergo elastic compression and the shear stress distribution to be representative of the long-term.

Incremental creep tests in ice-poor frozen soils should be interpreted with caution. Load increments should be as

large as possible and applied for as long as possible so that stress history effects may be minimised.

Finally, it is determined that pile compressibility effects will generally only affect the creep data during the first 48 hours of loading, after which time, the shear stresses may be considered representative of the long-term.

CHAPTER 9

CONCLUDING REMARKS

This thesis has dealt with a wide variety of design and construction problems associated with piling in permafrost. In the light of this research the following comments concerning general piling practice in the arctic are presented.

9.1 Site Investigation

The selection of pile type and installation method are governed primarily by the nature of the subsurface soil conditions. Therefore, a site investigation is an essential part of the foundation design program. The site investigation should address the following concerns

1. Soil Conditions.

   The soil profile must be adequately determined particularly throughout the anticipated embedded depth. Special attention should be given to determining if boulders or dense gravel strata are present at the site, since this condition may prove to be an important design factor especially in warm permafrost.

   The nature and extent of segregated ice should be identified since this will determine whether thawing can be permitted. A knowledge of the ice structure will also indicate whether the frozen soil is ice-rich or ice-poor. The distinction between these two conditions

is dependent primarily upon the ice structure. A conservative approach is to assume that the soil is ice-rich if the average bulk density is less than 1.7 Mg/m^3. This criterion should be refined as more creep data becomes available. The ground temperature profile is of importance in design and in governing pile selection. The temperature at the tip of the pile and the thickness of the permafrost should be evaluated and talik zones, if present, should be located.

2. Availability of Local Materials and Equipment.

If the site is underlain by thaw-unstable permafrost, a gravel pad should be constructed over the site. Hence, a suitable gravel source must be located.

For small projects the cost of equipment mobilisation is a major portion of the overall budget and so the choice of pile and installation method is often governed by the availability of suitable local materials.

9.2 Selection of Piling System

Once the site investigation has identified the permafrost conditions the final pile foundation system may be selected.

For small structures timber piles are generally the cheapest pile type. However, timber piles cannot be driven and must be installed in either drilled or steamed holes. Steel piles are usually more expensive than timber piles but they can be driven into most types of permafrost and can

support heavy loads. Pipe piles can also be converted into thermal piles. Concrete piles are usually the most expensive pile type in North America and hence are seldom used. Concrete piles may be lightly driven and can suuport very high structural loads. Bored piles are not recommended at this time since it has been demonstrated that present day cements are unsuitable for cast-in-place piling. Laboratory studies have shown that permafrost cement-based concrete can develop adequate compressive strength for use as bored piles. However, the salt additive present in the cement diffuses into the thin zone of unfrozen soil surrounding the pile, which is produced when the concrete slurry temperature is greater than 0 ^{0}C. The freezing point of this thin zone of saline soil is depressed and hence the adfreeze strength is reduced at warmer temperatures. It is anticipated that this problem may be overcome by placing the concrete slurry at a temperature colder than 0^{0} C. Nevertheless, a comprehensive field study of this problem must define allowable adfreeze strengths before this construction method can be considered as a viable piling alternative.

Piles may be installed using impact or vibratory driving, slurrying and steaming techniques. Steaming introduces large quantities of heat into the permafrost and should only be used in cold permafrost. Placement in oversized drilled holes has been very popular at sites where pile driving has been considered unreliable. In this method the annulus is backfilled with a sand slurry and allowed to

refreeze. This method may be used for all types and sizes of piles but is particularly attractive for placing thermal piles since these piles cannot be driven.

Pile driving is the most efficient installation method. Impact driving of steel piles has been very successful in fine-grained frozen soils. Stiffened H piles may also be driven into coarse-grained frozen soils.

The wave equation analysis has been used to predict blow counts and end bearing stresses and thus to evaluate the potential for tip damage during driving. It is concluded that steel H piles may be driven into frozen clays, silts and medium dense sands using standard driving equipment, even in cold permafrost. However, instantaneous strength properties of frozen coarse-grained soils must be determined before the analysis can be extended to predict pile behaviour in dense permafrost.

A review of the literature on vibratory driving in frozen soils has revealed that high-frequency vibratory methods are the most efficient piling method at this time. Vibratory driving has tremendous potential in dense frozen soils, where problems have been encountered using conventional steaming, driving and slurrying techniques. The vibratory energy is converted into heat at the pile and the pile advances through the permafrost by liquefying the thawed soil at the pile tip.

A summary of piling techniques is presented in Figure 9.1. This chart provides guidelines for determining the

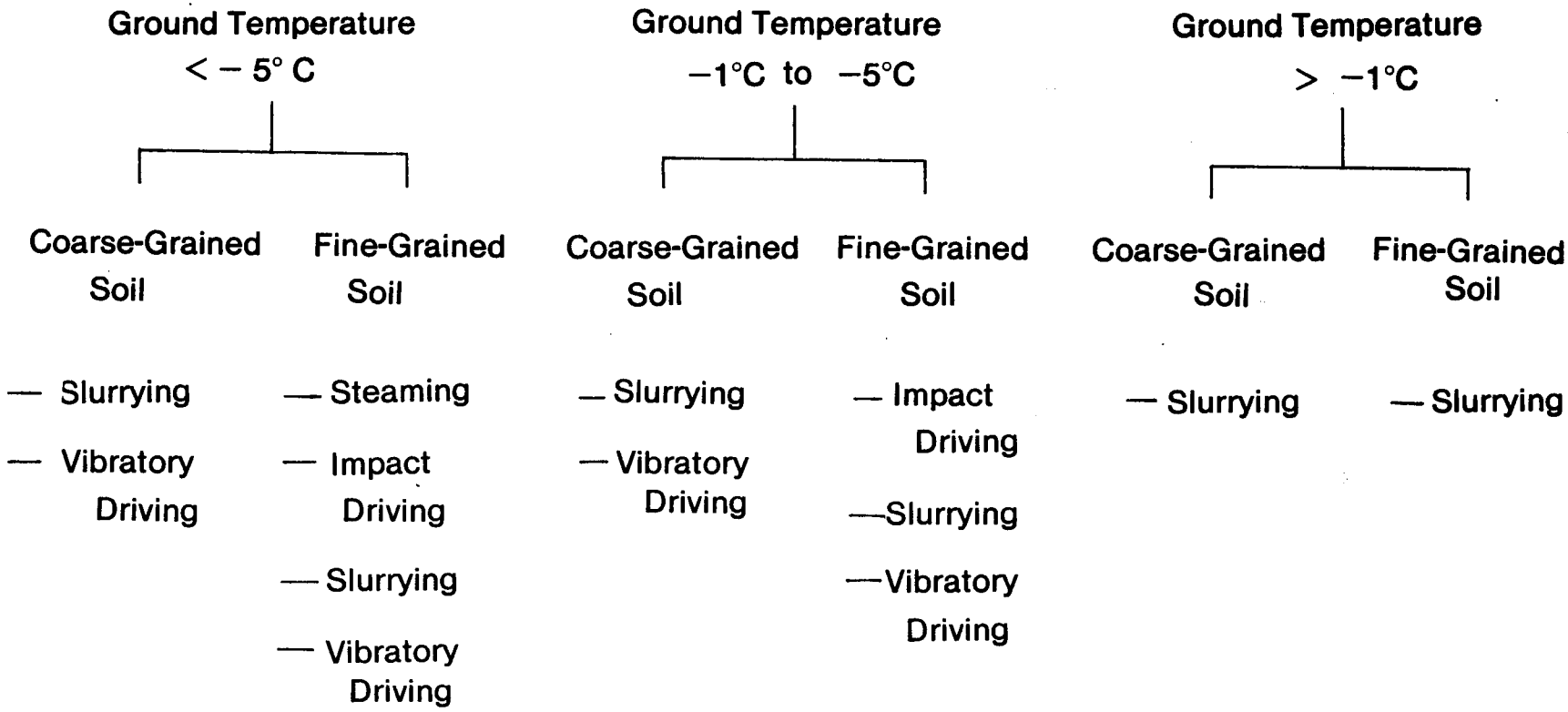

Figure 9.1 Proposed Pile Selection Procedures

suitable piling alternatives. The ground temperature and the soil type are the major geotechnical factors that determine which methods may be considered. Vibratory driving and slurrying are the most versatile installation methods but neither technique can be used in all types of frozen soils. Slurrying techniques must be used in warm permafrost since thermal piles cannot be driven. Moreover, vibratory driving has advantages over slurrying in dense frozen soils since drilling in these soils is often very difficult.

Economic considerations usually govern the final selection of the piling system. For small-scale projects the choice of pile type and installation method will be governed by the availability of local materials and equipment and at this time this usually precludes the use of vibratory driven piles. However, for large-scale projects the initial high cost of equipment mobilisation may be offset by the construction time and effort saved by using the more efficient vibratory piling system.

In recent times, the Soviets have experimented with combined steaming and vibratory techniques. These methods appear very promising and offer potential for installing piles and well casings in dense frozen soils.

9.3 Pile Design

Pile design must satisfy both thermal and rheological considerations. The thermal aspect can be subdivided according to the following headings

1. Degradation of the permafrost beneath the structure
2. Heat Conduction down the pile
3. Freezeback time for slurried piles
4. Analysis of thermal piles.

The above concerns may be analysed using the well established procedures outlined in Chapter 3.

The rheological aspect of design ensures safety against gross failure and excessive settlement. If competent bedrock is within practical piling distance then end bearing piles are usually preferred. However, if this approach is impractical then the pile must develop adequate support in the permafrost soils. Design against skin friction failure is based upon allowable adfreeze strengths. The long-term adfreeze strength may be directly related to the long-term cohesive strength by means of a simple coefficient which is dependent only upon the pile type(Equation 5.1). In this way, the allowable adfreeze strength may be determined from Tables 5.1 and 5.2.

Design against excessive settlement may be based either upon field creep tests or theoretical predictions of pile creep. The implications of poor pile testing techniques have been studied and guidelines for data interpretation have been presented (Chapter 8). However, long-term static and incremental load tests are needed to improve interpretation of stage-loaded tests.

Simple shear laboratory studies have outlined the manner in which the shaft stress is transferred to the

permafrost via the adfreeze bond. It is concluded that the shear strain is continuous across the adfreeze bond, provided that the applied shear stress does not exceed the long-term adfreeze strength.

Long-term creep tests on frozen soils have been reviewed and creep laws have been proposed for a wide range of permafrost soils. It is concluded that the long-term creep behaviour of all frozen soils may be described by primary creep laws and that the long-term deformation behaviour of ice may be approximated by steady-state creep. The long-term creep of a composite body of segregated ice and frozen soil is governed by secondary creep within the network of segregated ice. Hence, it may be argued that the flow law for ice provides the upper limit to the flow law for ice-rich frozen soils. Nevertheless, long-term quality controlled tests on ice-rich soils are required to refine the creep laws proposed in this thesis.

In the light of the laboratory studies and the proposed constitutive relationships pile creep has been analysed using the theory of simple shearing of concentric cylinders. The analysis holds for both primary and secondary creep and is applicable to both ice-rich and ice-poor soils. Design charts for piles in ice or ice-rich soils, frozen clay, frozen silt and frozen sand are presented in Figures 5.4 to 5.7 respectively.

End bearing support is negligible for piles in homogeneous frozen soils. However, if the permafrost

stiffness increases significantly with depth then an end bearing design may be justified. Creep of end bearing piles has been predicted using the expanding cylindrical cavity theory and design charts for piles in ice or ice-rich soils, frozen clay, frozen silt and frozen sand are presented in Figures 5.8 to 5.11 respectively. A critical and detailed analysis of pile creep test data in frozen soils has confirmed the validity of the proposed designs.

In general, pile design in ice-rich soils is governed by settlement. Pile design in ice-poor soils should satisfy both settlement and strength criteria. Guidelines for determining allowable bearing capacities are presented in Figure 5.18. It is recognised that the geotechnical properties of warm (greater than -1 ^{0}C) permafrost are poorly defined and that the thermal balance in such soils is in a very delicate state of equilibrium. Hence, in marginal permafrost it is recommended that special precautions be taken to chill the ground to below -1 ^{0}C or to prethaw and compact the permafrost. Further, pile support in all frozen soils should only be determined for that portion of the pile which is embedded in permafrost of temperature colder than -1 ^{0}C.

In conclusion, it is emphasised that case histories and field studies are needed in which relevant and detailed frozen soil creep data are clearly recorded.

References

Anderson,D.M. and Morgenstern,N.R.,1973. "Physics chemistry and mechanics of frozen ground.A review", In North American Contribution Permafrost Second International Conference, Yakutsk, USSR, pp.257-288, 5

Anderson,D.M. and Tice,A.R.,1971. "Low temperature phases of interfacial water in clay-water systems", Soil Sciences Society American Proceedings, Vol.35, No.1, pp.47-54, 5

Anderson,F.M.,1971a. "Freeze-thaw cycling of cements", Unpublished, Progress Report 50, Halliburton Services Ltd., Duncan, Oklahoma., 141

Anderson,F.M.,1971b. "Shear bond of cementing compositions to ice", Unpublished, Progress Report 34, Halliburton Srevices Ltd., Oklahoma., 142

Anderson,F.M.,1971c. "Bonding of cements to frozen sand and gravel", Unpublished, Halliburton Services Ltd., Oklahoma., 142

Baguelin,F., Bustamante,M., Frank,M. and Jezequel,J.,1975. "La capacite portante des pieux", Annales de l' Institut Technique du Batiment et des Travaux Publics, Supplement 330, Series SF/116, 216pp., 81

Baker,R.W.,1978. "The influence of ice crystal size on creep ", Journal of Glaciology, Vol.21, No.85, pp.485-500, 6, 7, 12

Barnes,P.,Tabor,D. and Walker,J.C.F.,1971. "The friction and creep of polycrystalline ice", Proceedings of the Roval Society, London, Vol.324A, pp.127-155, 7, 65

Bowles,J.E.,1974. "Analytical and Computer Methods in Foundation Engineering", McGraw-Hill, 519pp., 120, 121

Buchko, N.A., Kuznetsov, V.S., and Tsokurenko, K.M.,1975. "Use of thermal piles for creating frozen cut-off curtains", Translated From Gidrotekhnicheskoe Stroitelstvo, No.5, pp.26-30, 38

Colbeck,S.C. and Evans,R.F.,1973. "A flow law for temperate glacier ice", Journal of Glaciology, Vol.12, No.64, pp.71-86, 147

Crory,F.E.,1963. "Pile foundations in permafrost", Proceedings Permafrost International Conference, Lafayette, pp.467-472, 78, 97

Crory,F.E.,1973. "Installation of driven test piles in permafrost at Bethel air force station Alaska", U.S.Army Cold Regions Research Engineering Laboratory, Technical Report 139, 17pp., 98, 119, 125, 180

Crory,F.E.,1975. "Bridge foundations in permafrost areas", U.S.Army Cold Regions Research Engineering Laboratory, Technical Report 266, 30pp., 98, 119, 122, 128

Cunningham,W.C., Fehrenback,J.R. and Maier,L.F.,1972. 'Arctic cements and cementing", Journal Petr leum Canadian Technology, Oct.-Dec., pp.49-55, 132

Davis,E.A.,1960. "Relaxation of a cylinder on a rigid shaft", Journal of Applied Mechanics, March, pp.41-44, 156

Davison, B.E., Rooney, J.W., and Bruggers, D.E.,1978. "Design variables influencing piles driven in permafrost", unpublished, 12pp., 29, 34, 35, 117, 119

Dokuchayev,V.V. and Markin,K.,1972. "Pile Foundations in Permafrost", in Russian, 143pp., 99

Duncan,J.M. and Dunlop,P.,1969. "Behaviour of soils in simple shear tests", Proceedings 7th. International Conference on Soil Mechanics and Foundation Engineering, Vol.1, Mexico, pp.101-109, 59

Emery,J.J. and Nguyen,T.Q.,1974. "Simulation of ice flow problems", In Applications of Solid Mechanics, Second Symposium (CSME-CSCE-ASME), McMaster University, Vol.1, pp.30-45, 8

Eroshenko, V.N., and Fedoseev, Yu.G.,1976." Effect of ice content and cryogenic structure of frozen ground on the bearing capacity of a pile", Translated From Osnovaniya, Fundamenty i Mekhanika Gruntov, No.6, pp.20-21, 46

Fletcher,N.H.,1968. "Surface structure of water and ice II. A revised model", Philosophical Magazine, Vol.18, pp.1287-1300, 65

Frank,R.,1974. "Etude Theorique du Comportement des Pieux Sous Charge Verticale. Introduction de la Dilatance", Ph.d thesis, Pierre et Marie Curie University, France, 234pp., 81

Frederking,R.,1974. "Downdrag loads developed by a floating ice cover: field experiments", Canadian Geotechnical Journal, Vol.11, No.3, PP.339-347, 98

Glen,J.W.,1955. "The creep of polycrystalline ice", Proceedings of the Royal Society of London, Vol.228A, pp.519-538, 52, 54, 149, 180

Glen,J.W.,1975. "The mechanics of ice", U.S.Army Cold Regions Research and Engineering Laboratory, Monograph II-2cb, 47pp., 6, 8, 11

Gold,L.W.,1972. "The failure process in columnar-grained ice", National Research Council Division of Building Research, Technical Paper 369, 108pp., 11, 12

Goncharov, Yu.M.,1964. "Construction of pile foundations in permafrost Regions", Problems of the North, No.10, pp.161-171, 32, 180

Hawkes,I. and Mellor,H.,1972. "Deformation and fracture of ice under uniaxial stress", Journal of Glaciology, Vol.11, No.61, pp.103-131, 11, 123

Haynes,F.D. and Karalius,J.A.,1977. "Effect of

temperature on the strength of frozen silt", U.S.Army Cold Regions Research Engineering Laboratory, Report 77-3, 27pp., 23, 26, 122

Haynes,F.D., Karalius,J. and Kalafut,J.,1975. "Strain rate effect on the strength of frozen silt", U.S.Army Cold Regions Research Engineering Laboratory, Research Report 350, 27pp., 23, 122

Hobbs,P.V.,1974. "Ice Physics", Clarendon Press, Oxford, 837pp., 6

Holloway,D.M.,1975. "Wave equation analysis of pile driving",U.S.Army Engineering Waterways Experimental Station Soils and Pavements Laboratory, Vicksburg, 105pp., 120, 121

Hooke,R.L.,Dahlin,B.B. and Kauper,M.T.,1972. "Creep of ice containing fine dispersed sand", Journal of Glaciology, Vol.11, No.63, pp.327-336, 12, 74

Houston,B.J. and Hoff,G.C.,1975. "Cold weather construction materials. Part 1 Regulated-set cement for cold weather concreting", U.S.Army Cold Regions Research Engineering Laboratory, Special Report 245, 22pp., 132

Huck,R.W. and Hull,J.R.,1971. "Resonant driving in permafrost", Foundation Facts, Vol.7, No.1, pp.11-15, 118

Huck,R.W.,1967. "Interim report on the behaviour of timber piles under static load in permafrost", U.S.Army Cold Regions Research Engineering Laboratory, 19pp., 97

Hult,J.A.H.,1966. "Creep in Engineering Structures", Blaisdell Publishing Company, Massachusets, 115pp., 18, 164

Inland-Halliburton,1978. "Inland-Halliburton Class G Cement. Technical Manual", Inland Cement Services and Halliburton Services Ltd., 50pp., 141

Jellinek,H.H.G.,1959. "Adhesive properties of ice", Journal of Colloid Sciences, Vol.14, pp.268-280, 65

Johnston,G.H. and Ladanyi,B.,1972. "Field tests of grouted rod anchors in permafrost", Canadian Geotechnical Journal, Vol.9, No.2, pp.63-80, 78, 86, 98

Kaplar,C.W.,1969. "Laboratory determination of dynamic moduli of frozen soils and ice", U.S.Army Cold Regions Research Engineering Laboratory, RR 163, 45pp., 159

Ladanyi,B. and Johnston,G.H.,1974. "Behaviour of circular footings and plate anchors embedded in permafrost", Canadian Geotechnical Journal, Vol.11, No.4, pp.531-553, 88, 89, 91

Ladanyi,B.,1972a. " Design of laterally loaded piles in permafrost", Report for Mackenzie Valley Pipeline Research Limited, Calgary, Alberta, 27pp., 41

Ladanyi,B.,1972b. "An engineering theory of creep of frozen soils", Canadian Geotechnical Journal, Vol.9, No.1, pp.63-80, 8, 19

Langdon T.G.,1973. "Creep mechanisms in ice", In

Proceedings Symposium Physics and Chemistry of Ice, Royal Society of Canada, Ottawa, pp.356-361, 6, 7

Lee, T.M.,1963. " Note on freezeback time of slurry around piles in permafrost", unpublished, 10pp., 38

Long, E.L.,1963. "The Long thermopile", Proceedings Permafrost International Conference, Lafaette, pp.487-491, 31, 38

Long, E.L.,1973. "Designing friction piles for increased stability at lower installed cost in permafrost", North American Contribution Permafrost Second International Conference, Yakutsk, U.S.S.R., pp.693-699, 31

Madzula,J.S.,1966. "Status of long term static load tests at the Alaska field station", U.S.Army Cold Regions Research Engineering Laboratory, Technical Note, 19pp., 97

Maier,L.F., Carter,M.A., Cunningham,W.C. and Bosley,T.G.,1970. "Cementing practices in cold environments", Society of Petroleum Engineers of AIME, Paper No. SPE2825, 8pp., 134

Maksimov, G.N.,1967. "Time of natural freezing around piles driven into permafrost", Translated From Osnovaniya, Fundamenty i Mekhanika Gruntov, No.3, pp.12-14, 180

McRoberts,E.C., Law,T.C. and Murray,T.K.,1978. "Creep tests on undisturbed ice-rich silt", Third International Conference on Permafrost, 1978, Vol.1, Edmonton, Canada, pp.539-545, 16

Mellor,M. and Testa,R.,1969. "Creep of ice under low stresses", Journal of Glaciology, Vol.8, No.52, pp.147-152, 148, 150

Miller,J.M.,1971. "Pile foundations in thermally fragile frozen soils", Proceedings of the Symposium on Cold Regions Engineering, University of Alaska, Vol.1, pp.34-72, 100

Morgenstern,N.R., Roggensack,W.D. and Weaver,J.S.,1979. "Pile creep in ice-rich soils",in press, 180

Morgenstern,N.R., 1978. Personal communication, 43, 180

National Research Council Canada,1976. "Handbook for the Design of Bases and Foundations of Buildings and Other Structures on Permafrost", NRC TT-1865, 141pp., 44, 78, 99

Nees, L.A.,1951. "Pile foundations for large towers on permafrost", Proceedings of American Society of Civil Engineers, Vol.77, pp.935-947, 37

Nixon, J.F., and McRoberts, E.C.,1976. "A design approach for pile foundations in permafrost", Canadian Geotechnical Journal, Vol.13, No.1, pp.40-57, 41, 84, 88, 146, 150, 152

Nixon, J.F.,1978. "Foundation design approaches in permafrost areas", Canadian Geotechnical Journal, Vol.15, No.1, pp.96-112, 16, 37, 38

O'Connor,M.J. and Mitchell,R.J.,1978. "The energy surface: a new concept to describe the behaviour of

frozen soils", Third International Conference on Permafrost, Proceedings, Vol.1, Edmonton, Ca ada, pp.119-126, 166

Odqvist,F.K.G.,1966. "Mathematical Theory of Creep and Creep Rupture", Oxford Mathematical Monograph, Clarendon Press, Oxford, 168pp., 8, 71

Perkins,T.K. and Ruedrich,R.A.,1973. "The mechanical behaviour of synthetic permafrost", Society of Petroleum Engineers of AIME Journal, Vol.13, No.8, pp.211-220, 26

Porkhaev, G.V., Targulyan, Yu.O., and Kolesov, A.A.,1977. "Driving piles in permafrost with hole sinking by steam vibroleader", Translated From Osnovaniya. Fundamenty i Mekhanika Gruntov , No.3, pp.12-14, 32

Randolph,M.F. and Wroth,P.C.,1978. "Analysis of deformations of vertically loaded piles", Journal of the Geotechnical Engineering Division,Proceedings of the ASCE, Vol.104, No. GT12, pp.1465-1488, 94

Reed-Hill,R.E.,1973. "Physical Metallurgical Principles", Second Edition, Van Nostrand Company, 920pp., 12

Reid, R.L., Tennant, J.S., and Childs, K.W.,1975. "The modelling of a thermosyphon type permafrost protection device" Transactions of The ASME, August, pp.382-386, 38

Rockefellor,W.C.,1967. "Mechanical resonant systems in high-power applications", American Society of Mechanical Engineers, Vibration Conference, Boston, 12pp., 129

Roggensack,W.D.,1977. "Geotechnical Properties of Fine-grained Soils", Ph.D Thesis, University of Alberta, 449pp., 6, 7, 16, 148

Rooney,J.W., Nottingham,D.A. and Davison,B.E.,1976. "Driven H-pile foundations in frozen sands and gravels", Proceedings Second International Symposium on Cold Region Engineering, Fairbanks, Alaska, pp.169-188, 1

Roscoe,K.H.,1953. "An apparatus for the application of simple shear to soil samples", Proceedings 3rd. International Conference on Soil Mechanics and Foundation Engineering, Vol.1, pp.186-191, 59

Rowley,R.K., Watson,G.H. and Ladanyi,B.,1973. "Vertical and lateral pile load tests in permafrost", North American Contribution Permafrost Second International Conference, Yakutsk, pp.712-721, 98

Sanger, F.J.,1969. "Foundations of structures in cold regions" , Cold Regions Science and Engineering. Monograph III-C4, 71pp., 32, 33, 34, 162

Sayles,F.H. and Haines,D,1974. "Creep of frozen silt and clay", U.S.Army Cold Regions Research Engineering Laboratory, Technical Report 252, 50pp., 13, 147

Sayles,F.H.,1968. "Creep of frozen sands", U.S.Army Cold Regions Research Engineering Laboratory, Technical

Report 190, 54pp., 13, 20, 147
Sayles,F.H.,1973. "Triaxial and creep tests on frozen Ottawa sand", International Conference Permafrost North American Contribution, Yakutsk, pp.384-391, 13, 20, 26, 147, 156
Scott, R.F.,1956. "Freezing of slurry around wood and concrete piles", Arctic Construction and Frost Effects Laboratory, May, 61pp., 38
Sivanbaev, A.V., and Kolesov, A.A.,1976. "Method of pile driving in plastic-frozen soils", Translated From Osnovaniya, Fundamenty i Meckhanika Gruntov, No.1, pp.5-6, 36
Sivanbaev,A.V., Shilin,N.A., Nikhotin,N.I. and Neklyudov,V.S.,1977. "Results of field tests of piles in permanently frozen ground", Translated from Osnovaniya, Fundamenti i Mekhanika Gruntov, No.5, pp.35-36, 114
Smith,A.E.L.,1962. "Pile driving analysis by the wave equation", Transactions of the American Society of Civil Engineers, Vol.127, Part 1, pp.1145-1193, 2, 120, 121
Steinemann,S.,1958. "Experimental investigation of the plasticity of ice", U.S.Airforce, Cambridge Research Laboratory, Research Translation AMST-G-166+, 11
Thompson,E.G. and Sayles,F.H.,1972. "In situ creep analysis of a room in frozen soil", Proceedings of the ASCE, Vol.98, No.SM9, pp.899-915, 16
Tice,A.R.,Anderson,D.M. and Banin,A.,1973. "The prediction of unfrozen water contents in frozen soils from liquid limit determinations", Symposium on Frost Action in Roads, Oslo, Vol.1, pp.329-344, 5
Tsytovich,N.A.,1975. "The Mechanics of Frozen Ground", Mcgraw-Hill, N.Y., 426pp., 5, 73
U.S.Army /Airforce,1973. "Draft. Arctic and subarctic construction: foundations for structures" Technical Manual, TM5-852-4/AFM 88-19 Chapter 4, 324pp., 42
Vialov,S.S., Dokuchayev,V.V., Sheynkman,D.P., and Goncharov,Yu.M.,1973. "Ground ice as the bearing stratum for construction", U.S.S.R. Contribution Permafrost Second International Conferfence, Yakutsk, pp.537-545, 46, 99
Vialov,S.S., Targulyan,Yu.O. and Vsorskiy,D.P.,1969. "Interplay of frozen ground with piles during vibratory driving", Tech. Translation FSTC-HT-23-944-68, U.S.Army Foreign Science and Technology Center, 13pp., 117, 118, 119
Vialov,S.S.,1959. "Rheological Properties and Bearing Capacity of Frozen Soils", Translation 74, U.S.Army Cold Regions Research Engineering Laboratory, translated in 1965, 219pp., 13, 78, 88, 99
Vialov,S.S.,1962. "Strength and creep of frozen soils and calculations in ice-soil retaining structures", U.S.Army Cold Regions Research Engineering Laboratory, Translation 76, 301pp., 19

Vialov,S.S.,1978. "Long term settlement of foundations on permafrost", Third International Conference on Permafrost, Proceedings Vol.1, pp.898-903, 100

Voitkovskii,K.F.,1960. "Mekhanicheskiye svoystva lda (The mechanical properties of ice)", Moscow, Izd. Akademii Nauk, English Translation AFCRL-62-838, AMS-T-R#391+, 92pp., 11, 60, 78

Weertman,J.,1973. "Creep of ice", In Proceedings Symposium Physics and Chemistry of Ice, Royal Society of Canada, Ottawa, pp.320-337, 6, 7

Womick,O. and LeGoullon,R.B.,1975. "Settling a problem of settling", Northern Engineer, Vol.7, No.1, pp.4-10, 100

Woodward-Clyde Consultants,1976. " Review report. Alyeska field VSM load tests,1975", for Alyeska Pipeline Service Company, 28pp., 148

Woodward-Lundgren and Assoc.,1971. "Final Report-Results of Pile and Anchor Installation and Load Tests, and Recommended Design Procedures", Alyeska Pipeline Service Co., April, 55pp., 1, 116, 119

APPENDIX A

ANALYSIS OF PRIMARY CREEP DATA, SAYLES (1973)

To facilitate data reduction the results were analysed in terms of strain rather than strain rate. Inspection of Equation 2.5 reveals that for constant stress and temperature, the creep data will give a straight line of gradient, b, on a double logarithmic plot of strain against time. A summary of the creep data is presented, according to the above format, in Figure A.1. It is observed that this data does support the simple power relationship between strain and time. The intercept on the strain axis, at a time equal to one hour, is defined as 'A'. A summary of b and A values obtained from Figure A.1 are presented in Table A.1. Inspection of this table reveals that the time exponent, b, is essentially insensitive to the magnitude of the applied stress and assumes an average constant value of 0.26. Each data set has been modified to comply with a constant exponent of 0.26. In this way, Figure A.2 presents the modified plots and Table A.2 summarises the modified A values.

Analysis of these data yields a 'c' value of 1.316 and an 'f' value of 1.3, which is equivalent to a "pseudo" friction angle of 7.5 ^{0} Comparison of the primary creep data presented by Vialov (1962) and Sayles (1968) suggests that 'k' is somewhat insensitive to material type and is approximately equal to 1.0. Thus in this analysis, for 'k' equal to 1.0,'w' assumes a value of 21.0 MPa.hr /^{0}C . A summary of these parameters is presented in Table A.3. This table also summarises creep data from other investigators.

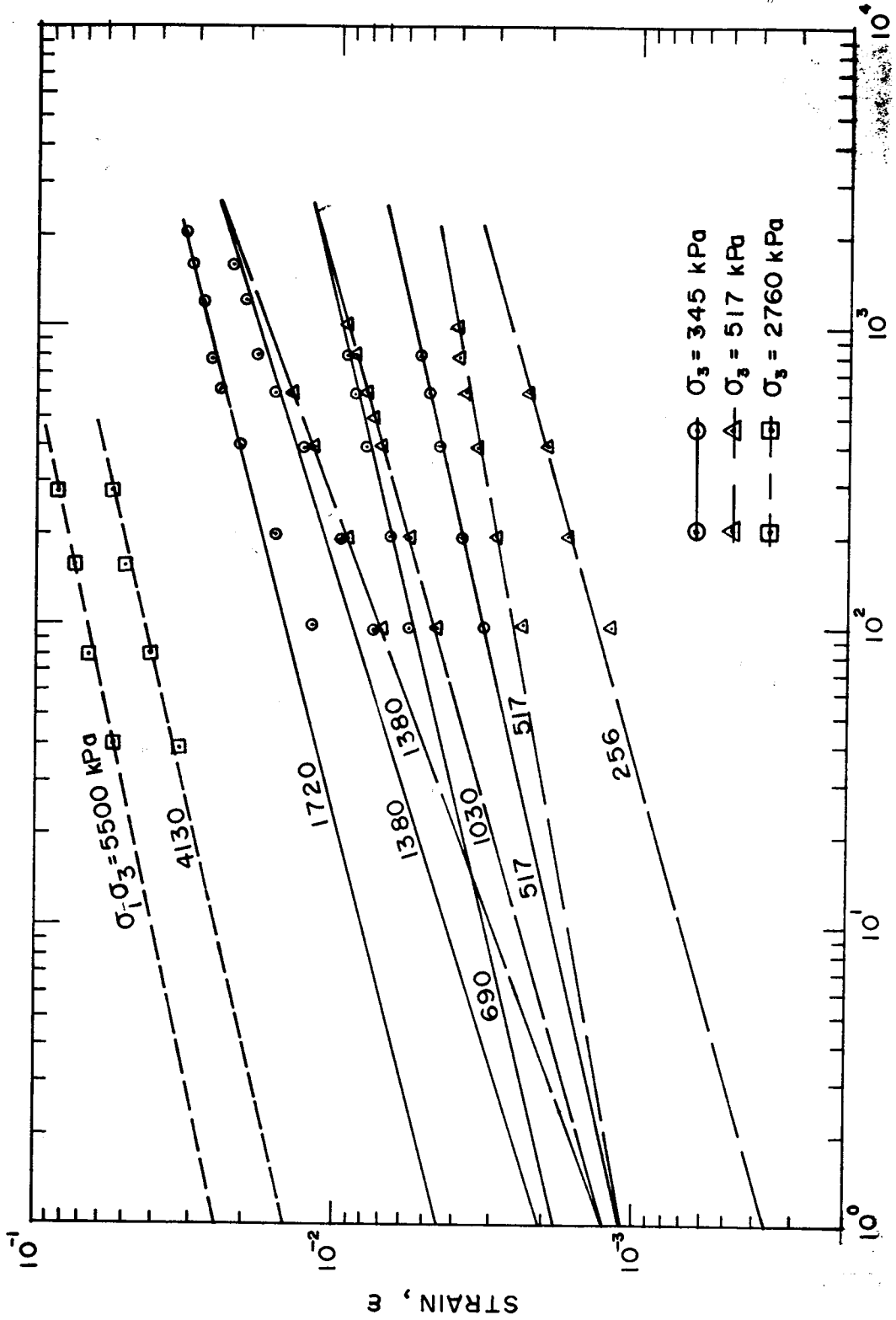

Figure A.1 Strain Versus Time for Frozen Ottawa Sand (Sayles (1973))

Confining Stress, σ_3 (kPa)	Deviatoric Stress, $\sigma_1-\sigma_3$ (kPa)	b	A x 10^3 (hr^{-b})
345	517	0.233	1.12
345	690	0.24	1.82
345	1380	0.315	2.05
345	1720	0.259	4.50
517	256	0.287	0.37
517	517	0.189	1.10
517	1030	0.289	1.26
517	1380	0.376	1.26
2760	4130	0.24	14.4
2760	5500	0.22	24.2

Table A.1 Summary of 'A' and ' b ' Values

-Data From Sayles (1973)

Confining Stress, σ_3 (kPa)	Deviatoric Stress, $\sigma_1-\sigma_3$ (kPa)	Modified b	Modified A x 10^3 (hr^{-b})
345	517	0.26	0.92
345	690	0.26	1.6
345	1380	0.26	3.1
345	1720	0.26	4.4
517	256	0.26	0.43
517	517	0.26	0.64
517	1030	0.26	1.4
517	1380	0.26	2.4
2760	4130	0.26	12.0
2760	5500	0.26	20.0

Table A.2 Summary of Modified A and λ/m Values -Data from Sayles (1973)

Soil	c	b	w ($MPa.hr^{\frac{b}{c}}/°C^k$)	k
Suffield Clay[3]	2.38	0.333	0.73	1.2
Bat-baioss Clay[1]	2.50	0.45	1.25	0.97
Hanover Silt[3]	2.04	0.151	4.58	0.87
Callovian Sandy Loam[1]	3.70	0.370	0.88	0.89
Ottawa Sand[2]	1.28	0.449	44.7	1.0
Manchester Fine Sand[2]	2.63	0.631	2.29	1.0
Ottawa Sand (this study)	1.32	0.263	21.0	1.0

1 Vialov (1962)

2 Sayles (1968)

3 Sayles and Haynes (1974)

Table A.3 Constants for Primary Creep Equation

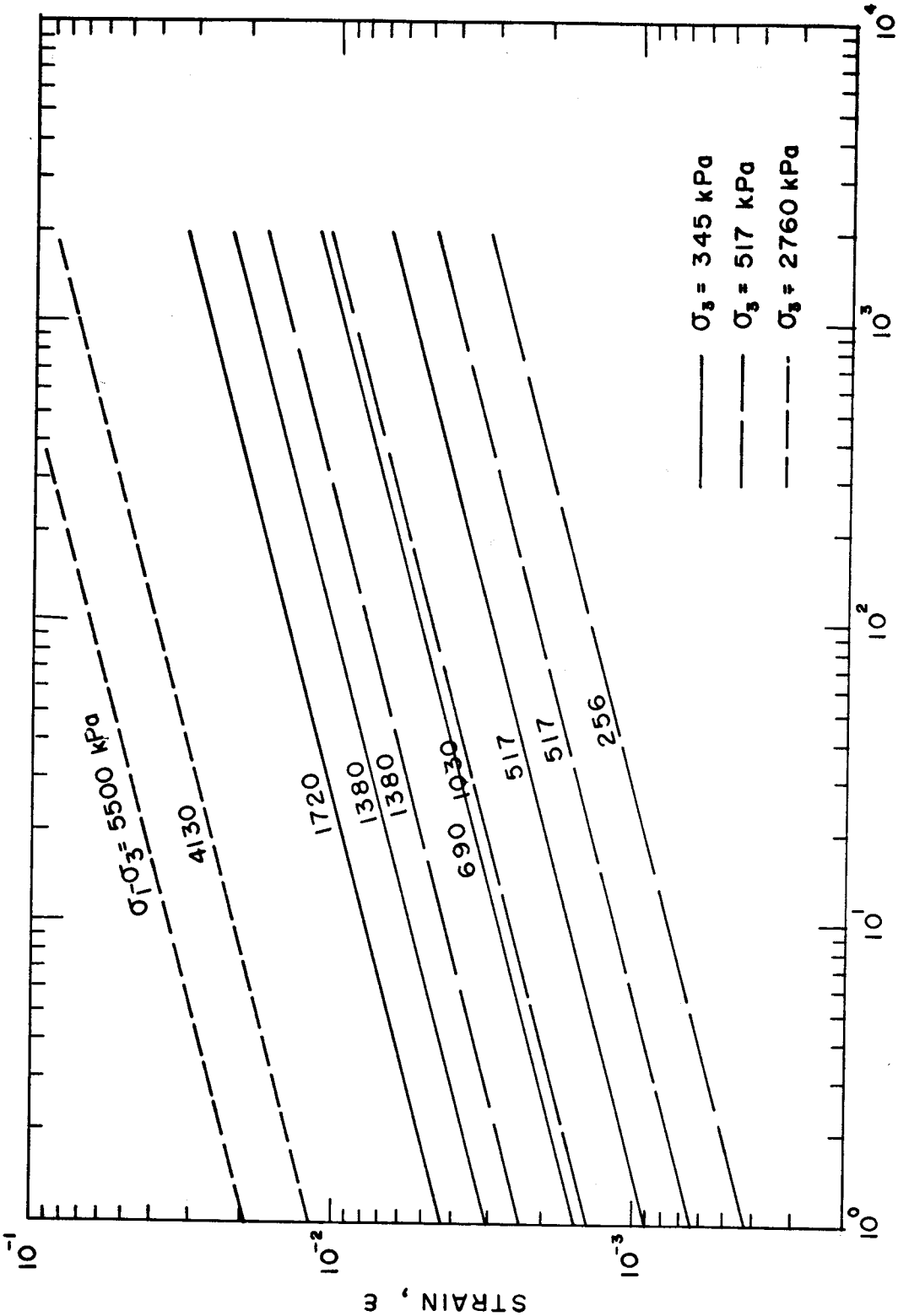

Figure A.2 Modified Strain Versus Time for Frozen Ottawa Sand (Sayles (1973))

APPENDIX B

SUMMARY OF LABORATORY CREEP TEST RESULTS

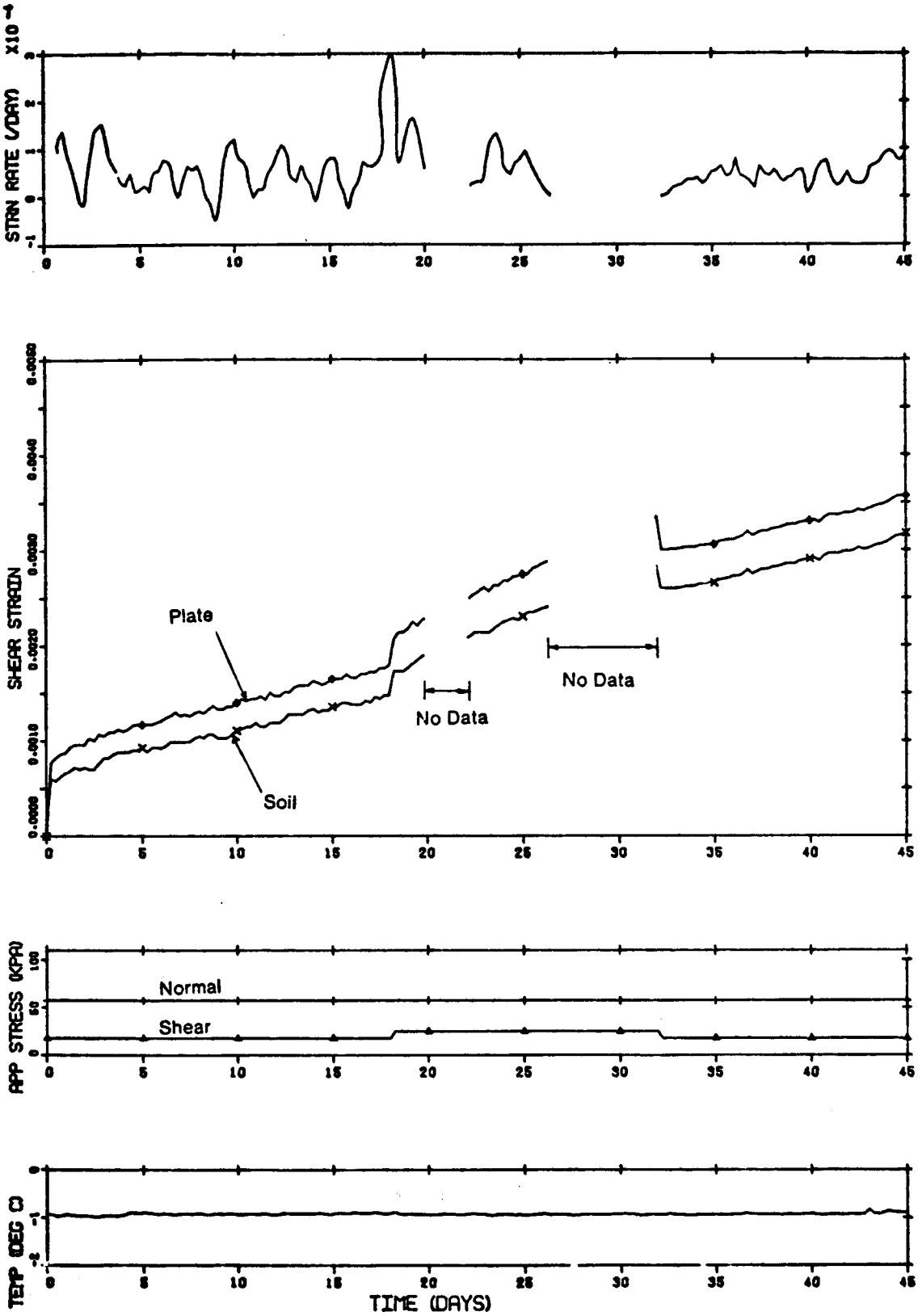

Figure B.1 SHEAR CREEP OF ICE IN TS#1 (γ_i =0.90 MG/CU.M)

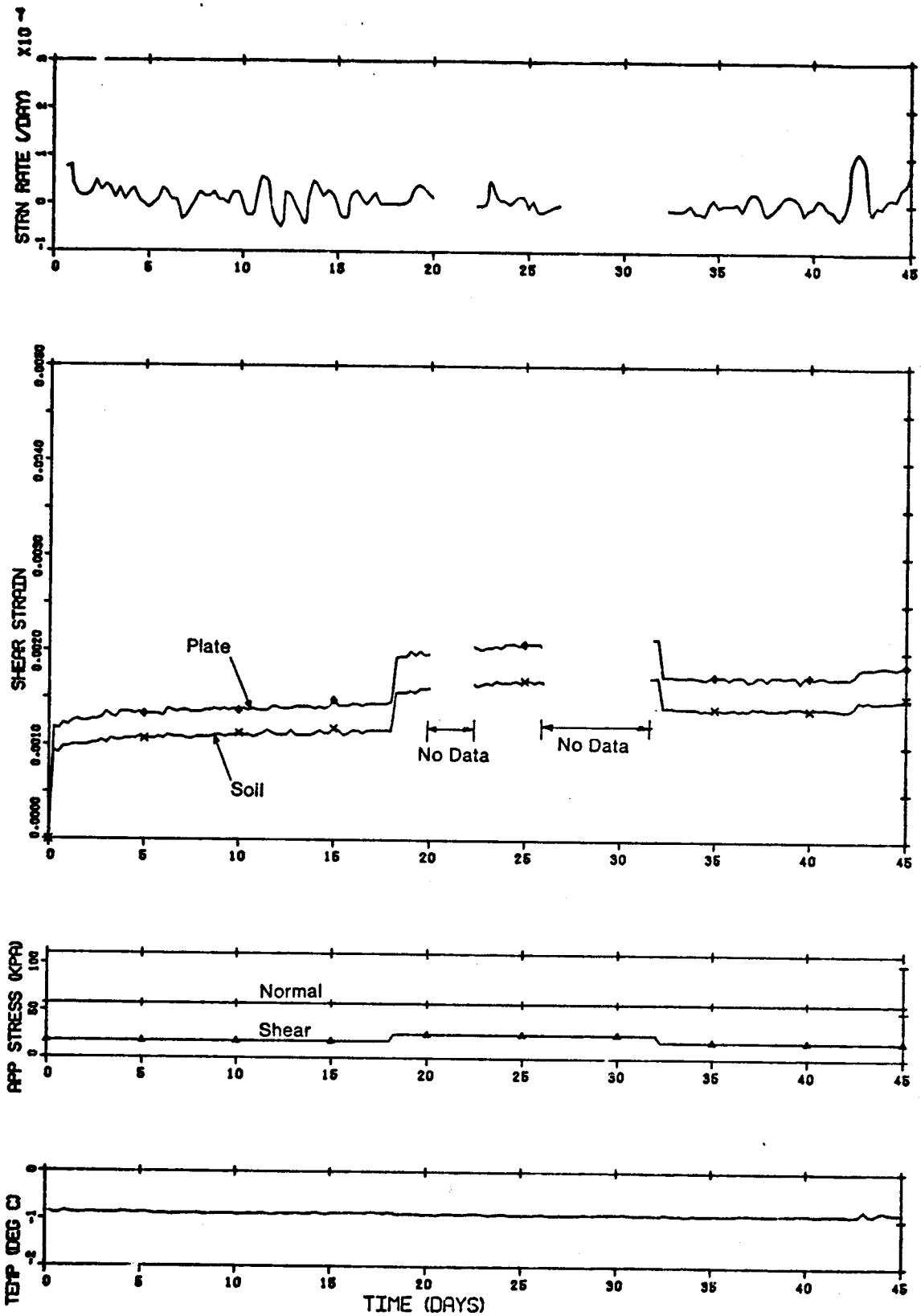

Figure B.2 SHEAR CREEP OF SILT2 IN TSH1 (γ_t =1.59 MG/CU.M)

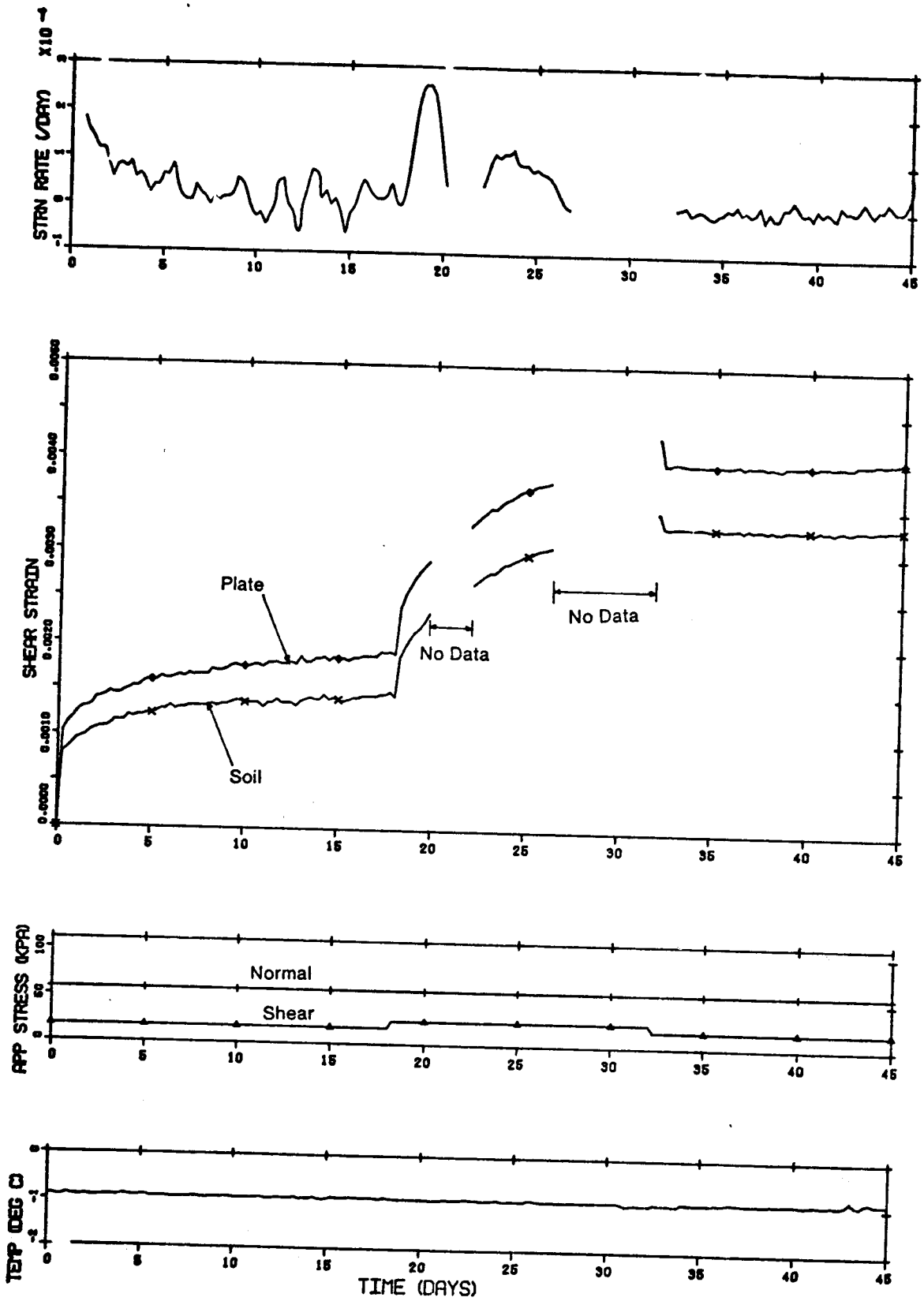

Figure B.3 SHEAR CREEP OF SAND IN TS#1 (γ_t ≈2.03 MG/CU.M)

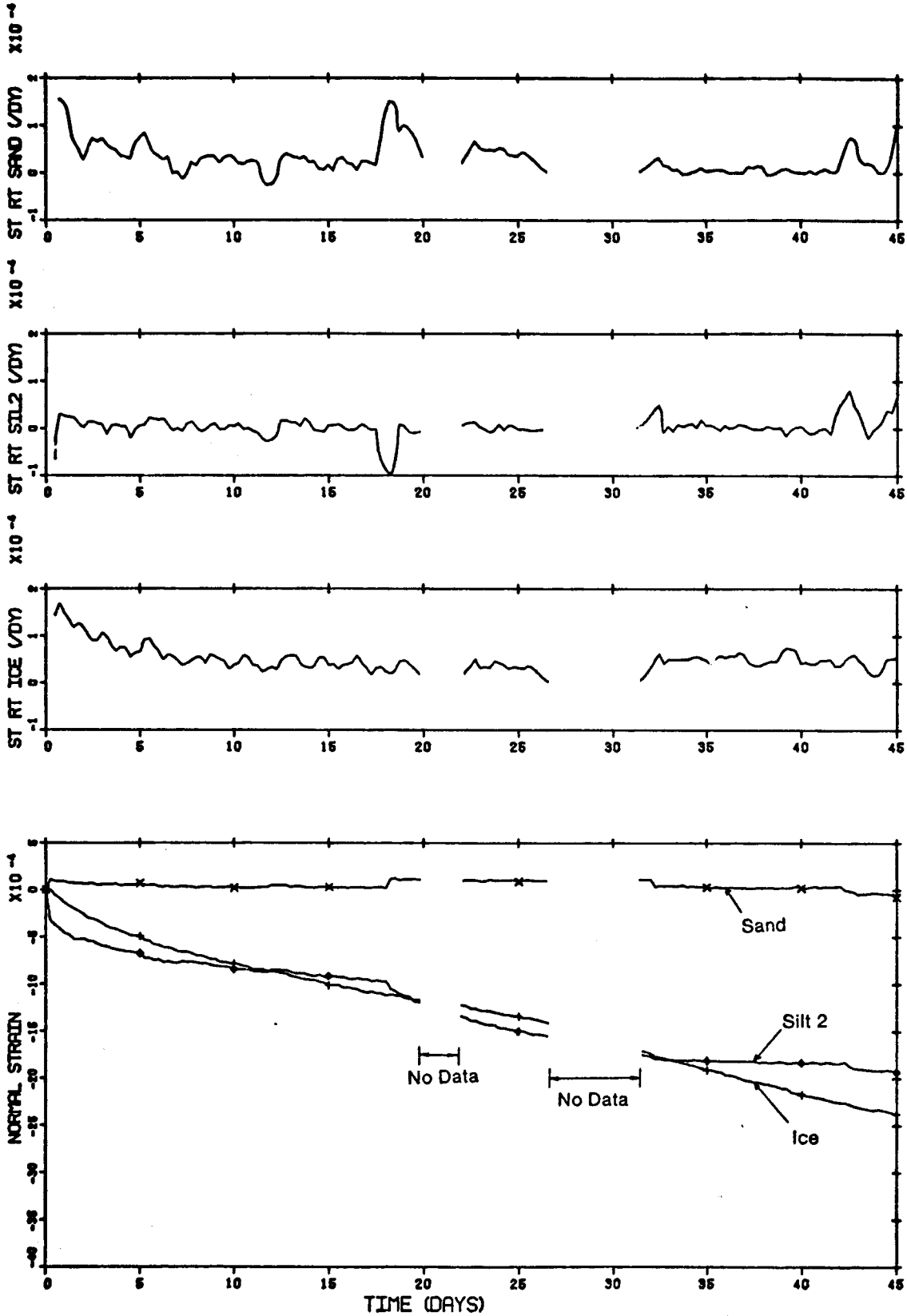

Figure B.4 VERT CREEP OF ICE,SILT2 AND SAND IN TS#1

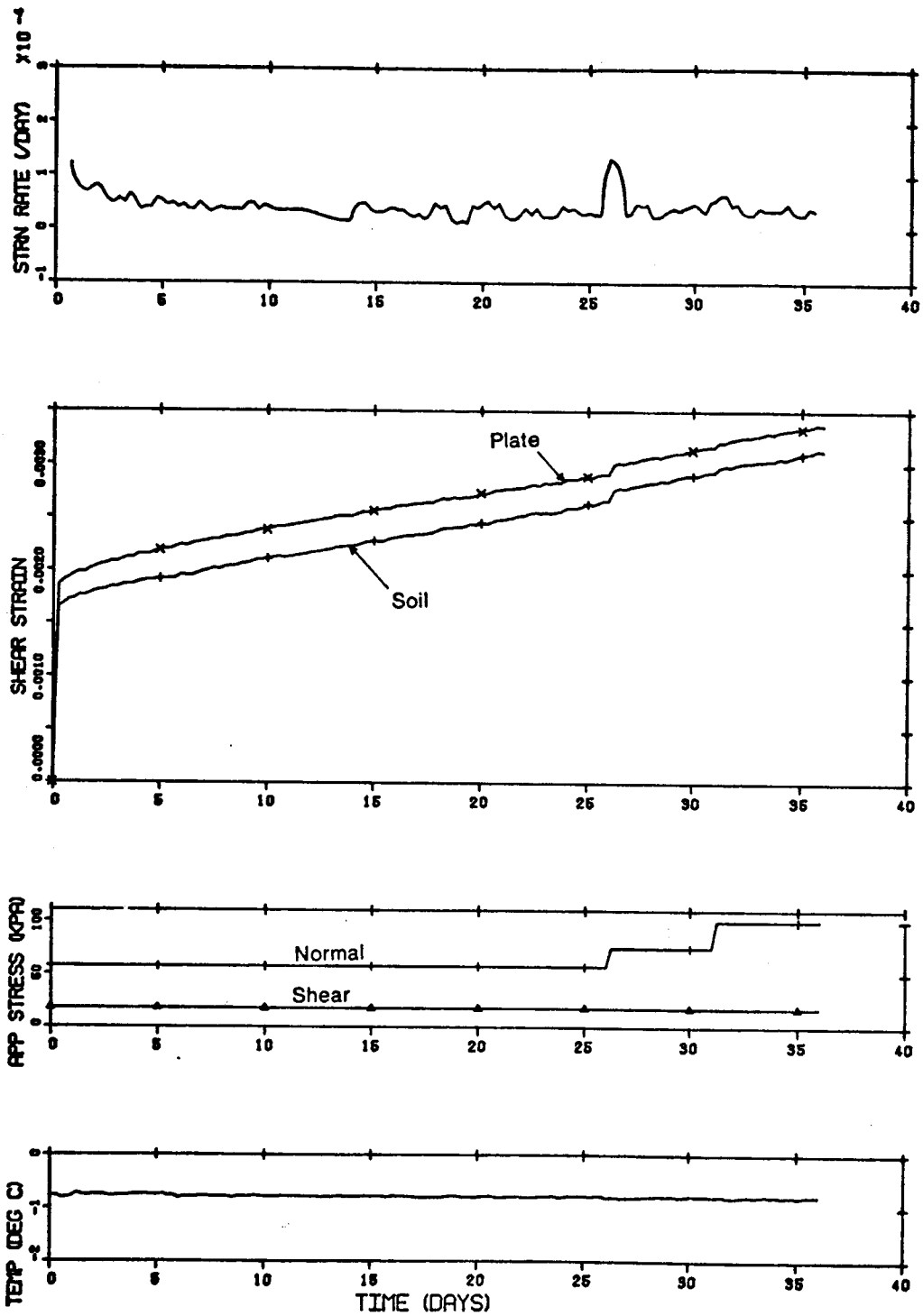

Figure B.5 SHEAR CREEP OF ICE IN TS#2 (γ_f =0.90 MG/CU.M)

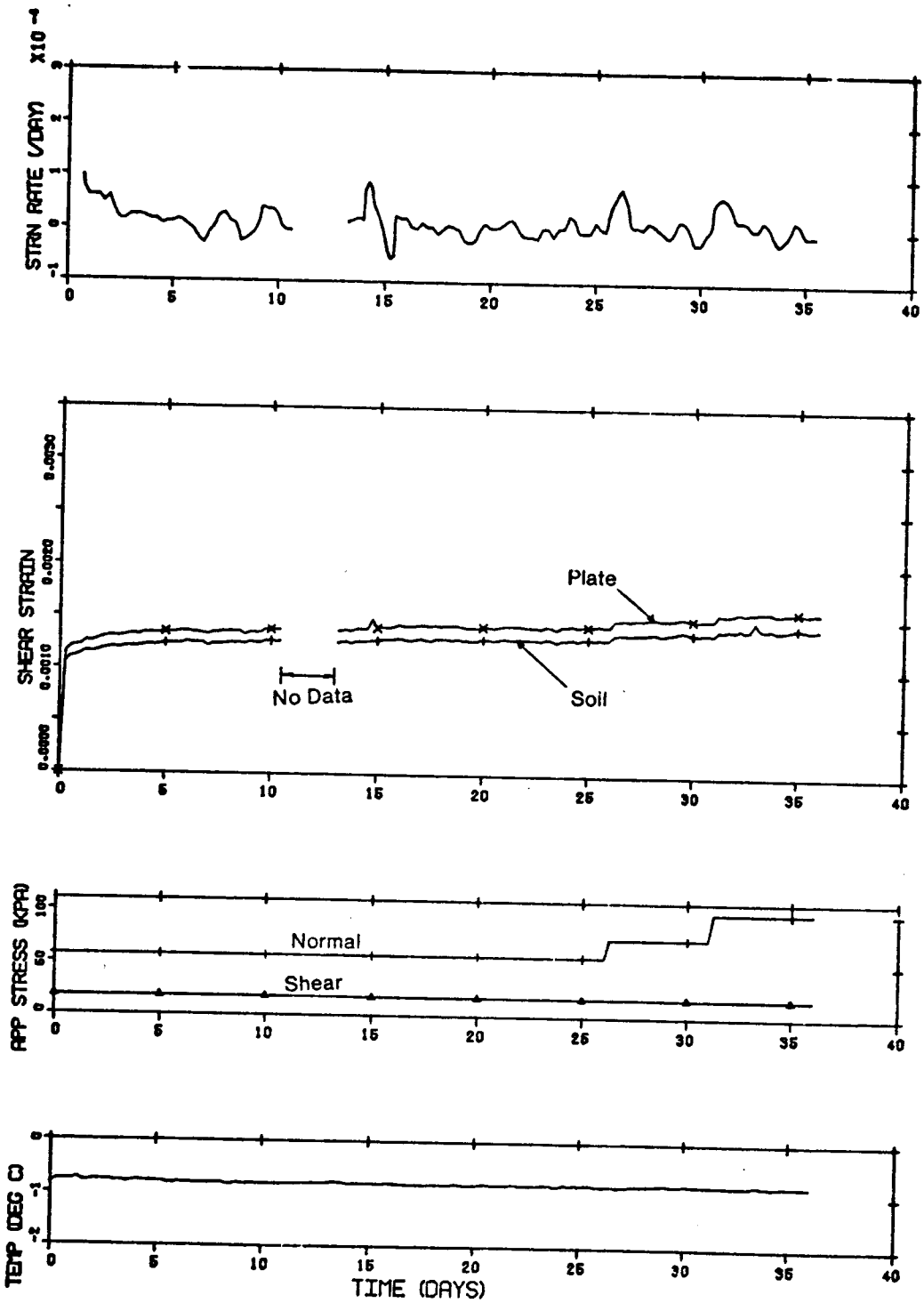

Figure B.6 SHEAR CREEP OF SILT2 IN TS#2 (γ_f =1.54 MG/CU.M)

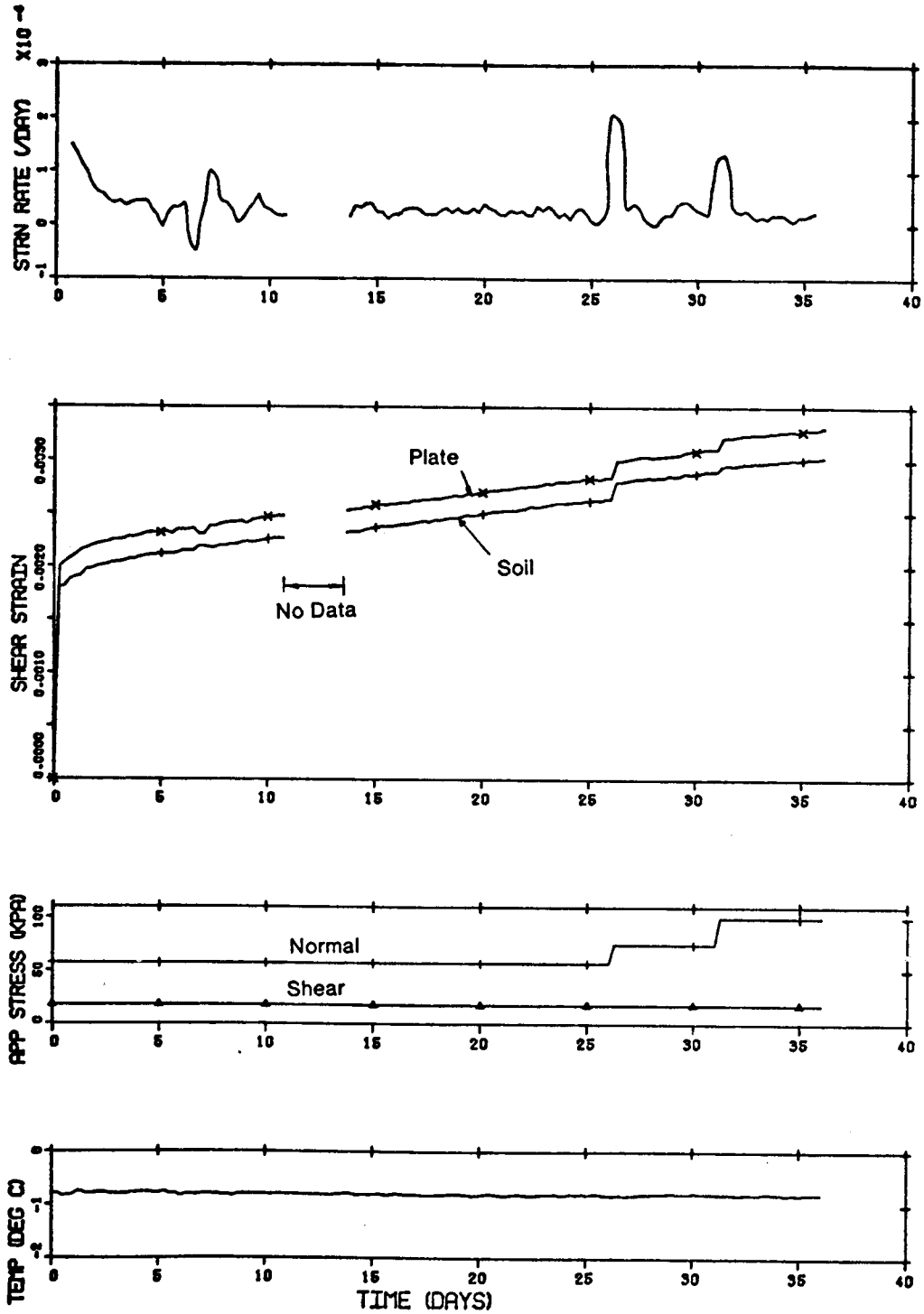

Figure B.7 SHEAR CREEP OF SAND IN TS#2 (γ_t =2.05 MG/CU.M)

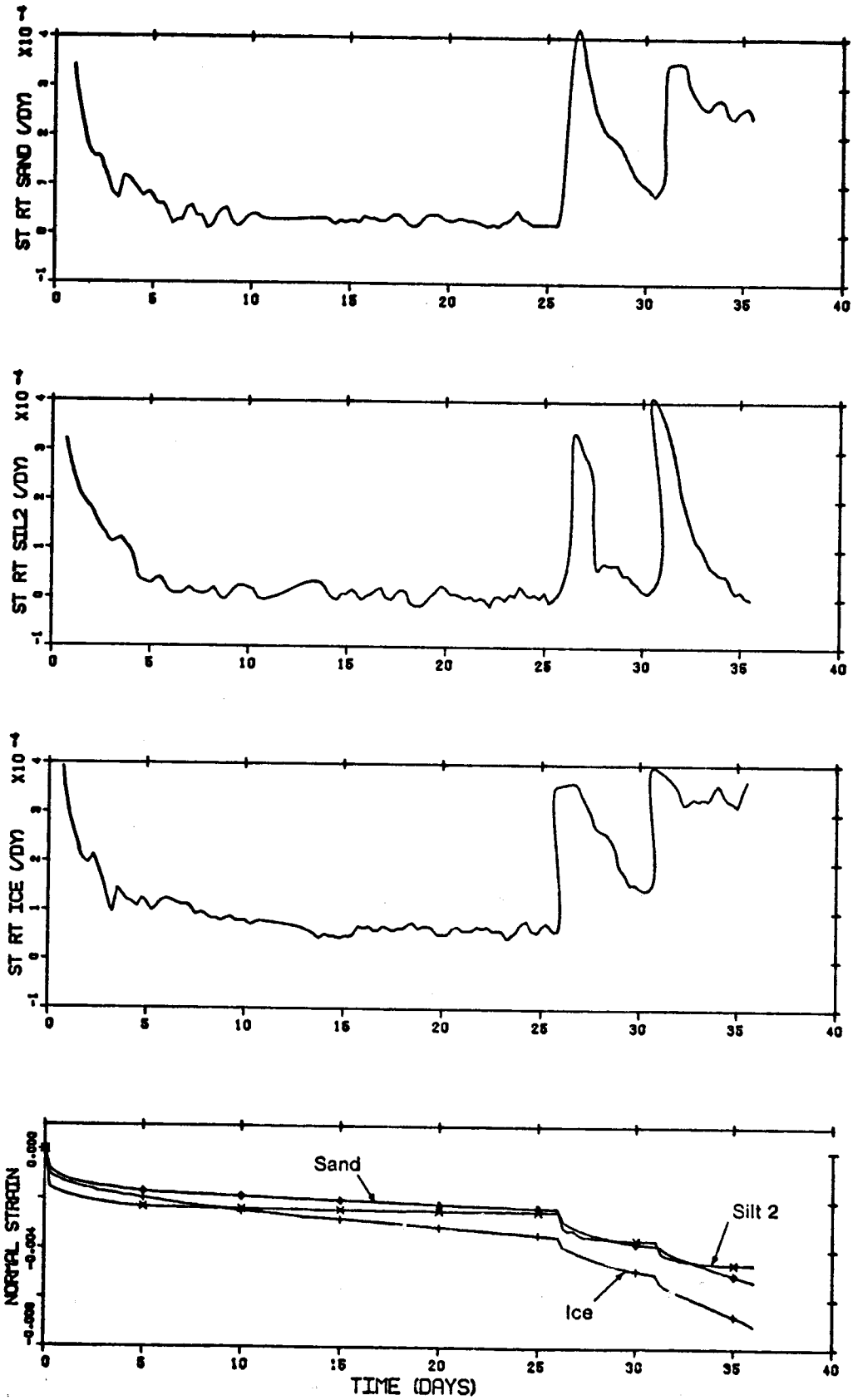

Figure B.8 VERT CREEP OF ICE,SILT2 AND SAND IN TS#2

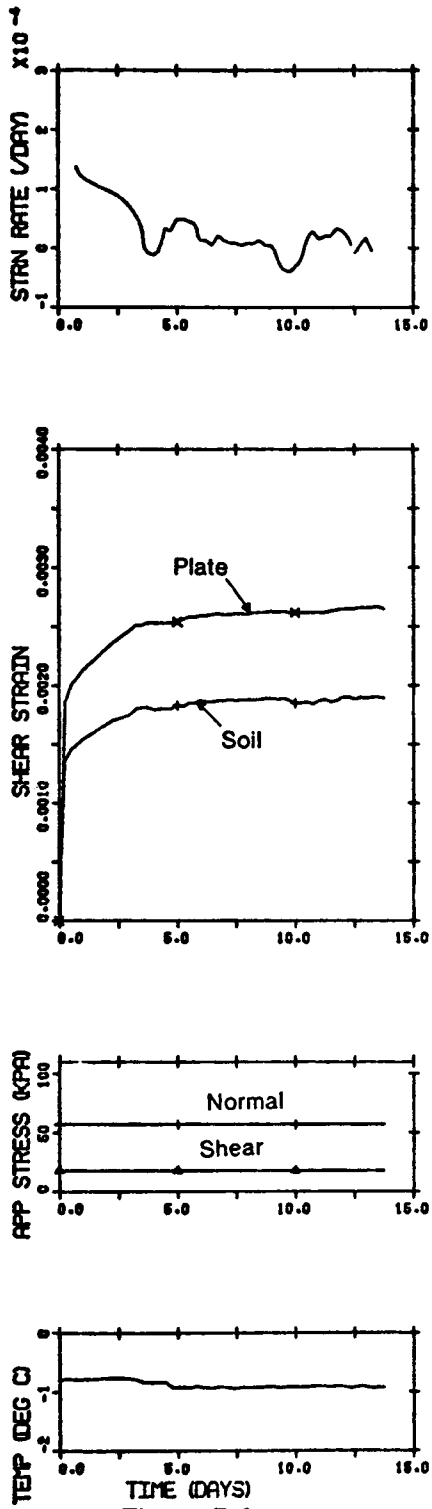

Figure B.9
SHEAR CREEP OF SILT1 IN TS#3 (γ_t =1.76 MG/CU.M)

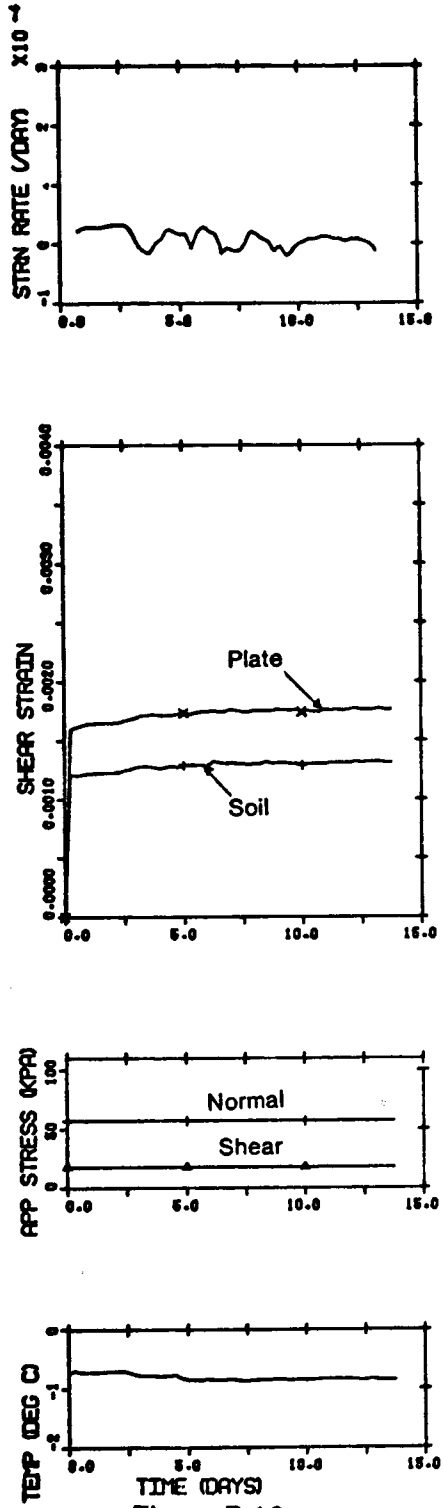

Figure B.10
SHEAR CREEP OF SILT2 IN TS#3 (γ_t =1.42 MG/CU.M)

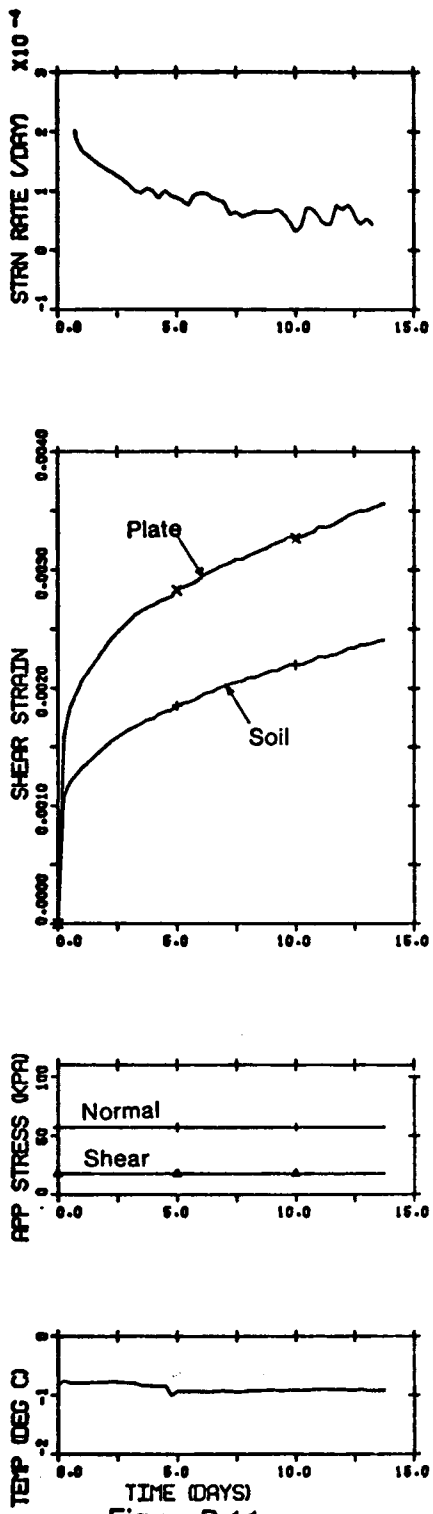

Figure B.11
SHEAR CREEP OF SILT3 IN TS#3 (γ_t =0.96 MG/CU.M)

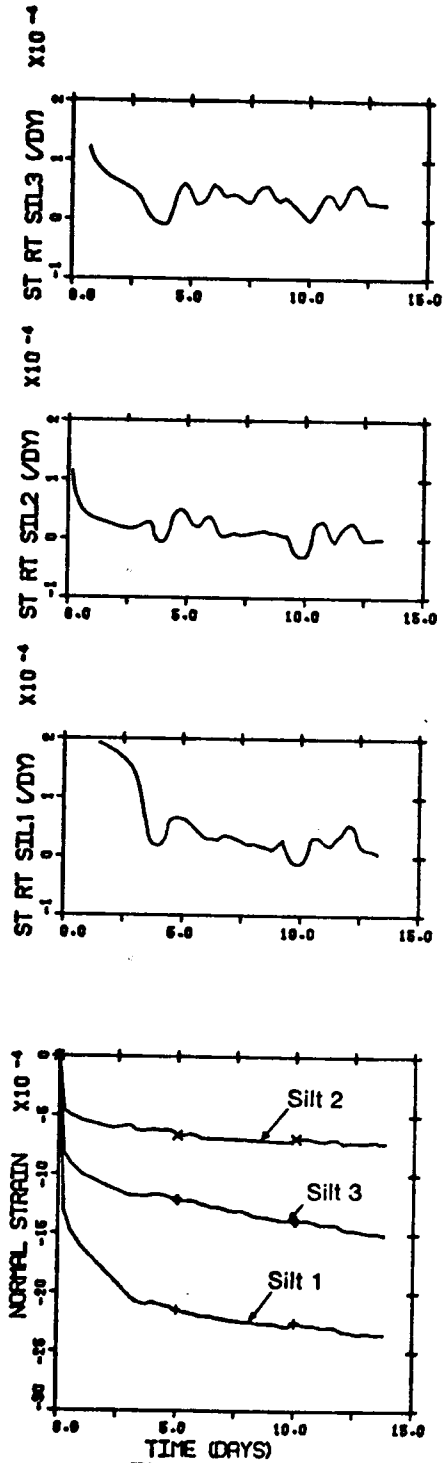

Figure B.12
VERT CREEP OF SILT1,SILT2 AND SILT3 IN TS#3

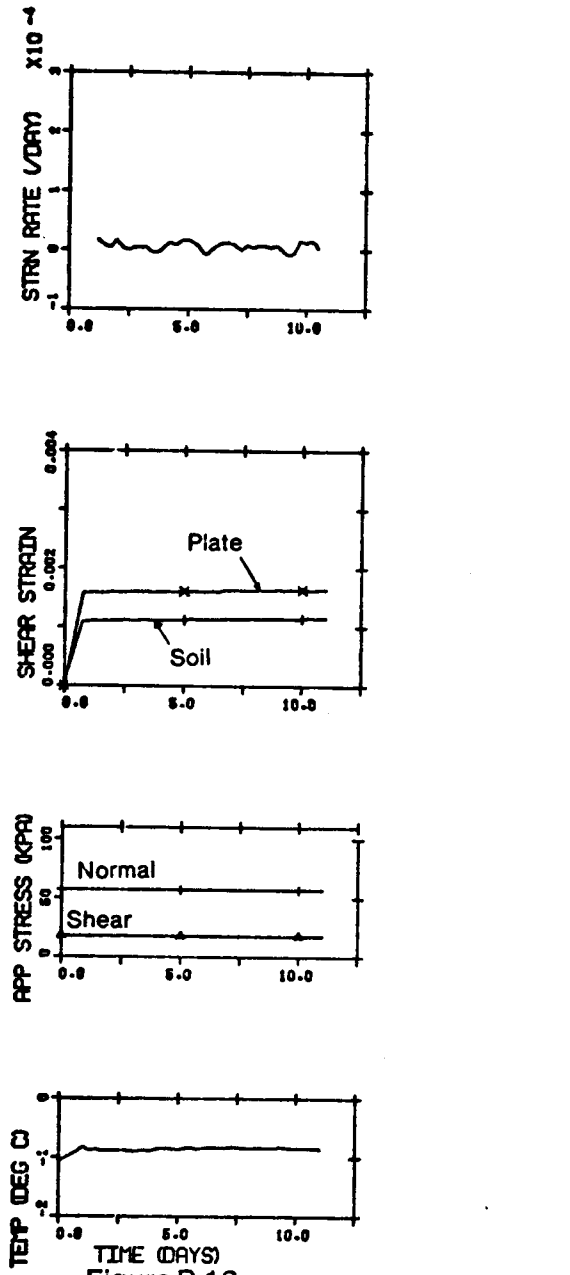

Figure B.13
SHEAR CREEP OF SILT2 IN TS#4 (γ_f =1.42 MG/CU.M)

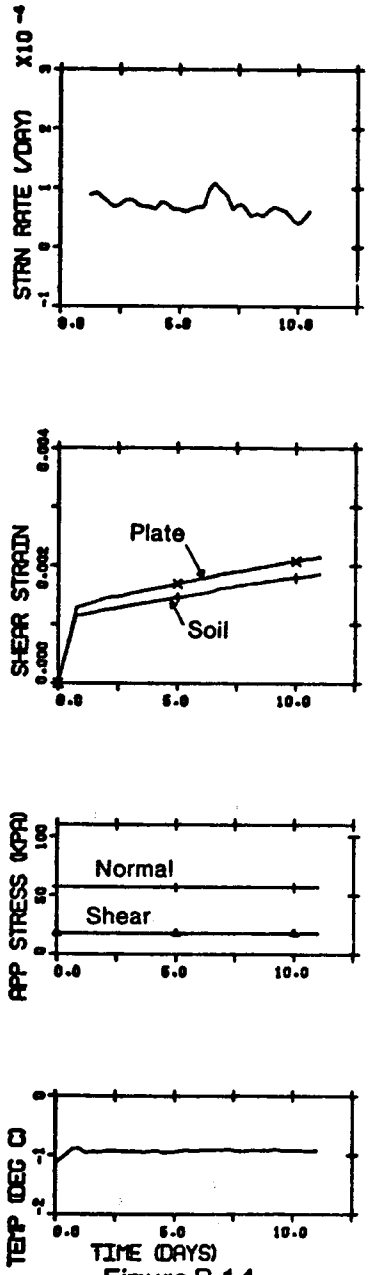

Figure B.14
SHEAR CREEP OF SILT3 IN TS#4 (γ_f =0.96 MG/CU.M)

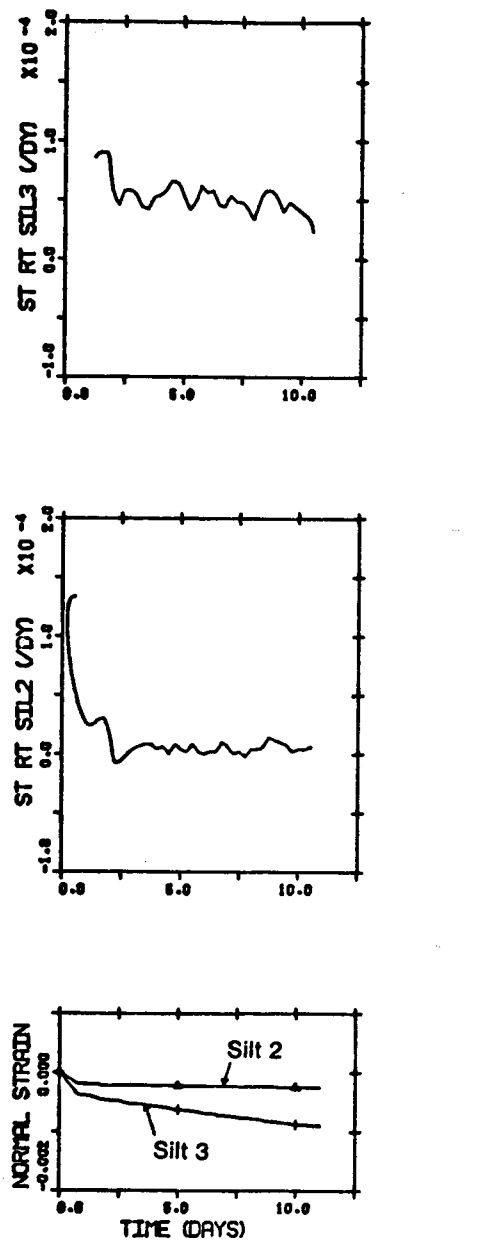

Figure B.15
VERT CREEP OF SILT2 AND SILT3 IN TS#4

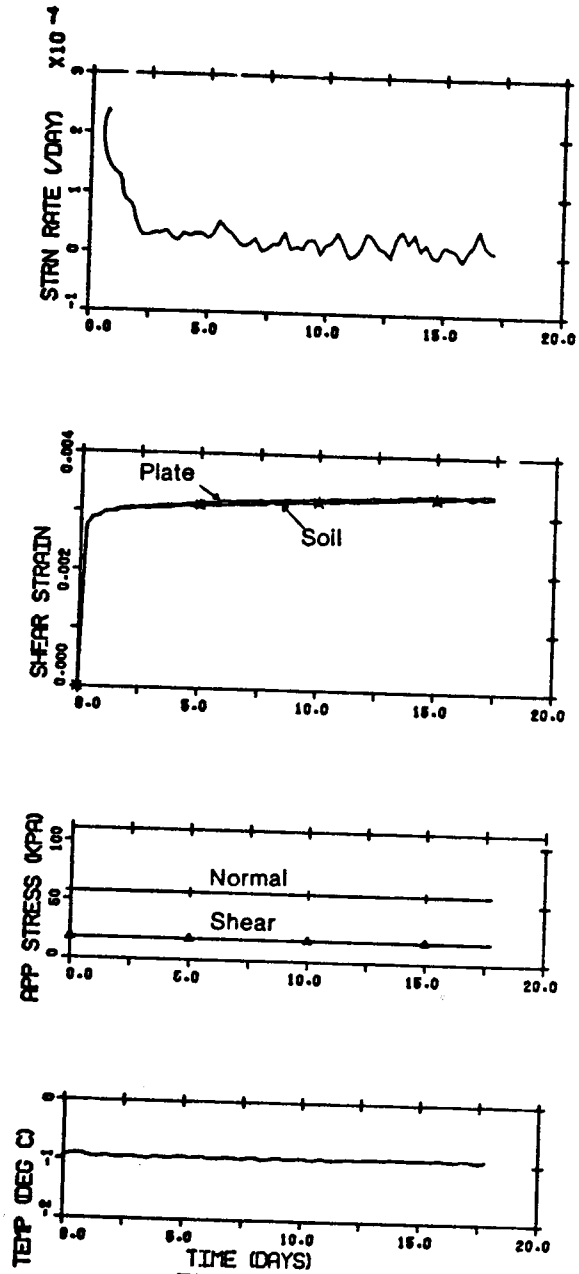

Figure B.16
SHEAR CREEP OF SILT1 IN TS#5 (γ_t =1.85 MG/CU.M)

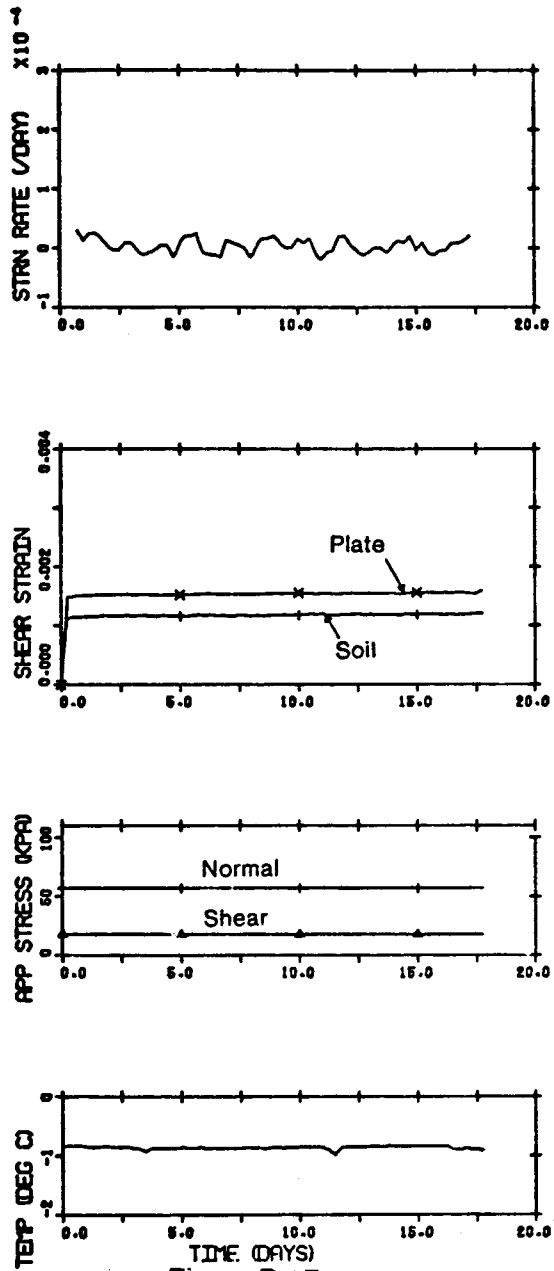

Figure B.17

SHEAR CREEP OF SILT2 IN TS#5 (γ_t =1.42 MG/CU.M)

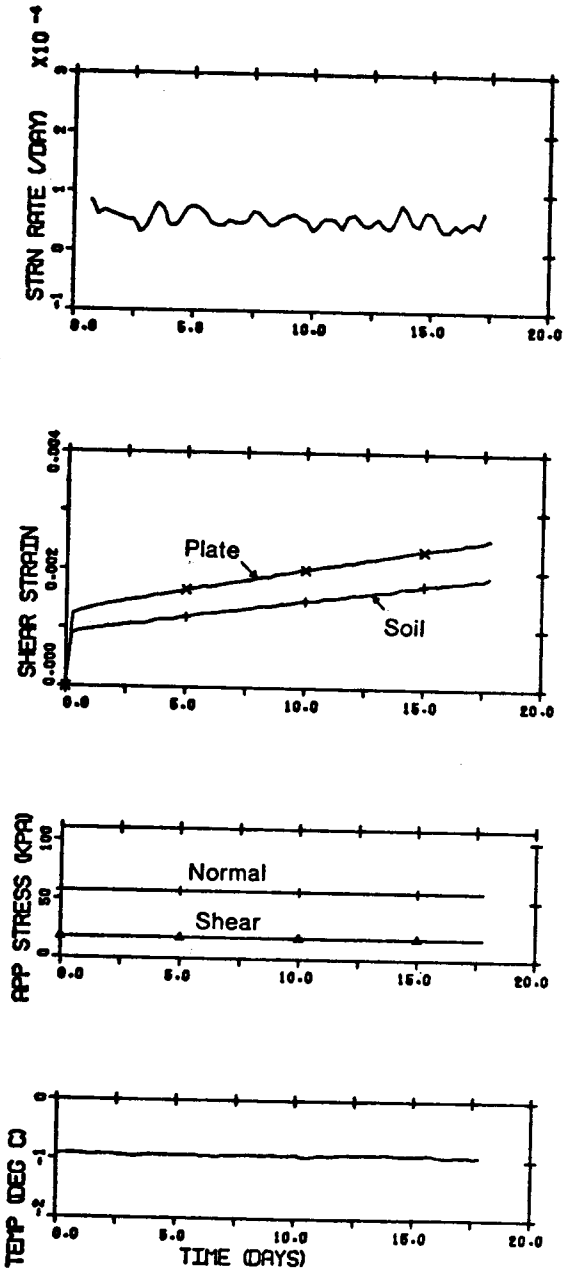

Figure B.18
SHEAR CREEP OF SILT3 IN TS#5 (γ_f =0.96 MG/CU.M)

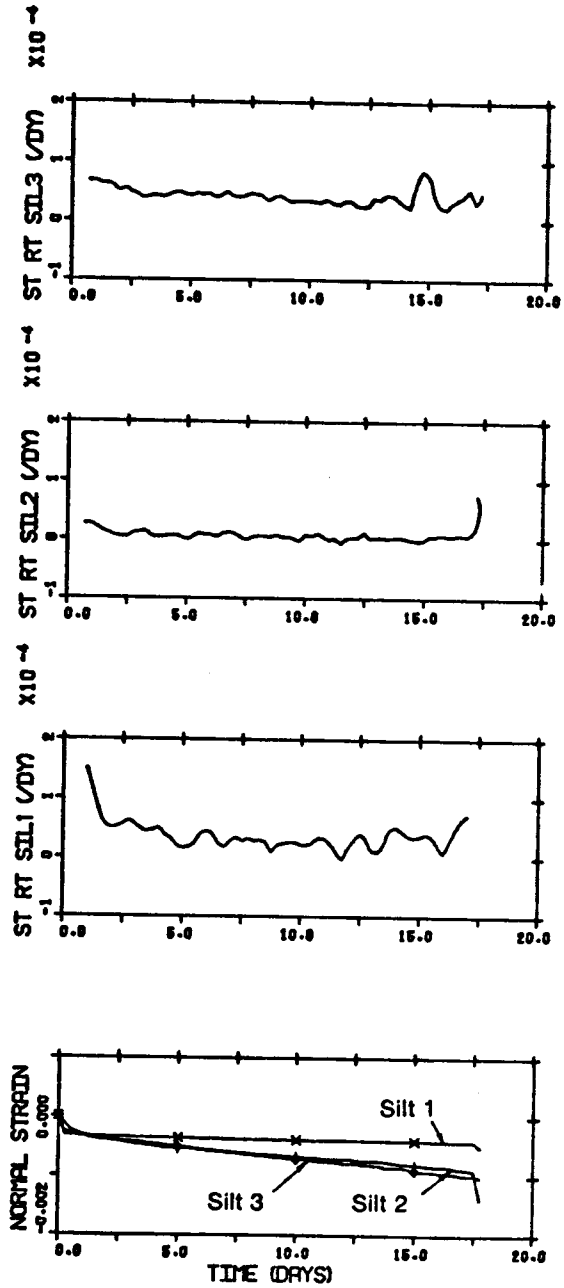

Figure B.19
VERT CREEP OF SILT1,SILT2 AND SILT3 IN TS#5

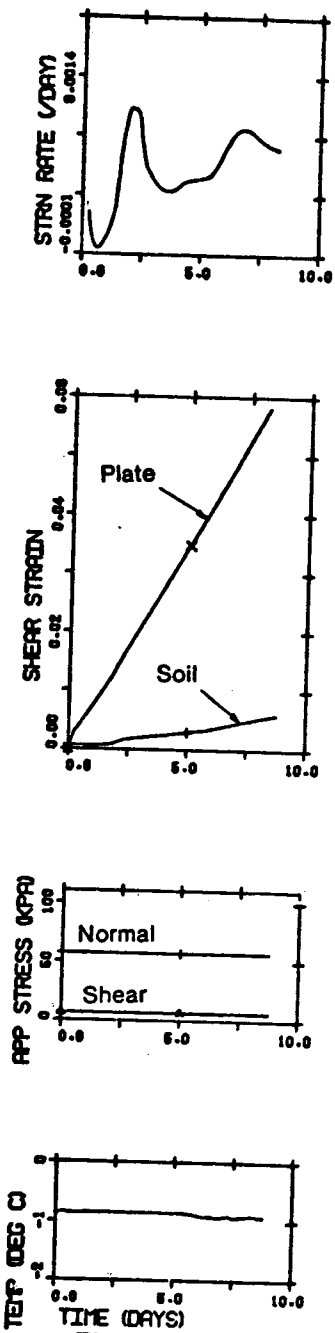

Figure B.20

SHEAR CREEP OF ICE IN TS#6 (γ_f =0.89 MG/CU.M)

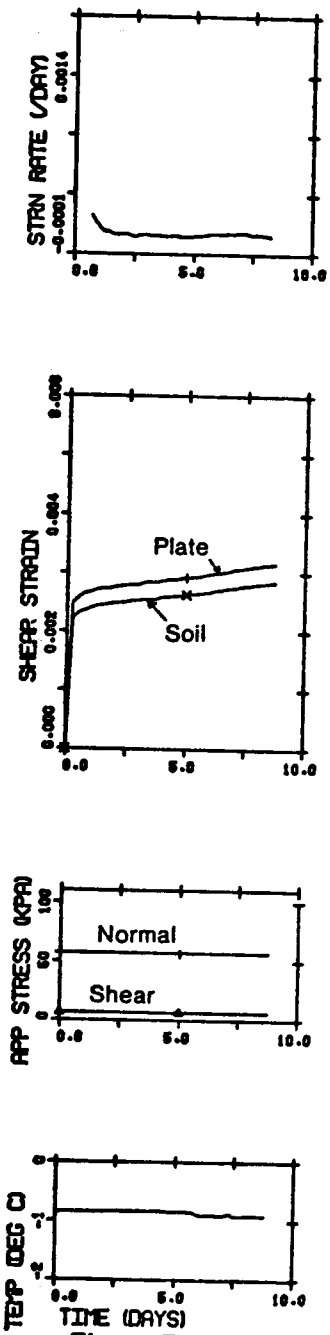

Figure B.21
SHEAR CREEP OF SILT1 IN TS#6 (γ_f =1.89 MG/CU.M)

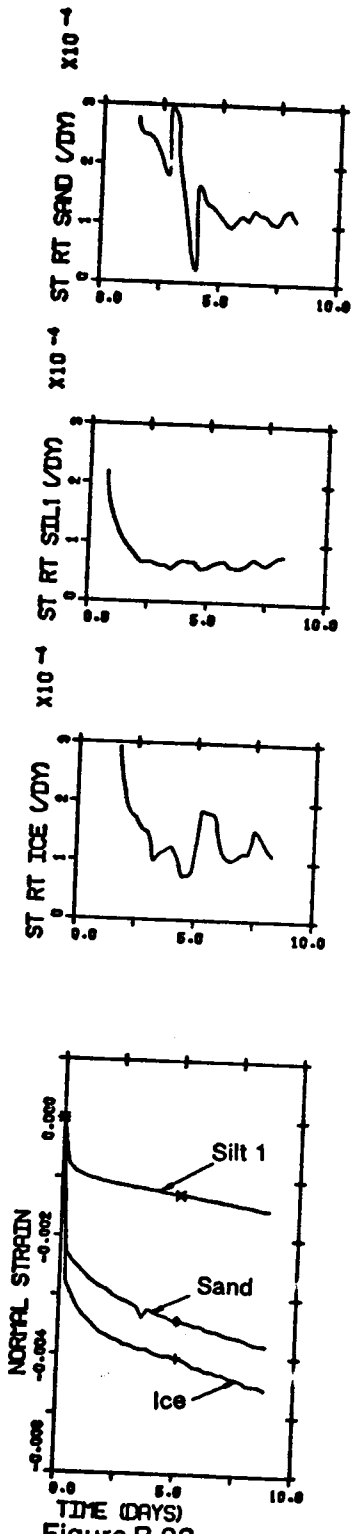

Figure B.23
VERT CREEP OF ICE,SILT1 AND SAND IN TS#6

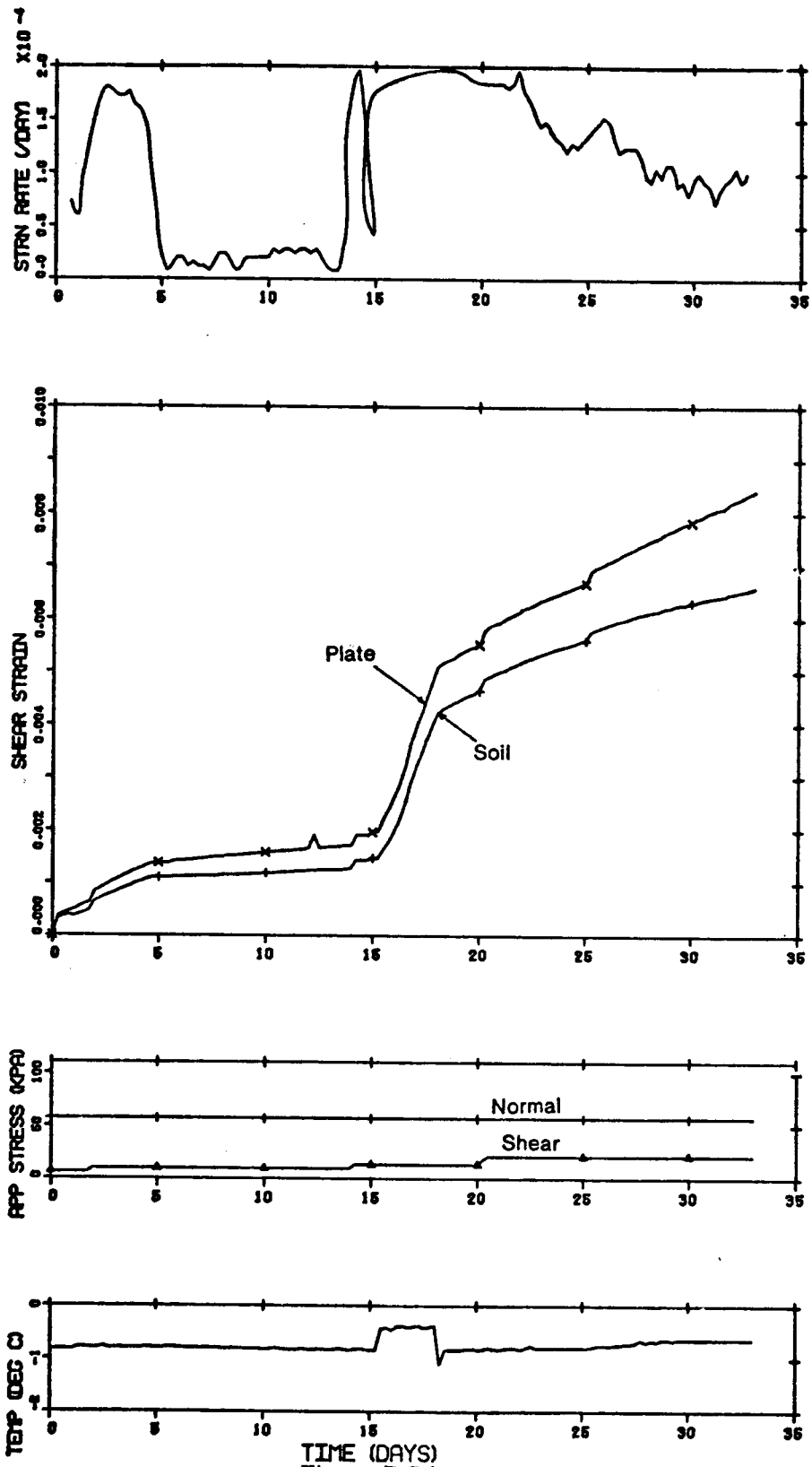

Figure B.24
SHEAR CREEP OF ICE IN TS#7 (γ_f =0.89 MG/CU.M)

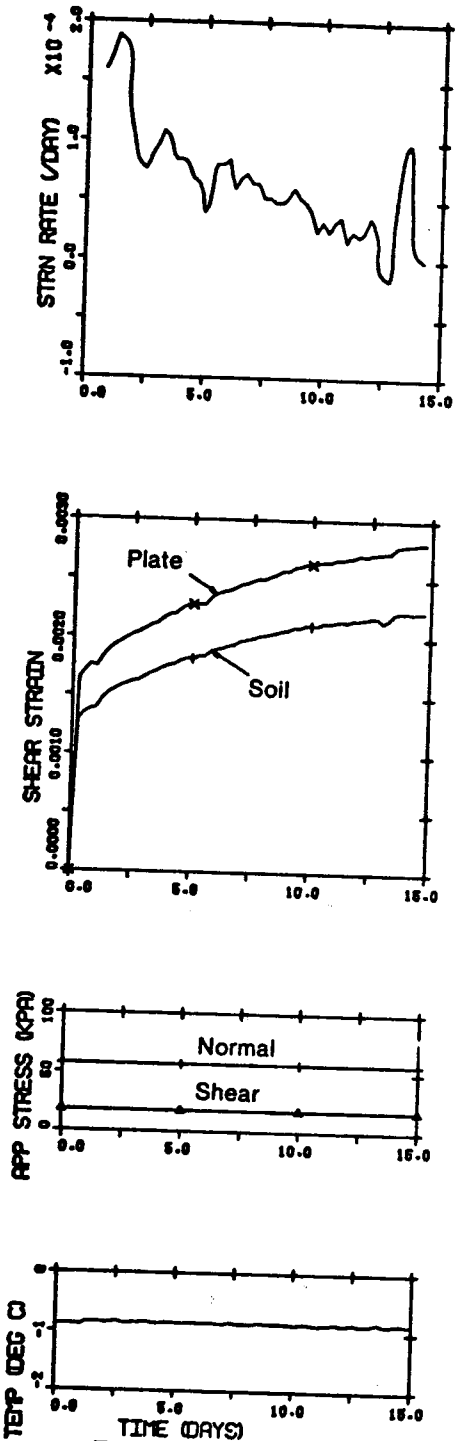

Figure B.26

SHEAR CREEP OF SAND IN TS#7 (γ_f =2.05 MG/CU.M)

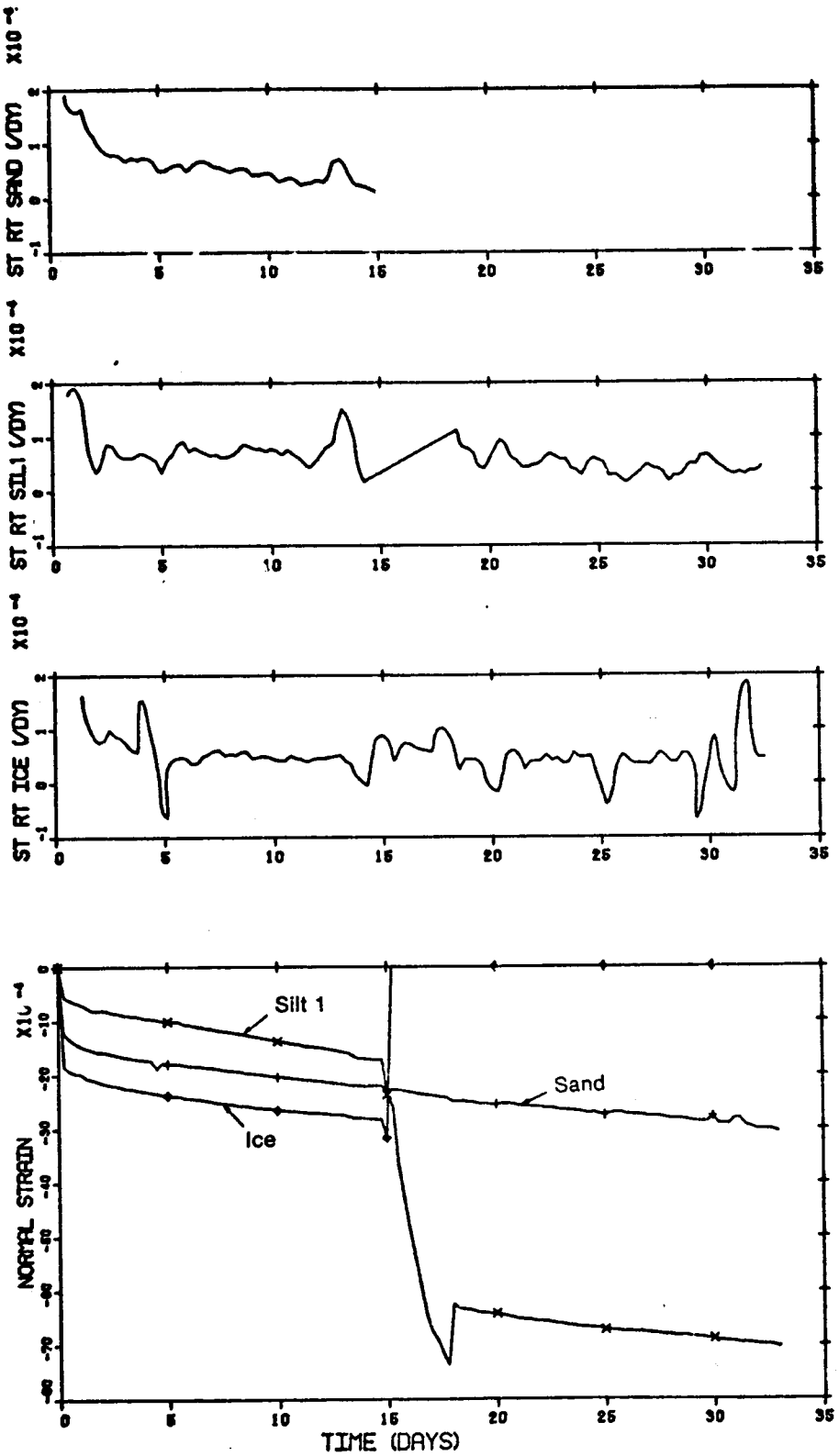

VERT CREEP OF ICE,SILT1 AND SAND IN TS#7

Figure B.27

APPENDIX D

COMPUTER LISTING - WAVE EQUATION

```
C  ************************************************************************
C  ************************************************************************
C  **                                                                    **
C  **       END BEARING RESISTANCE ONLY - NO TENSION AT TIP              **
C  ** THIS PROGRAM ANALYSES A STATICALLY-DRIVEN PILE USING THE WAVE      **
C  ** EQUATION. IT COMPUTES THE VARIATION OF PILE SET, DISPLACEMENT      **
C  ** AND INTERNAL STRESSES WITH TIME. THE SOIL MODEL ASSUMES AN         **
C  ** ELASTIC QUAKE OF 0.1 AND PROVIDES AN END-BEARING RESISTANCE        **
C  ** WHICH IS A FUNCTION OF THE VELOCITY OF THE PILE TIP. DURING       **
C  ** REBOUND THE PILE RESISTANCE IS DETERMINED BY ASSUMING THAT         **
C  ** THE  RESISTANCE AT THE ONSET OF REBOUND IS EQUAL TO SIGL.          **
C  **                                                                    **
C  ************************************************************************
C  ************************************************************************
C     V=VELOCITY
C     D=DISPLACEMENT
C     DD=PLASTIC DISPLACEMENT
C     R=SOIL RESISTANCE
C     C=SPRING COMPRESSION
C     F=FORCE IN SPRING
C     E=COEFFICIENT OF RESTITION
C     W=WEIGHT
C     K=SPRING MODULUS
C     Q=QUAKE
C     SIGL=LOWER LIMIT OF TIME-DEPENDENT STRESS
C     SIGU=UPPER LIMIT OF TIME-DEPENDENT STRESS
C     RO=DENSITY
C     YM=YOUNGS MODULUS
C     AL=PILE LENGTH
C     TFL=LOWER TIME LIMIT OF TIME-DEPENDENT STRESS
C     REND=VALUE OF SOIL RESISTANCE AT THE ONSET OF REBOUND
C     DT=TIME INTERVAL
      REAL V(50),D(50),DD(50),R(50),C(50),F(50),E(2),
     /W(50),KD(50),K(50)
      READ(1,100)DT,E(1),E(2),Q,V(1),AP,B,AN,TFL,RO,YM,AL,W(1),W(2),K(1)
      RO=RO/386
      J=0
      K1=0
      I=0
      JA=0
      MA=0
      COEFF=4.5*AP
      FA=0.0
      DL=DT*4/12*(YM/RO)**0.5
      N=AL/DL
      DL=AL/N
      N=N+2
      LN=N-1
      DO 39 I=3,N
      W(I)=RO*AP*DL*12*386
   39 K(I)=AP*YM/12/DL
      K(2)=AP*YM/12/DL
      TIME=0.0
      DO 1 I=2,N
    1 V(I)=0.0
      DO 2 I=1,N
      F(I)=0.0
      C(I)=0.0
      DD(I)=0.0
      D(I)=0.0
    2 R(I)=0.0
```

APPENDIX E

THAW PENETRATION AROUND A BORED PILE DURING CURING

In this analysis the water/cement/aggregate ratio of the "permafrost cement" concrete is assumed to be 0.44/1.0/2.75 by weight, respectively. The density of the concrete was assumed to be 2.1 Mg/m^3 and the heat of hydration of permafrost cement was taken as 10000 cals/kg.

Thus, for a 0.5 m diameter pile, the mass of cement per unit length is 98 kg/m. Therefore, the total heat released to the permafrost is 4.12 kJ/m. An upper estimate of the thickness of the thawed annulus may be obtained if sensible heat is ignored. Hence, the heat of hydration will melt 12.3 kg/m of ice. This is equivalent to a thawed annulus of thickness 9 mm in ice and 20 mm in permafrost containing 20 % ice by weight.

APPENDIX F

COMPUTER LISTING OF FREEZEBACK PRESSURE ANALYSIS PROGRAM

```
C*****THIS PROGRAM COMPUTES THE CHANGE IN RADIAL STRESS WITH TIME, AROUND***
C*****A SLUFFIED PILE.******
      DIMENSION R(10),RSTRS(10),SBI(10),SL(10),SB(10)
      R(1)=.125
      G=500.
      DRA=.001
      C=2.04
      SLINF=-0.20
      AK=0.01309
      BBB=(C-1)*G*AR*2**(1-C)*3**((C+1)/2)
      NDR=8
      NNDR=NDR-1
      T=1.0E-23
      DO 1 I=1,NNDR
    1 R(I+1)=2*R(I)
      DO 5 I=1,NDR
    5 SBI(I)=DRA*4*G*R(1)/R(I)**2
      E=DRA*4*G*R(1)
      GOTO 4
    3 T=T*10.
    4 TS=T**0.151
      D=BBB*E*(C-1)*TS
      DO 2 I=1,NDR
      SB(I)=SBI(I)/((1+BBB*SBI(I)**(C-1)*TS))**(1/(C-1))
      SL(I)=2*E*(1/(R(I)**2*D)+1/D*ALOG10(R(I)**2/(R(I)**2+
     /D)))+SLINF
      IF(T.LT.0.001)SL(I)=SLINF
    2 RSTRS(I)=(SL(I)-SB(I))*500
      WRITE(6,10)T,(RSTRS(I),I=1,8)
      IF(T.LT.0.001)T=0.001
      IF(T.LT.10000.)GOTO 3
   10 FORMAT(F12.3,3X,8F8.2)
      STOP
      END
```